ABSTRACT

HALL, RACHAEL SUZETTE. Diversification of Prenylated Natural Products Using Synthetic Biology. (Under the direction of Dr. Gavin Williams).

Terpenes are natural products biosynthesized by the condensation of the hemiterpenes dimethylallyl pyrophosphate (DMAPP) and isopentenyl pyrophosphate (IPP) to form linear chains. These linear products can be further modified by various enzymes to produce a wide variety of terpenoid natural products. Because of their structural complexity, terpenes and their analogues are difficult to chemically synthesize, and biosynthetic approaches are being explored. However, hemiterpene biosynthetic pathways involve at least six enzymes and are difficult to leverage for production of precursor analogues. As an alternative, a synthetic-biology approach involving the design and construction of an artificial biosynthetic pathway has been developed. Subsequently, this platform could enable the high-scale synthesis of diverse terpenes that are modified with non-natural chemical functionality, using simple, cell-permeable, chemical precursors.

Prenylation, or the addition of a prenyl moiety to a molecule, is important for the activity of several families of natural products and even some proteins. This prenylation can either form the carbon skeleton of the molecule or occur on the periphery. One aromatic prenyltransferases responsible for this type of transformation, FgaPT2, has been investigated for its promiscuity toward a variety of prenyl donors. In addition, the artificial pathway for terpene analogues has been successfully coupled with FgaPT2 prenylation to produce natural product analogues *in vitro* and *in vivo*. Two other prenyltransferases, FtmPT1 and CpaD, and a chain-length determining mutant of FgaPT2, CpaD, and FtmPT1 have also been characterized with a panel of pyrophosphate analogues and coupled to the artificial pathway.

Diversification of Prenylated Natural Products Using Synthetic Biology

by
Rachael Suzette Hall

A thesis submitted to the Graduate Faculty of
North Carolina State University
in partial fulfillment of the
requirements for the degree of
Doctor of Philosophy

Chemistry

Raleigh, North Carolina

2019

APPROVED BY:

Dr. Gavin Williams
Chair of Advisory Committee

Dr. Reza Ghiladi

Dr. Wei-Chen Chang

Dr. Robert Kelly

BIOGRAPHY

Rachael Hall was born and raised in Friendsville, TN. She moved to Murfreesboro for her undergraduate studies at Middle Tennessee State University, where she received an ACS-certified BS in chemistry and performed undergraduate research in the lab of Dr. Scott Handy. For there, Rachael started her MS work also at MTSU with Dr. Amy Phelps in chemical education, studying how partner-selection methods affected the lab classes she was teaching. Then Rachael moved to Raleigh, NC to begin her PhD work with Dr. Gavin Williams, characterizing the enzymes that prenylate natural products.

TABLE OF CONTENTS

LIST OF TABLES

LIST OF FIGURES

CHAPTER 1: Terpene and prenylated natural products

1.1. Introduction

Natural products are typically good drug candidates because they have evolved to interact with biological targets. Terpenes and prenylated natural products are fantastic examples of medically relevant compounds as they have been used to treat a number of different medical conditions ranging from inflammation to cancer (**Figure 1.1**). While these classes of natural products have the same biosynthetic origin, they vary greatly with respect to structure and biological activity. These molecules have proven difficult targets for total synthesis and diversification, because of their complex scaffolds, number of stereocenters, and lack of synthetic handles on their hydrocarbon backbone.[1] Full and partial biological synthesis of these molecules might offer a complimentary approach to traditional organic synthesis. Investigations and engineering efforts are underway to take advantage of biological machinery to make these drugs.

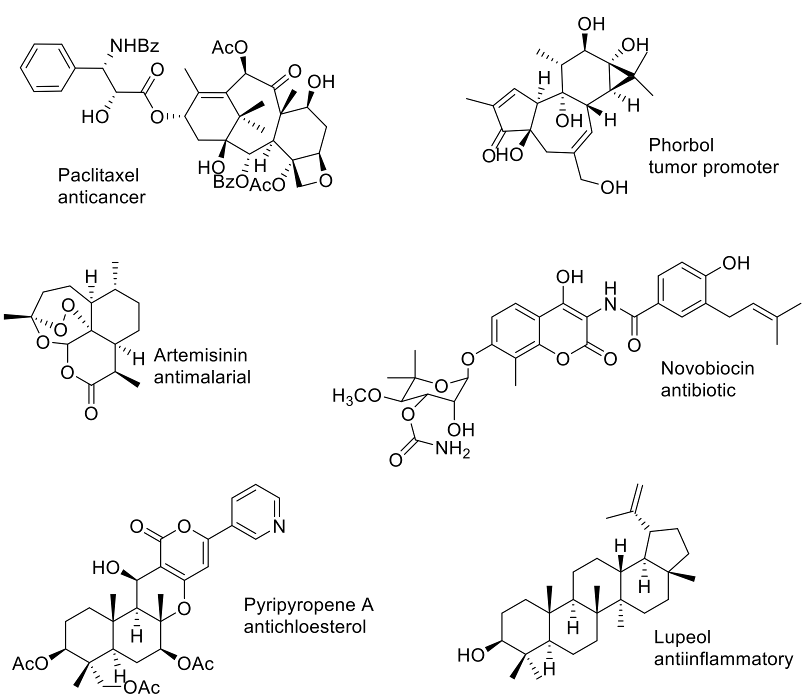

Figure 1.1 Examples of bioactive terpenoid natural products.

1.2. Terpene biosynthesis

Terpenes are one of the most diverse families of natural products. This diversity may be surprising given that these molecules originate from only two biological starting materials, dimethylallylpyrophosphate (DMAPP) and isopentenylpyrophosphate (IPP). This diversity comes from the downstream processing of these molecules. In the biological synthesis, the hemiterpenes DMAPP and IPP are condensed by a prenyltransferase to form linear chains.[2] These linear products can be further modified by various enzymes such as terpene cyclases, cytochrome P450s, or prenyltransferases to produce a very wide variety of terpenoid natural products.

There are two known natural pathways for the biosynthesis of hemiterpenes (**Figure 1.2**). In the 1-deoxy-D-xylulose-5-phophate (DXP) pathway, also known as the 2-*C*-methyl-D-erythritol-4-phosphate (MEP) pathway, pyruvate and glyceraldehyde-3-phosphate serve as carbon sources. In the mevalonate (MEV) pathway, acetyl-CoA serves as the sole carbon source. Gruchattka et al. performed *in silico* modeling of terpene pathways in *Escherichia coli* (DXP pathway) and *Saccharomyces cerevisiae* (MEV pathway) to investigate each microorganism's ability to serve as a host for heterologous production by calculating the maximum production of IPP possible and the energy and carbon cost of maximal production. When the steps to convert the carbon source in the media into the precursors of hemiterpenes were included in the models, the maximal production of IPP in *E. coli* through the DXP pathway was nearly 50% higher than the MEV pathway in *S. cerevisiae.*[3]

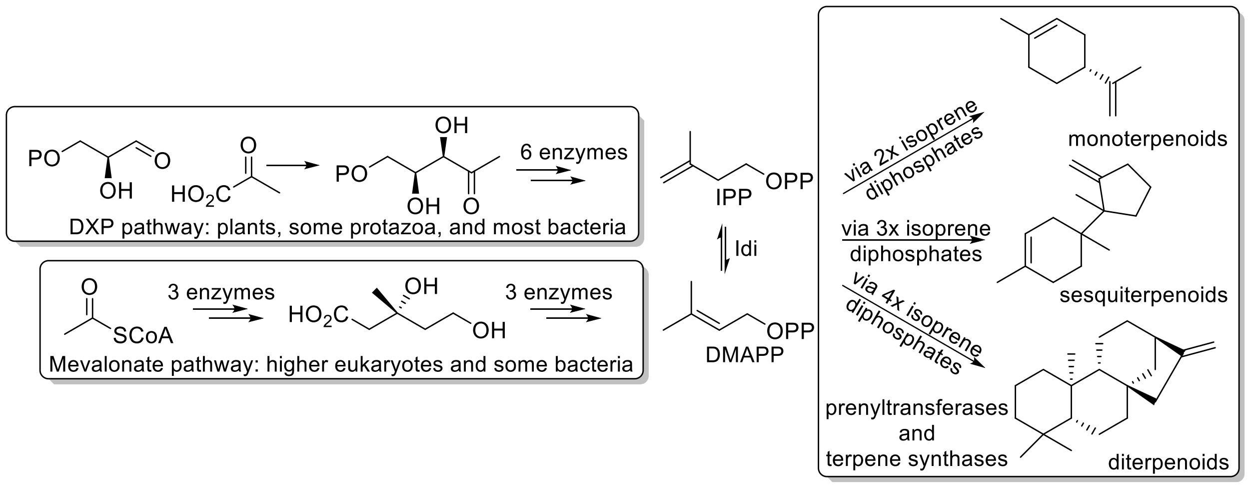

Figure 1.2. Terpene biosynthesis.

In the biosynthesis of lycopene, a red diterpene pigment, CrtE is a prenyltransferase, or specifically a prenylelongase, which synthesizes geranylgeranyl pyrophosphate (GGPP) by condensing DMAPP with three successive molecules of IPP. CrtB forms phytoene via condensation of two GGPPs. Then CrtI dehydrogenates phytoene to give lycopene (**Figure 1.3**).[4] Because of their characteristic colors, lycopene and other carotenoids can be used to screen for the production or consumption of simple linear terpenes.[5] Overproduction of an enzyme that increases of one the carotenoid precursors would increase the color of the cells, while overproduction of an enzyme that uses a precursor would have reduced carotenoid production.

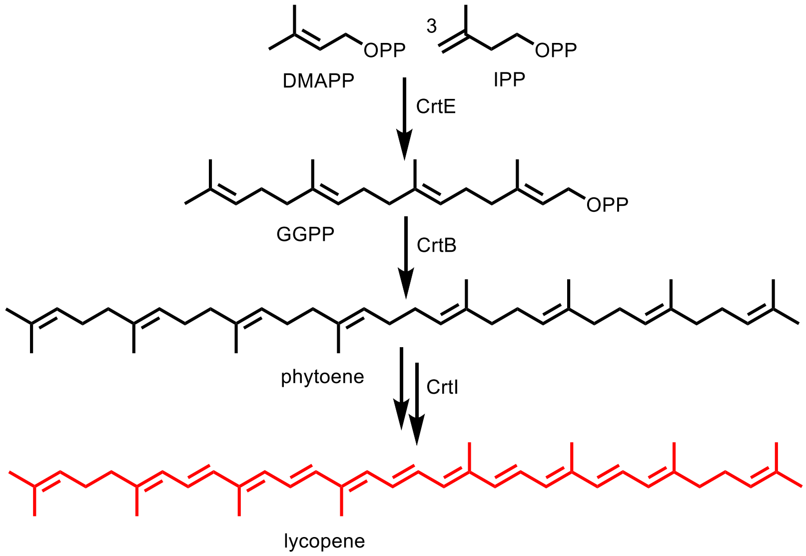

Figure 1.3. Lycopene Biosynthesis.

CrtE is only one example of a prenylelongase. There are many which perform a variety of condensations (head-to-tail, head-to-head, head-to-middle, head referring to the pyrophosphate end) of pyrophosphates of different lengths (DMAPP, IPP, GPP, FPP, GGPP, etc.), and these ultimately decide how long the prenyl chain will be and therefore also which class of terpene the final product will be.[6,7] With this perspective in mind, let's reframe the prenylelongases mentioned in the synthesis of lycopene: CrtE performs a head-to-tail condensation synthesizing long-chain pyrophosphates by adding C5 units to the end of the growing chain, and CrtB condenses two GGPP head-to-head to produce phytoene. Dr. Sean Lund, a former Williams Lab member, studied IspA, another prenylelongase which can condense DMAPP and IPP to GPP or GPP and IPP to FPP. An isozyme of IspA, avian farnesylpyrophosphate synthase (FPS), has been studied by the Poulter lab and engineered via amino-acid mutation to produce longer chains, geranylgeranyl, geranylfarnesyl, and longer in this case.[7] For the non-typical condensations, lavandulyl diphosphate and analogues thereof are good examples. They are formed by a head-to-middle condensation with DMAPP. If DMAPP and DMAPP are condensed in this manner, lavandulyl diphosphate is produced; if GPP and DMAPP, sesquilavandulyl diphosphate or its isomer isosesquilavandulyl diphosphate.

The mechanism proposed by work out of Poulter's lab on the avian FPS mentioned earlier is as follows: the pyrophosphate dissociates from DMAPP or GPP to form a resonance-stabilized carbocation, which is then attacked by the alkenic portion of IPP; then the hydrogen on the carbon next to the resultant carbocation and allylic to the pyrophosphate is removed to form GPP or FPP.[8] They made molecules similar to DMAPP which replaced a terminal methyl with a trifluoromethyl group with methane sulfonate or chlorine in the place of the pyrophosphate, and determined how those substitutions affected rate of solvolysis (proxy for S_N1) or displacement of chlorine by iodine (proxy for S_N2). The trifluoromethyl group retarded the rate of solvolysis, i.e. rate of C1-O bond cleavage and mildly increased the rate of direct nucleophilic attack and replacement of Cl by I. They also looked at the how the trifluoromethyl substitution would affect the rate of the enzyme-catalyzed reaction and determined that again the substitution slowed the rate of reaction dramatically. Because solvolysis and enzymatic reactions were slowed by the same type of substitution, they proposed that they occur by a similar mechanism.[8]

Another lab who often publishes mechanistic studies on prenyltransferases, Martin Tanner's lab out of British Columbia, recently published their work looking into the mechanism of the head-to-head condensation of two FPP to produce squalene.[9] They were trying to study this mechanism by making mimics of the proposed allylic carbocation intermediate, specifically in the form of a guanidinium or amidinium moiety flanked by a phosphonylphosphinate and a hydrocarbon chain, which could bind to the enzyme and inhibit it. To their surprise, the neutral urea-containing control molecule they made was actually the most potent inhibitor. The explanation they propose, the active site doesn't directly stabilize the carbocation; instead, the tight binding of the pyrophosphate and hydrocarbon portions promote catalysis and the pyrophosphate anion can stabilize the newly formed carbocation. Their alternate explanation is that the neutral inhibitor is binding to the "non-ionizing FPP-binding site" or to the site where the nucleophilic FPP binds.[9]

Following elongation, linear precursors can be cyclized to form a variety of products (**Figure 1.4**). According to the proposed mechanism, the allylic diphosphate is first cleaved to form a resonance-stabilized carbocation intermediate which can then undergo a variety of transformations dictated by the terpene cyclase.[10] Even a single terpene cyclase can produce a variety of products by cyclizing the linear terpene to produce many different configurations (**Figure 1.4**).[11–13] Dean Tantillo's lab has produced a large body of work (with only a few general pieces cited here) computationally studying the carbocation rearrangements necessary to produce different terpenes and the feasibility of different possible pathways to the same product.[11,14–17]

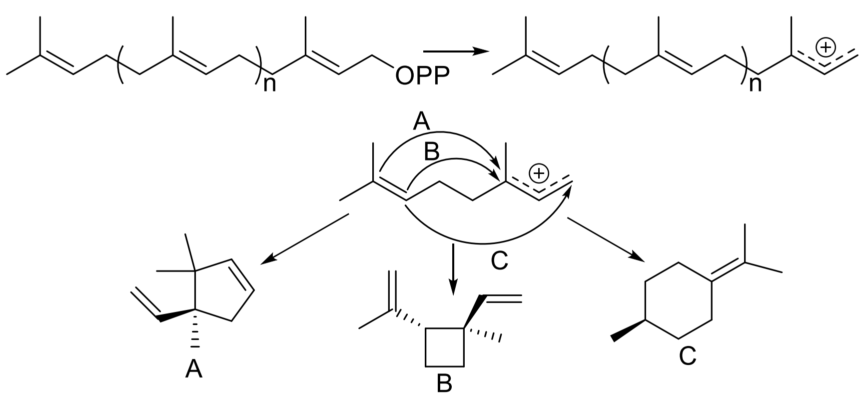

Figure 1.4. Potential products from a hypothetical cyclization of the geranyl cation.

1.3. Engineering efforts

Several engineering efforts have been undertaken to improve the titers of these pathways to heterologously produce useful terpene natural products in microorganisms.[18,19,28–30,20–27] Many of these efforts can be grouped together based on their method for increased product production: increasing precursor supply, engineering downstream enzymes, or balancing flux throughout from primary metabolite to final product, just to name a few. These broad efforts can be even further broken down; increasing precursor supply could be achieved by optimization of the existing pathway, decreasing shunt pathways, and/or adding additional heterologous pathways that also make the precursor. The following paragraphs will discuss recent examples of different types of engineering efforts and their success.

For terpene production in *Escherichia coli* the starting point is often optimization of the existing precursor production through DXP pathway modification. Lv et al. optimized production of isoprene in *E. coli* by engineering precursor-synthesizing enzymes that were thought to be rate-limiting based on previous work, along with promoter manipulation to balance the flux between precursor pathway and product pathway.[31] Specifically they made an error-prone library of a “dxs/dxr/idi’ construct they had made previously which contained their three enzymes of interest and screened those mutants using lycopene-producing *E. coli*, more lycopene indicating higher precursor production and thus increased activity of key enzymes. Then using their top-performing mutant from the lycopene screen for isoprene production, there was a 60% improvement in isoprene formation. Following their “inter-module” optimization, balancing precursor production with final product formation, they saw a 4.7-fold increase in isoprene production compared to the wild-type strain.[31]

There have been strides in other organisms which also use the DXP pathway. Not as much is known about the balance in these organisms so many of the recent papers have been laying the foundation to determine which enzymes could be important targets in this new context. For example, Ya-jing et al. looked at the transcriptional profile of DXP-pathway genes in *Bacillus subtilis* 916.[32] They needed to determine where these genes were located in the genome, their redundancy, and at which phase(s) their transcription takes place. The nine genes of interest were found in seven different operons and were transcribed during exponential and stationary phases.[32] In another example, Englund et al. used overexpression of individual DXP-pathway genes of interest to determine which would be important for terpene production in *Synechosytis* sp. PCC 6803, an unicellular cyanobacterium. Upon finding those targets, overexpression of the three genes gave a 2-fold increase in isoprene production. Then they used a genome-scale model to determine which other genes could increase flux toward the terpene pathway, and using that information they got another 60% increase in isoprene production.[33]

Another way to increase terpene precursor production has been to transplant a natural pathway into an organism using the other: DXP into a MEV-utilizing organism or MEV into DXP-utilizing. Much of the work in this area has come out of the Keasling lab with their efforts to use part of the MEV pathway in *E. coli* to increase terpene production, complementing all their other work in engineering microbes for terpene production.[34–38] Focusing on their recent works, they have worked to engineer enzymes in the MEV pathway to produce more of the target terpene and also have chromosomally integrated the MEV pathway into *E. coli* using CRISPR-Cas9.[37,38] For the enzyme engineering, their target was isopentenol, the hydrolyzed version of IPP, so the method is a little different. Now they are trying to bypass the toxicity of high-levels of IPP and the need for ATP, by not going all the way to IPP in the first place. PMD, the enzyme which converts mevalonate pyrophosphate to IPP via decarboxylation, has some promiscuity toward the monophosphate of mevalonate to produce the monophosphate of IPP, or IP, which can then be dephosphorylated to isopentenol. They engineered PMD to better utilize mevalonate monophosphate, and these changes resulted in a 2.4-fold increase in isopentenol production compared to wild-type strains.[37] For their chromosomally integrated MEV system, they were attempting to overcome the hurdles of *E. coli* production of terpenes becoming industrially relevant by making a strain which produced bisabolene from sucrose by integrating the necessary sucrose-processing genes chromosomally and putting MEV genes under stress-response control. Once they integrated MEV, the production dropped dramatically compared to the plasmid system, so they used CRISPR-Cas9 to switch out promoters and optimize the integrated system. This strategy led to 5-fold improvement of bisabolene production. They also present an interesting discussion on how the switch from plasmid to chromosome is not very straightforward.[38] Keasling's lab, along with a few other labs and industry partners, has also worked to add the DXP pathway to yeast, which naturally contains the MEV pathway.[39] Prior to this work, cytosolic expression of the DXP pathway in yeast had not been successful, and the authors used a combination of methods to make this happen in a MEV-knockout yeast strain. The biggest problems came from production of soluble, active forms of IspG and IspH; they were most successful producing fusion proteins of flavodoxins and orthologs of IspG or IspH. Using their MEV-knockout strains with the above-mentioned fusion proteins and the rest of the DXP pathway, they were able to rescue growth under low-oxygen conditions.[39]

More creative ways to alter or increase precursor supply have been explored. Many of these efforts have altered the feedstock in some way: using a sugar the microbes do not typically utilize or feeding in a molecule which can be turned into DMAPP or IPP once taken up by the cell. For example, Kwak et al. used *S. cerevisiae* which had been previously engineered to utilize xylose and with some engineering of flux through the native and heterologous pathways, made more squalene and amorphadiene than could previously be made using glucose as the carbon source.[40] Recently Stephanopoulos' lab has published a couple of papers using alternative pathways to increase precursor supply. In one instance, they used side reactivity of a native aldolase to make DXP from dihydroxyacetone and arabinose which could then supplement the supply for the DXP pathway. The activity was enough to rescue DXP-pathway inhibited cultures and increase lycopene production.[41] In another instance, they added in two heterologous kinases and the alcohol precursors of DMAPP or IPP to increase lycopene production.[42] Our lab has also demonstrated the same concept but with different kinases and a broader range of downstream coupling steps.[43]

A few labs have abandoned cells entirely and have made terpenes *in vitro*. Bowie's lab has produced a large body of work producing terpenes from glucose using enzymes.[44–48] Their system has 27 enzymes which converts glucose to monoterpenes, while also generating the necessary cofactors for the transformations. They demonstrated success with three monoterpenes by switching out the terminal monoterpene synthase, making more than can be made in a cell because of toxicity limits.[46] In addition, work out of the Schulz lab converted acetic acid to sesquiterpenes in a cell-free system. Their system used 10 enzymes (plus additional cofactor-regenerating enzymes), and once again the final enzyme could be switched out to produce a different FPP-cyclization product, patchoulol or geosmin in this case. They reported >40 % yield from acetic acid to FPP and >90% yield from FPP to terpene.[49]

Other engineering methods have focused more on increasing the efficiency of the terpene synthases following precursor production. For example, taxadiene and amorphadiene synthases (from taxol and artemisinin biosynthesis respectively) have been recent targets for optimization, and mutants were made to increase yield an identify important active-site residues.[50–53] In addition, an FPP analogue was used with amorphadiene synthase to save a few steps in the semi-synthesis of artemisinin.[54]

These advancements have made great strides toward the goal of high-level heterologous production of terpene natural products. They have explored the complex network of genes and knockouts necessary to increase metabolic flux to the natural terpene pathways. They have also transplanted one natural terpene pathway into an organism that typically uses the other. In addition, they have investigated the balance between the natural pathway and the heterologous pathways to transform DMAPP and IPP into complex natural products of interest. These types of investigations are necessary if high-level production of these molecules via fermentation is to become a reality.

While these investigations have provided very useful information about terpene heterologous production, they are limited. Many of these studies do not produce the natural product of interest, but instead a precursor: amorphadiene instead of artemisinin or taxadiene instead of paclitaxel. Also these engineering efforts do not lend themselves well to further diversification of terpenes because they increase the quantity of natural substrate instead of utilizing alternative sources.

However, there have been a few potential methods for diversification discussed in the literature. Many of the terpene cyclases are multiproduct, and their product distribution can be shifted based on pH, metal ion, or substrate geometry.[55] Also enzyme engineering of these terpene cyclases with mutations can also change their major product.[56] Outside of terpene cyclases, prenylelongases, which synthesize the linear pyrophosphates cyclized by the cyclases, have also been reported to be multiproduct in some cases.[57] There is also potential to use prenylelongases which do not do the typical head-to-tail condensations and instead perform head-to-torso or head-to-middle condensations producing branched alkyl pyrophosphates.[58] As for other modifications to the linear pyrophosphate, a GPP methyltransferase has been reported recently which can make a C11 pyrophosphate via methylation.[59] The reported methods with the most potential to produce new pyrophosphates are ones which sequentially phosphorylate cell-permeable alcohols to pyrophosphates, but the production of non-natural alkyl pyrophosphates using this method has not be reported to date.[42,43] It is important to note that some efforts to produce analogues have been with the intent of producing enzyme inhibitors which could be useful for further study of the enzyme of interest or the production of antibiotics in the case of inhibition of enzymes necessary for life.[60–62]

1.4. Prenylated natural products

Prenylation, or the addition of a prenyl moiety to a molecule, is important for the activity of several families of natural products and even some proteins.[63–67] These prenyl groups can either serve as a scaffold to further build the molecule by providing carbons for the backbone, or they can also increase the lipophilicity of these molecules so they can interact with the membrane or pass through the cell to interact with their biological target. Many families of natural products are the result of appending a prenyl group onto a different family of natural products: for example, meroterpenoids and more specifically ergot alkaloids (**Figure 1.5**). Meroterpenoids are formed by the prenylation of the product of a type-III polyketide synthase, product of a non-ribosomal peptide synthase, or some other small molecule by a prenyltransferase.[68,69] Ergot alkaloids and other dimethylallyl-tryptophan (DMAT) natural products are formed by the prenylation of the indole ring of tryptophan or a small peptide containing tryptophan.[70–72]

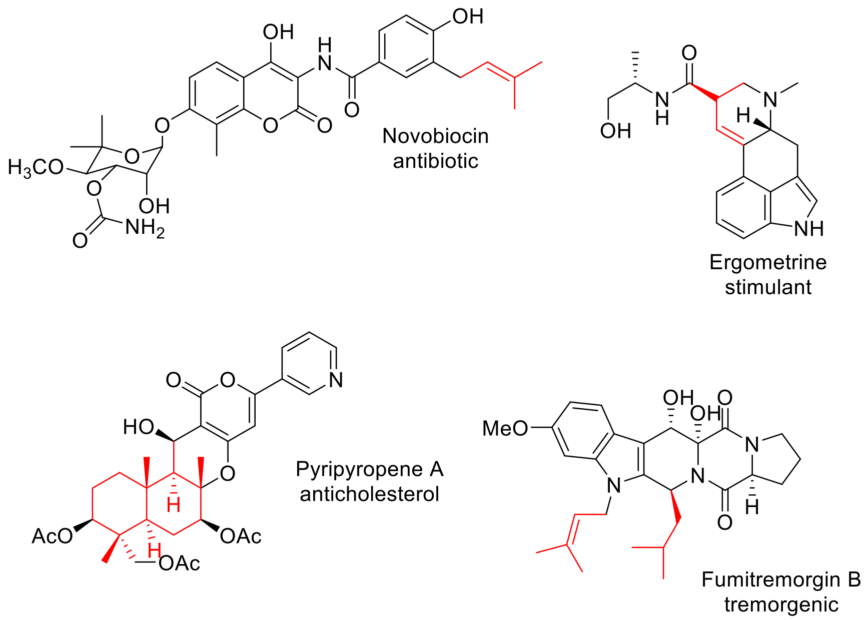

Figure 1.5. Examples of hybrid natural products. Prenyl moieties highlighted in red.

There are a few different types of prenyltransferases which prenylate aromatic rings (**Figure 1.6**). They tend to group phylogenetically based on origin (fungal or bacterial), prenyl donor (small to longer chain pyrophosphates), and/or aromatic substrate (amino acid, polyketide, phenzazine, and xanthones).[68,72,73] For example, the enzymes responsible for prenylating xanthones or hydroxybenzoates or those using longer chain prenyl donors (>C20) tend to be magnesium-dependent membrane proteins containing aspartate-rich binding motifs for substrate binding. On the other hand, those that prenylate individual amino acids, simple polyketides, and phenazines with small-chain prenyl groups tend to be magnesium-independent soluble proteins with a characteristic fold, called a prenyltransferase (PT) barrel, with an alternating α-helix, β-sheet, β-sheet, α-helix (ABBA) structure.[73]

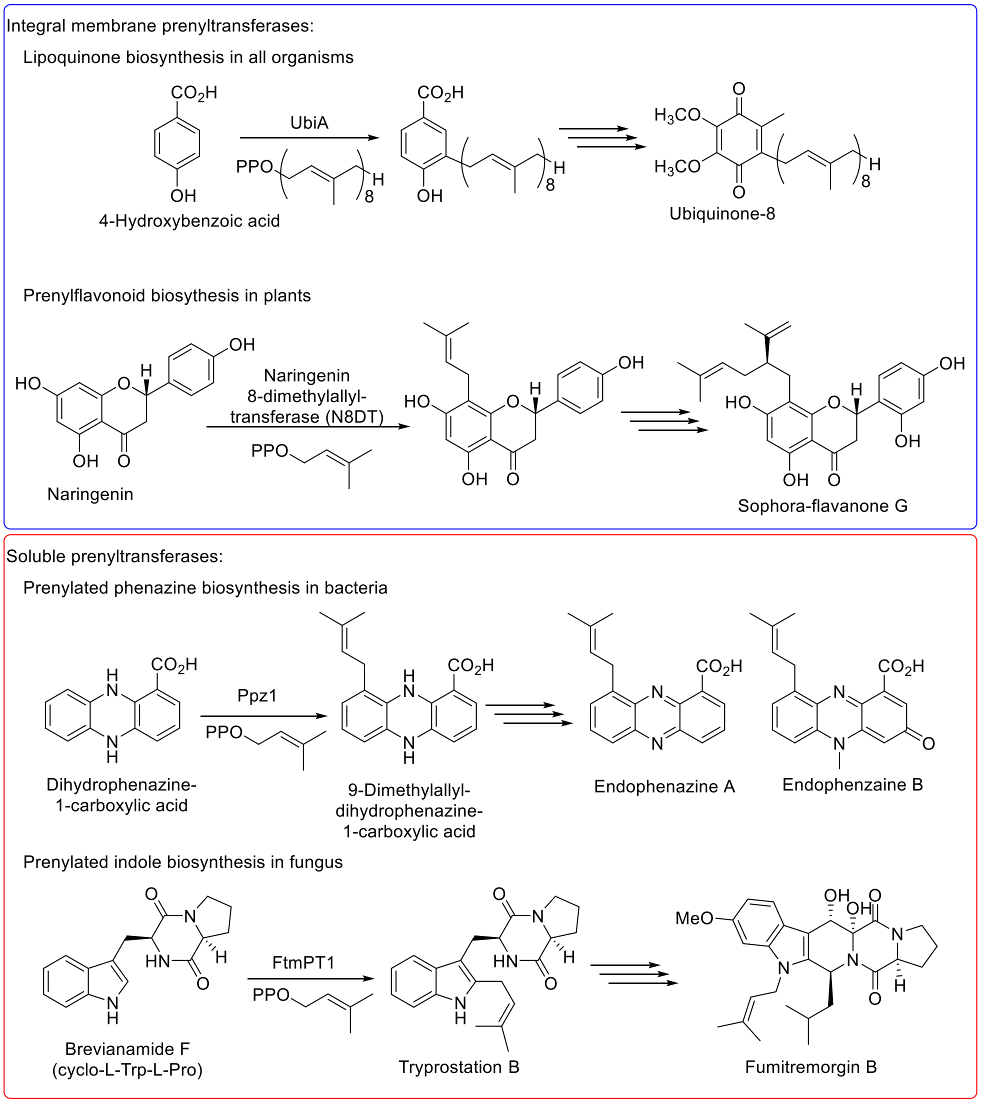

Figure 1.6. Examples of insoluble membrane prenyltransferases and soluble prenyltransferases.

The ABBA prenyltransferases responsible for forming these hybrid natural products are becoming better characterized. There has been some investigation into the substrate promiscuity relating to the aromatic portion of the product, and many of these enzymes have shown great promiscuity by accepting a wide variety of aromatic molecules.[68,73–78] The majority of the investigations into the promiscuity concerning the prenyl donor has dealt with the biologically available pyrophosphates such as DMAPP, geranyl pyrophosphate (GPP), farnesyl pyrophosphate (FPP), or geranylgeranyl pyrophosphate (GGPP). Most of these enzymes are selective for a specific biologically available prenyl donor.[79] The few investigations using non-natural prenyl donors have shown that there is some promiscuity with regards to prenyl donor, but it is important to note that these studies were limited to allylic pyrophosphates (**Figure 1.7**).[76,80–84] There has been success in engineering these enzymes to utilize different aromatic acceptors and prenyl donors.[85–94]

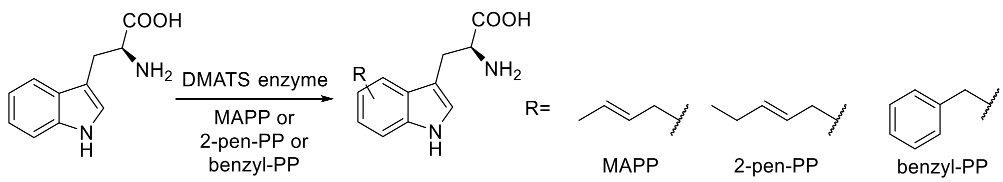

Figure 1.7. Prenylation of tryptophan with non-natural prenyl donors

With these hybrid terpene natural products, the potential for diversification has been investigated more than purely terpene natural products. With meroterpenoids the other family of origin is typically more investigated than the terpene portion, with many polyketide synthases (PKSs) and non-ribosomal peptide synthases (NRPSs) investigated for their ability to accept non-natural precursors.[95] Even with the limited investigations into alkyl pyrophosphate promiscuity, many of the enzymes have been promiscuous with the allylic pyrophosphates tested.[84] Perhaps the most exciting point of diversification is coupling various PKSs and NRPSs to various PTs, in a method termed "lego-lization" where one can imagine mixing and matching different chemical transformations to build new molecules like one could mix and match Lego pieces to build new structures.[96,97]

1.5. Overall goal and purpose

The following chapters will discuss progress on several specific aims: (1) development of a non-natural biosynthetic pathway to produce hemiterpene analogues and determining the scope and synthetic utility of an aromatic prenyltransferase, FgaPT2, involved in the formation of hybrid natural products; (2) use of this pathway to produce alkylated aromatic molecules *in vivo* and *in vitro* and changes to this pathway that would allow for further diversification; (3) determining the scope and utility of two further aromatic prenyltransferases, FtmPT1 and CpaD, which prenylate cyclic dipeptides. Additionally, potential future directions for these projects will be discussed. The first objective involves investigating potential enzymes which could be used to create an alternative pathway for the formation of pyrophosphates by sequentially phosphorylating cell-permeable alcohols and investigating the potential of these pyrophosphates as substrates for FgaPT2. The second objective combines the two major efforts of the Williams lab—polyketides/non-ribosomal peptides and terpenes—to produce analogues of hybrid natural products by prenylating tryptophan with natural and non-natural pyrophosphates formed by the new pathway. Modifications and mutations which allow for different prenyl donors and aromatic acceptors will be discussed. For the third objective, promiscuity with regard to both prenyl donor and aromatic acceptor for FtmPT1 and CpaD will be investigated using the same panel of non-natural pyrophosphates and several cyclic dipeptides. Lastly, the broad implications and further investigations to undertake will be discussed. This project aims to further characterize the enzymes involved in these pathways, their promiscuity toward non-natural prenyl donors, and their mechanisms with these non-natural donors.

CHAPTER 2: Probing the substrate promiscuity of PhoN and FgaPT2 to determine their synthetic utility in the context of terpene natural products

2.1. Introduction

As alluded to in Chapter 1, of the reported methods, sequential phosphorylation of cell-permeable alcohols has the most potential for terpene diversification. The aim would be to biologically synthesize non-natural pyrophosphate analogues and then diversify terpenoid natural products by using them in prenyltransferase, prenylelongase, and terpene cyclase reactions. A recent publication from our group describes a platform that could be used thusly, but so far has been reported to convert DMAA and ISO to DMAPP and IPP using sequential phosphorylation which was then utilized to supplement production carotenoids and 4-DMAT (more information in Chapter 3; **Figure 2.1**).[43] This platform could enable the high-scale synthesis of diverse terpenes that are modified with non-natural chemical functionality, using simple, cell-permeable precursors.

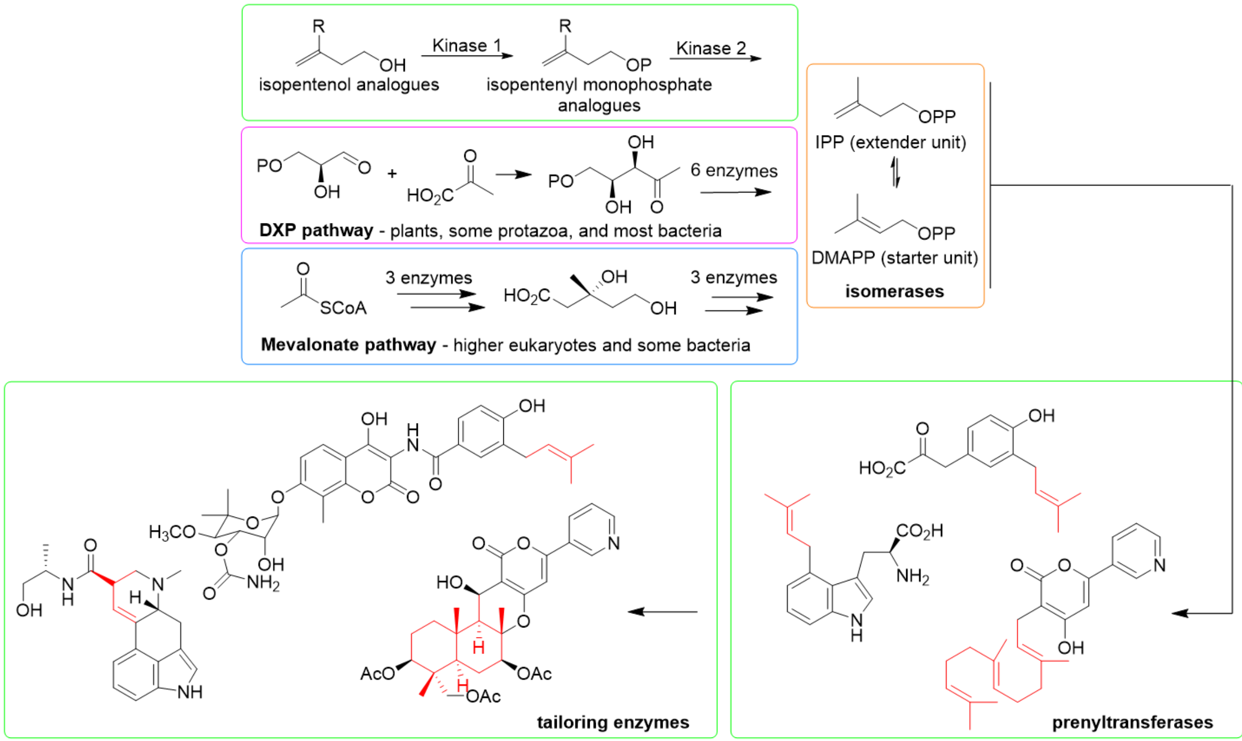

Figure 2.1. Biosynthesis of prenylated natural products, showing natural hemiterpene biosynthetic pathways and the designed artificial pathway coupled to downstream prenyltransferases

This chapter will discuss the development of such a platform to produce alkyl-pyrophosphates from cell-permeable small molecules by sequential phosphorylation of small-chain alcohols, by PhoN-Sf and IPK respectively, and the application of that platform to produce a library of alkylated molecules by use of an aromatic prenyltransferase (PT), FgaPT2. First, each of the proposed pieces of this pathway—PhoN-Sf, IPK, and FgaPT2—will be discussed regarding their origin and potential utility. They will be discussed in an order that may seem illogical but truer to the narrative of pathway setup: second phosphorylation by IPK, first phosphorylation by PhoN-Sf, and prenylation by FgaPT2. Next, the results of *in vitro* assays testing the promiscuity of each purified enzyme will be discussed. Then the potential of coupling all the enzymes *in vitro* and *in vivo* will be discussed.

2.1.1. Scope and utility of IPK

Isopentenyl monophosphate kinase (IPK) is responsible for the phosphorylation of IP to IPP in archaea which have a slightly different pathway to hemiterpenes when compared to eukaryotes. Instead of phosphorylating phosphomevalonate and then decarboxylation to produce IPP, phosphomevalonate is decarboxylated first to produce IP and then phosphorylated to produce IPP.[98] IPK has shown promiscuity for longer chain monophosphates like geranyl or farnesyl monophosphate *in vitro*, and it has been mutated to increase its activity with these longer changer monophosphates.[99,100]

Dr. Sean Lund probed the specificity of IPK from *Thermoplasma acidophilum*.[101,102] A panel of monophosphates was synthesized and tested as substrates with wild-type IPK (**Figure 2.2**). The panel of primary monophosphates included a wide variety of functional groups. Gratifyingly, ten of the monophosphates were successfully phosphorylated, and there were no apparent trends in monophosphate proximity to a double or triple bond, i.e. allylic, homoallylic, propargyl, etc., but there did appear to be a limit on the size or length because longer monophosphates were not utilized. This was a great first step to accessing pyrophosphates much different than the natural allylic and homoallylic pyrophosphates.

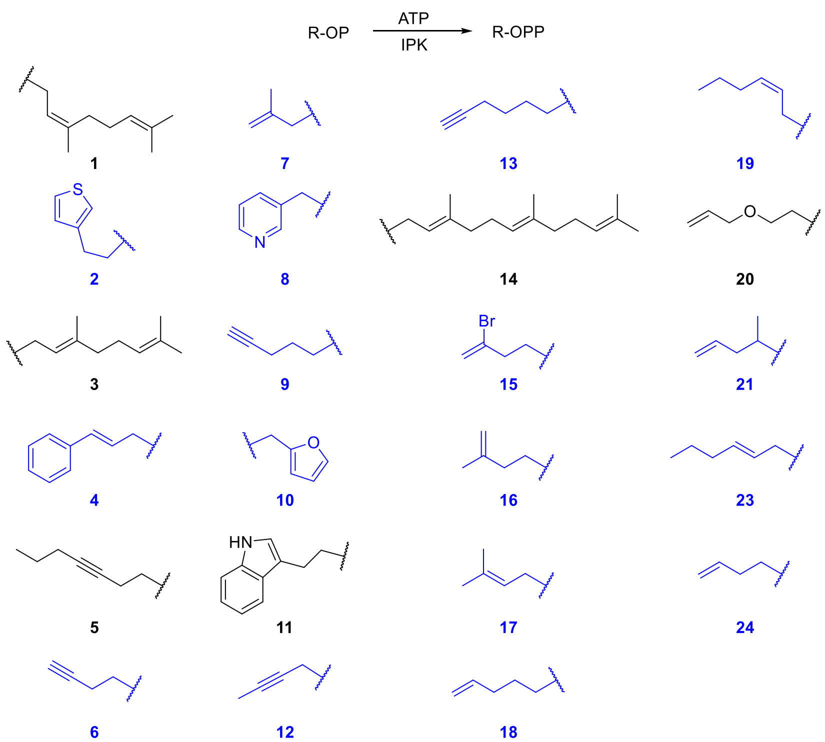

Figure 2.2. Substrate specificity of wild-type IPK. Successful phosphorylations as detected by LC-MS are in blue.

Also of note, IPK has been engineered recently to phosphorylate alcohol substrates in addition to monophosphates.[103] Liu et al. worked to rationally design mutations in an archaeal IPK (the same IPK of Dr. Lund's work) by comparing sequences of all similar enzymes in an online database. From there they looked at which residues were very conserved, and those were left unchanged. With that constraint, they modified the "changeable" residues within 5 Å of the substrate and along the substrate channel, which resulted in six saturation libraries. Three single mutants gave 7-fold activity increase with DMAA. Combining those mutations into one triple mutant resulted in an 8-fold increase compared to wild-type. They also expressed the triple mutant in betacarotene-producing *E. coli*, and with feeding alcohol into the culture, they achieved 1-fold increase in betacarotene production.[103]

2.1.2. Introduction to PhoN: significance and background

There were several candidates for the first kinase. However, Dr. Lund investigated several of those for the ability to phosphorylate DMAA or ISO to DMAP or IP respectively to no avail.[43] To this end, the remaining candidates on the list (FolK and PhoN-Sf) were investigated for this dissertation. FolK, or farnesol kinase, is a membrane-bound protein and hard to work with *in vitro* so it was abandoned early on.[104] PhoN-Sf is a non-specific acid phosphatase from *Shigella flexneri* whose natural substrate is unknown. While classified as a phosphatase, PhoN has also been shown to transfer a phosphate group from a phosphate donor to the hydroxyl group of another molecule, phosphorylating a wide variety of simple alcohols, carbohydrates, and nucleotides *in vitro*.[105–113] It achieves this by phosphorylating one of its own histidines, and then the phosphate group can be cleaved by nucleophilic attack of water or another hydroxyl-containing molecule.[114] PhoN can also be used to phosphorylate dihydroxyacetone (DHA) with a K_m of 3.6 M and k_{cat} of 40 s^{-1}, which is then used for an aldol condensation with an aldehyde by an aldolase in the synthesis of various carbohydrates.[108]

Engineering efforts of PhoN and related enzymes from different species of bacteria have been undertaken. Recently several phosphatases were immobilized on resin and their reaction conditions optimized to better control for transphosphorylation over unproductive hydrolysis.[113,115] The most investigated isozyme of PhoN is from *Salmonella enterica* (PhoN-Se). Several studies have sought to shift the pH optima closer to neutral or increase its phosphotransferase activity.[109,110,112,114] van Herk et al. used directed evolution to produce a V78L mutant with 25% greater product formation in less time than the wildtype at pH 6.0. Interestingly, PhoN-Sf already has a leucine at the position. Also PhoC, a similar enzyme from

Morganella morganii, has been engineered to increase phosphotransferase activity compared to phosphatase activity with a couple of mutations: I171T and G92D.[112,116]

2.1.3. Introduction to FgaPT2: significance and background

FgaPT2 is one of the most well studied members of the DMATS family (**Figure 2.3**). FgaPT2 is DMAPP specific and has not shown activity with any other natural pyrophosphates until recently where it has been shown to have low-level activity with GPP.[93,117] As far as non-natural pyrophosphates, FgaPT2 has shown some activity with 2-pen-PP, MAPP, and benzyl-PP but not with 3-methylbutanyl-PP or 4-methyl-3-pentenyl-PP.[81,118] It also generally requires an indole ring which is usually the site of prenylation; tryptophan derivatives, cyclic (di)peptides containing tryptophan, and molecules containing indole rings have all been prenylated by FgaPT2.[88,117,119–122]

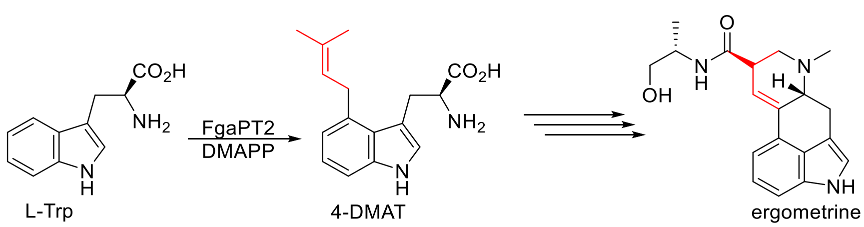

Figure 2.3. FgaPT2-catalyzed prenylation of the indole ring of tryptophan by DMATS. The prenyl moiety is shown in red. Ergometrine is just one of the possible products of that pathway.

FgaPT2 has also been engineered to modify its substrate specificity. The work to-date demonstrates that the substrate scope of FgaPT2 can often change with a few simple mutations.[85,87,123] FgaPT2 also catalyzes the regular prenylation of tyrosine at C3 of the phenol ring, and with a single amino acid mutation (K174F), favors tyrosine over tryptophan.[85] Fan et al. created a saturation library of arginine 244 in FgaPT2 and found thirteen mutants with differentially increased activity toward seven different tryptophan-containing cyclic dipeptides, prenylating regularly at C4 of the indole ring. Recently the K174X and R244X series were combined to produce double mutants which could reverse prenylate the indole ring now at C3 instead of C4.[87] In more work on FgaPT2 out of Shu-Ming Li's lab, FgaPT2 was mutated to switch its prenyl-donor specificity from DMAPP to GPP or FPP, and with one mutation (M328G), there was a 10-fold increase in activity with GPP and an almost 20-fold decrease in activity with DMAPP.[93]

FgaPT2 has also been studied with regard to its mechanism, and the results from these experiments have been used to propose mechanisms for other ABBA PTs. A few mechanisms for the prenylation of tryptophan at C-4 have been proposed. Two of the more obvious mechanisms are an associative type (S_N2), wherein the indole ring attacks the pyrophosphate carbon as the pyrophosphate group leaves or a dissociative type (S_N1), wherein the pyrophosphate leaves and then the indole ring attacks the resultant carbocation (**Figure 2.4**).[124] Positional isotope exchange (PIX) studies following the scrambling of the C-O bond in DMAPP during an FgaPT2-catalyzed prenylation of tryptophan suggest the dissociative type is more likely in this case.[125] The results of this experiment have been used to suggest similar mechanisms for other DMATS and for CloQ, a NovQ homologue, that have only been evaluated using computational methods.[126–129]

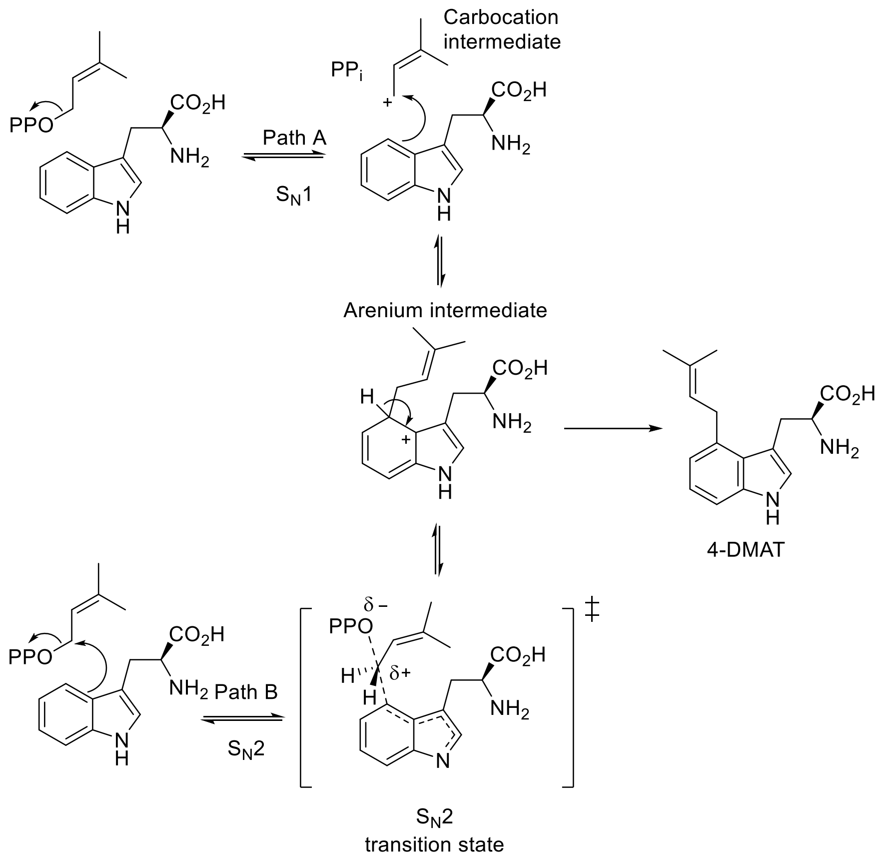

Figure 2.4. Proposed mechanisms for prenylation of tryptophan with DMAPP.

2.2. Results and Discussion

2.2.1. Probing the substrate promiscuity of PhoN

PhoN from *Shigella flexneri* was cloned, expressed in *E. coli* with an N-terminal His_6 tag, and purified using immobilized-metal affinity chromatography (IMAC). Purified PhoN was initially tested *in vitro* for its ability to phosphorylate dimethylallyl alcohol (DMAA) or isopentenyl alcohol (ISO) to produce dimethylallyl monophosphate (DMAP) or isopentenyl monophosphate (IP) respectively, using ATP as the phosphate donor. Following a co-elution liquid chromatography-mass spectrometry (LC-MS) experiment with synthesized DMAP and IP, the *m/z* and retention time of each putative product mass ion were consistent with their synthesized counterparts (**Figure 2.5**).

Given the confirmed ability of PhoN to phosphorylate DMAA and ISO, PhoN was next tested with an expanded panel of alcohols. Putative products were detected via high-resolution MS (HR-MS) analysis of the product mixtures and quantified by the comparison of extracted ion peak area to a known concentration of DMAP or cinnamyl-monophosphate that was spiked into the mixture (**Figure 2.6**). Cinnamyl-monophosphate was used in the place of DMAP to be able to distinguish the enzyme-catalyzed product from the standard DMAP in those few cases where the product was isomeric. The calibration curves were therefore generalizable for small- and medium-length monophosphates. The panel of molecules tested were the alcohol counterparts of the monophosphates tested with IPK. The panel was limited to molecules that contain double or triple bonds with few heteroatoms. There was much variety in size/length: 3 linear carbons all the way to 12 for acyclic, and small heteroaromatic to larger bicyclic aromatics. Many were like their natural pyrophosphate counterparts, DMAPP and IPP, with the alcohol allylic or homoallylic to the double bond and also the analogous alkynes with the alcohol propargylic and homopropargylic to the triple bond. However the alcohol was located several methylene units away from the double or triple bond in a few of the panel members, so this panel tested the synthetic potential of PhoN to synthesize monophosphates that could be used by IPK to make allylic non-natural alkyl pyrophosphates outside of the C5-unit limitation or non-allylic non-natural alkyl pyrophosphates.

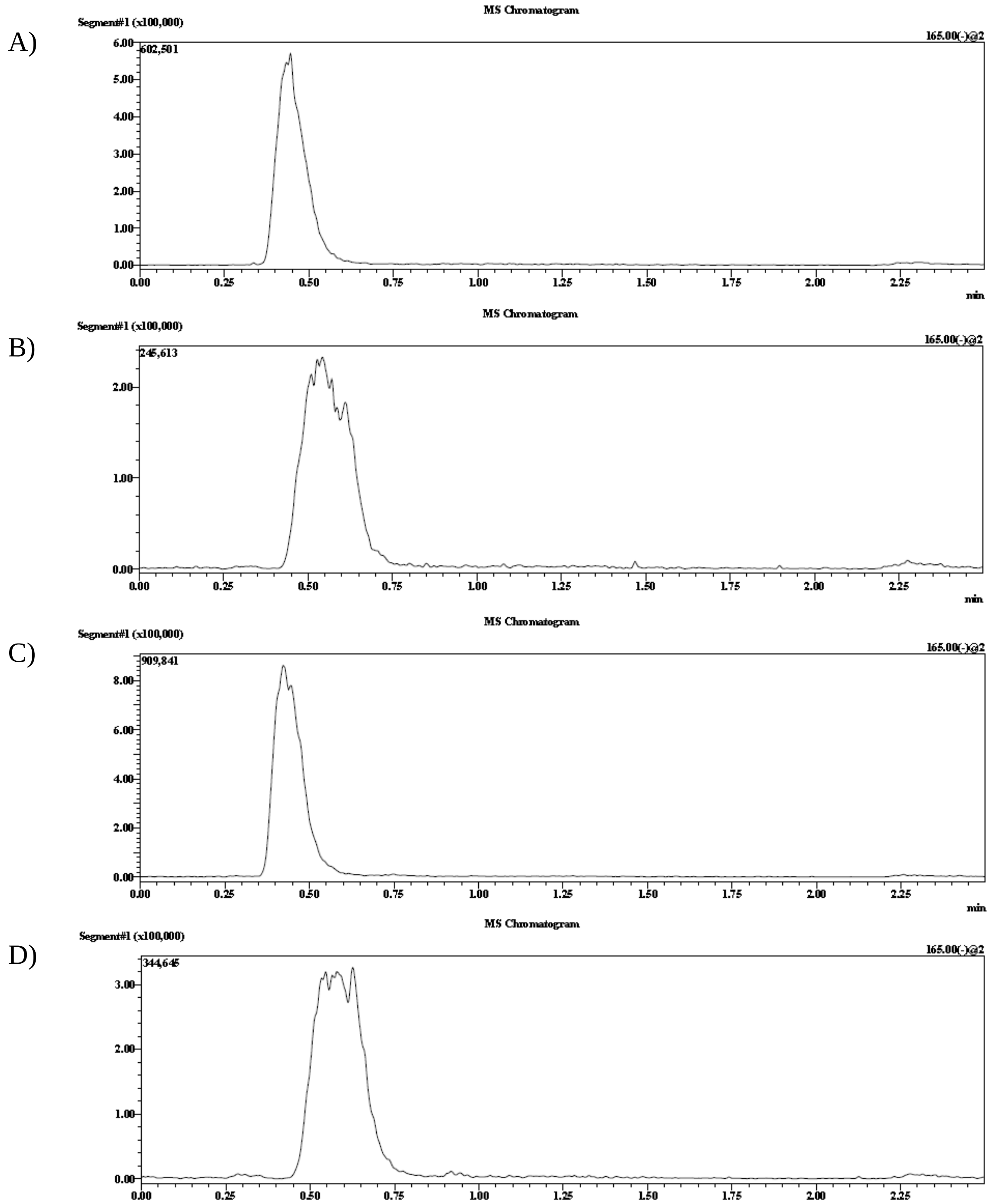

Figure 2.5. PhoN-catalyzed phosphorylation of ISO and DMAA. A) Reaction with ISO, B) Reaction with DMAA, C) Panel A reaction spiked with synthesized IP, D) Panel B reaction spiked with synthesized DMAP.

A)

B)

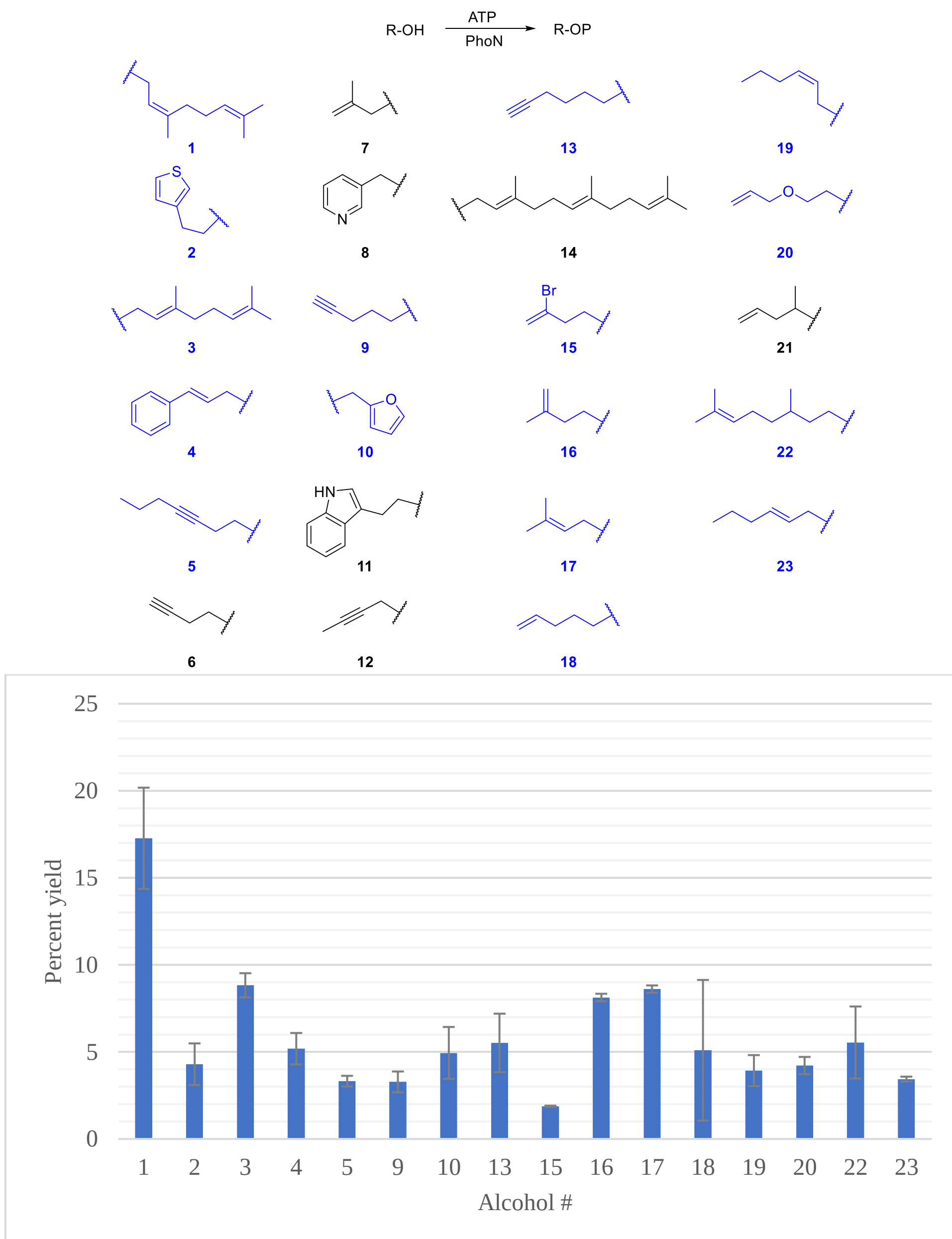

Figure 2.6. Reaction catalyzed by PhoN. A) PhoN was tested with a series of alcohols. Blue indicates mass ions were detected by HR-LC-MS consistent with the expected product. B) The percent yield of PhoN-catalyzed reactions was calculated using HR-LC-MS by comparison to an internal standard. Error bars indicate the standard deviation of reaction duplicates.

PhoN phosphorylated 16 of the 23 alcohols tested, and there did not appear to be any obvious substrate limitations beyond the known preference for primary alcohols.[107] Under the assay conditions, the alkyl monophosphate products (neryl monophosphate (NP, **1**), geranyl monophosphate (GP, **3**), DMAP (**17**), and IP(**16**)) found in nature were detected at the highest concentration apart from farnesyl monophosphate (FP, **14**) which was not detected at all. It is important to note that PhoN can also dephosphorylate the produced monophosphates once ATP has been depleted, so these results are a snapshot of the activity and could also indicate PhoN's ability to dephosphorylate the product as well as its transphosphorylating ability. The transphosphorylation activity over hydrolytic activity has been engineered in enzymes similar to PhoN-Sf. Yet, installing previously described mutations from PhoN-Se or PhoC-Mm engineering to PhoN-Sf was not successful in increasing the yield of desired monophosphate (data not shown).

Putting the PhoN possibilities in the context of Dr. Lund's IPK work, one can see that many different pyrophosphates could be synthesized by sequential phosphorylation of alcohols if the two were used in sequence (**Figure 2.7**). IPK tends to prefer shorter-chain monophosphates, but it has been engineered to accept GP and FP.[99] Depending on the desired chain length of the monophosphate, IPK could be engineered to accept longer-chain monophosphates. Using the two together, a very diverse panel of alkyl pyrophosphates could be synthesized from the respective alkyl alcohol: natural ones (IPP (**16**), DMAPP (**17**), and GPP (**3**)), other allylic pyrophosphates (**4**, **10**, **19**, and **23**), propargyl (**12**), homoallylic (**2**, **15**), and ones which are essentially alkyl because of how far removed their double or triple bond is from the pyrophosphate (**9**, **13**, and **18**).

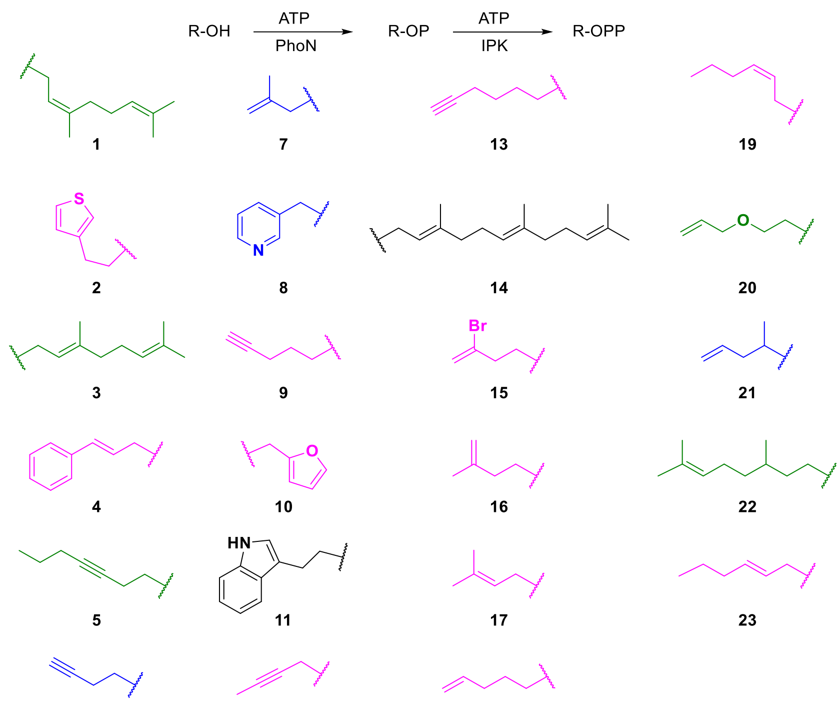

Figure 2.7. Potential pyrophosphates synthesized from alcohols by sequential phosphorylation. Green: utilized by PhoN; Blue: utilized by IPK; Magenta: utilized by both; Black: utilized by neither.

2.2.2. Probing the substrate promiscuity of FgaPT2

FgaPT2 was cloned, expressed in *E. coli* with an N-terminal His_6 tag, and purified using IMAC. Purified FgaPT2 was tested with a panel of synthesized alkyl pyrophosphates and L-tryptophan. The product mixtures were analyzed by HPLC and low-resolution LC-MS or LR-LC-MS. The substrate (Trp) and product peak areas were determined by high performance liquid chromatography (HPLC) at a detection wavelength of 269 nm, and the percent conversion was calculated (**Figure 2.8**). Product formation was confirmed by detection of expected mass ion in LR-LC-MS (data in Appendix I). The panel of molecules tested are the pyrophosphate counterparts of the alcohols and monophosphates tested previously. This panel could test if the allylic pyrophosphate is required for reaction, if propargylic or homoprogarylic pyrophosphates could also be utilized, and if there are limitations on length or bulk of the alkyl pyrophosphate substrate outside of a preference for DMAPP or GPP.

When these reactions were first tested, the only ones quantifiable by HPLC were smaller allylic pyrophosphates (**10**, **17**, **19**, and **23**) which is consistent with what has been previously reported for FgaPT2 and similar PTs. In addition, all the reactions were also analyzed using HR-LC-MS, which revealed that mass ions consistent with the expected product were also detected in instances where the pyrophosphate was not allylic (**6**, **12**, and **13** for example; data in Appendix I), contrary to expectations. Because of this, the sample-prep method was optimized so that the sample would be more concentrated prior to HPLC analysis. This provided detection and quantification at a few more orders of magnitude lower substrate conversion via HPLC (**Figure 2.9**).

With the new sample prep, the specificity of FgaPT2 with various alkyl pyrophosphates was confirmed to be surprisingly broad, contrary to expectations. The most active substrates were still allylic pyrophosphates (**4**, **10**, **16**, **17**, **19**, and **23**). However, “propargyl” (**12**), homopropargyl (**6**), and essentially alkyl pyrophosphates (**13**) were also utilized by FgaPT2 at low but replicable levels, and that activity has not been reported prior to this work.

A)

B)

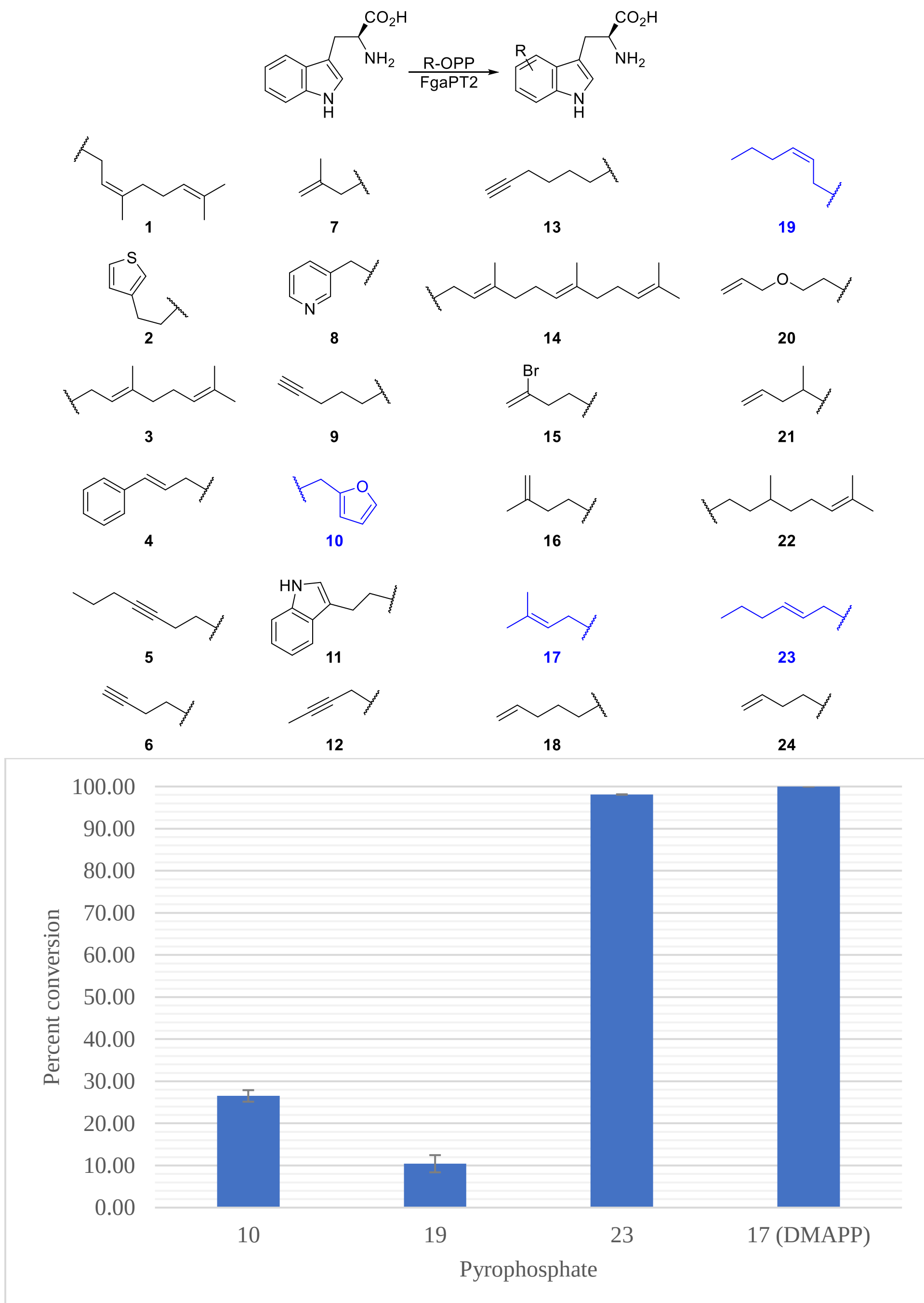

Figure 2.8. FgaPT2 *in vitro* activity. A) Pyrophosphate assays with FgaPT2. Blue indicates detection by HPLC and confirmation by LR-LC-MS. B) initial determined conversions with error bars as the standard deviation of duplicate reactions.

A)

B)

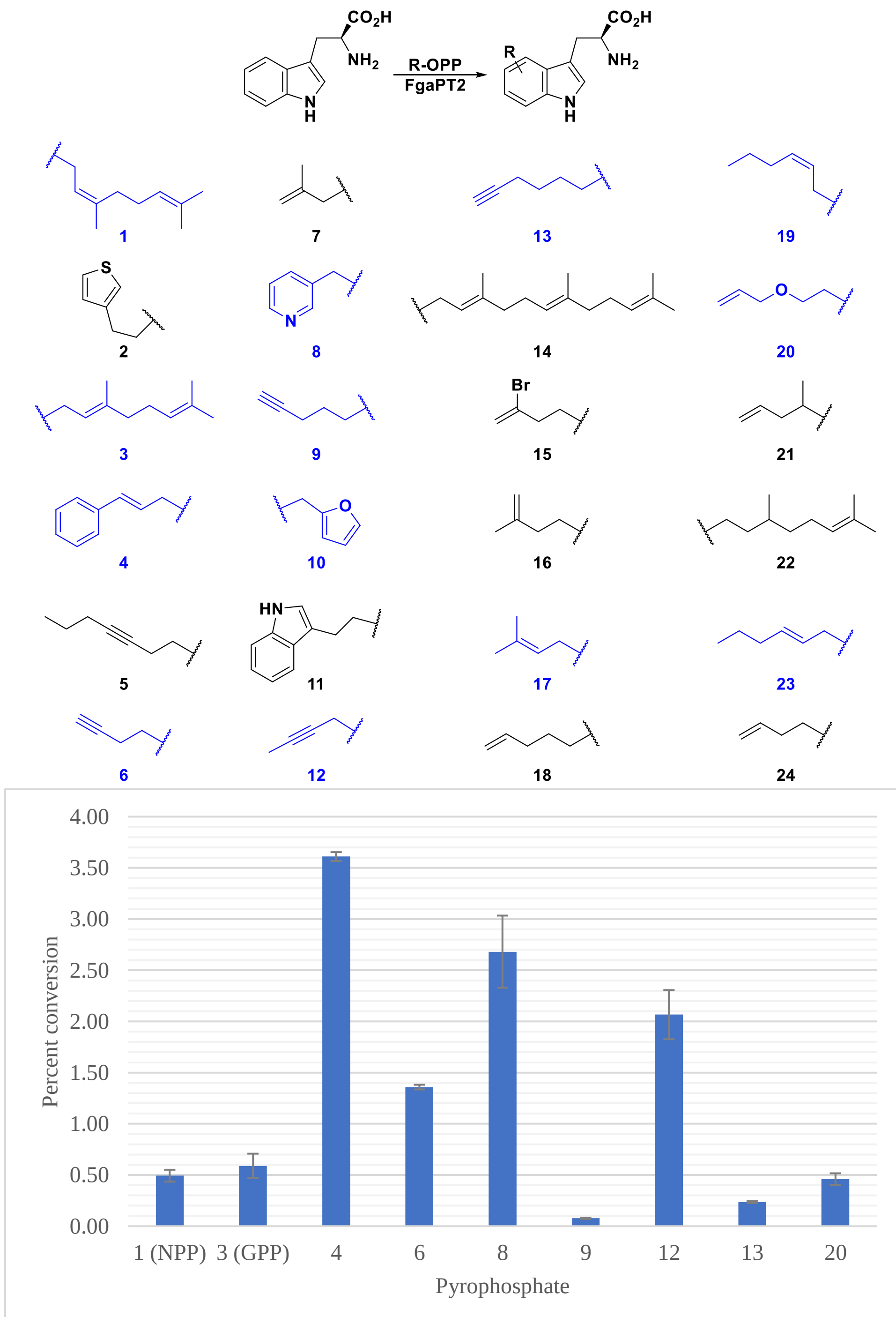

Figure 2.9. FgaPT2 *in vitro* activity analyzed with concentrated analytes. A) Pyrophosphate assays with FgaPT2. Blue indicates detection by HPLC and confirmation by LR-LC-MS. B) conversions detected upon concentration of reaction sample before analysis. Error bars are the standard deviation of duplicates.

From the initial panel, several testable questions arose, and three series (**A-C**) of pyrophosphates were synthesized to address them (**Figure 2.10**). Series A aimed to determine if the difference in activity for **10** and **2** was the heteroatom, the substitution position on the heteroatomic ring, or the proximity to the pyrophosphate, one or two methylenes away in this case. For series B, the purpose was to determine preference for double-bond geometry, chain length, and proximity of double bond to pyrophosphate. Finally, series C is very similar to B but this time for alkynes, so determining preference for chain length and proximity of triple bond to pyrophosphates.

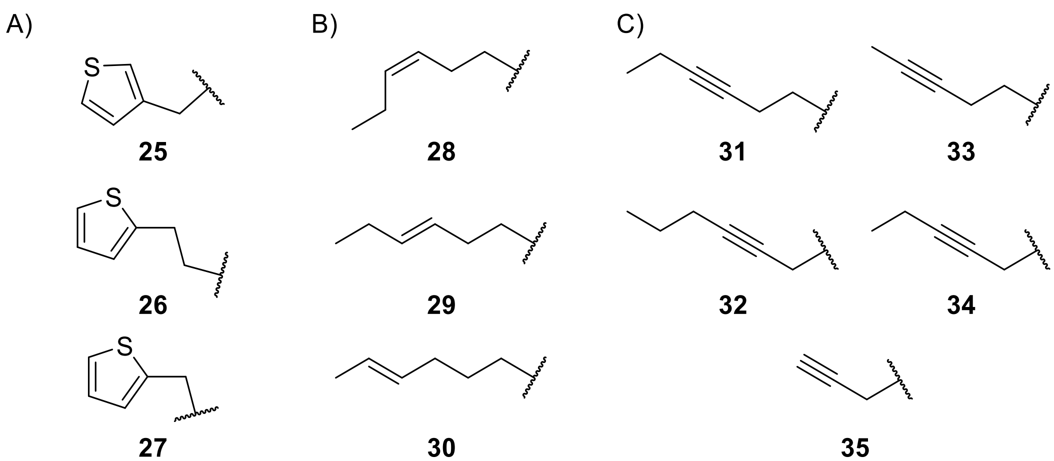

Figure 2.10. Extended pyrophosphate panel. A) thiophene series, B) alkene series, C) alkyne series.

For **10** vs. **2**, the thiophene-containing alcohols were cheaper than the furan counterparts, available in all variations desired for testing, and could be readily synthesized to pyrophosphates using known techniques, so they were chosen to compare to the furan (**10**, **Figure 2.11**). Reactions were setup as mentioned previously with synthesized alkyl pyrophosphates, purified enzyme, and L-Trp. In this case, product peaks were detected for **25** and **27** but not **26**. The results from this small panel suggest that the most important difference between **10** and **2** is proximity to the pyrophosphate. They also suggest there might be a preference for furan over thiophene (**10** vs. **27**) and for pyrophosphates at C-2 over C-3 (**25** vs. **27**).

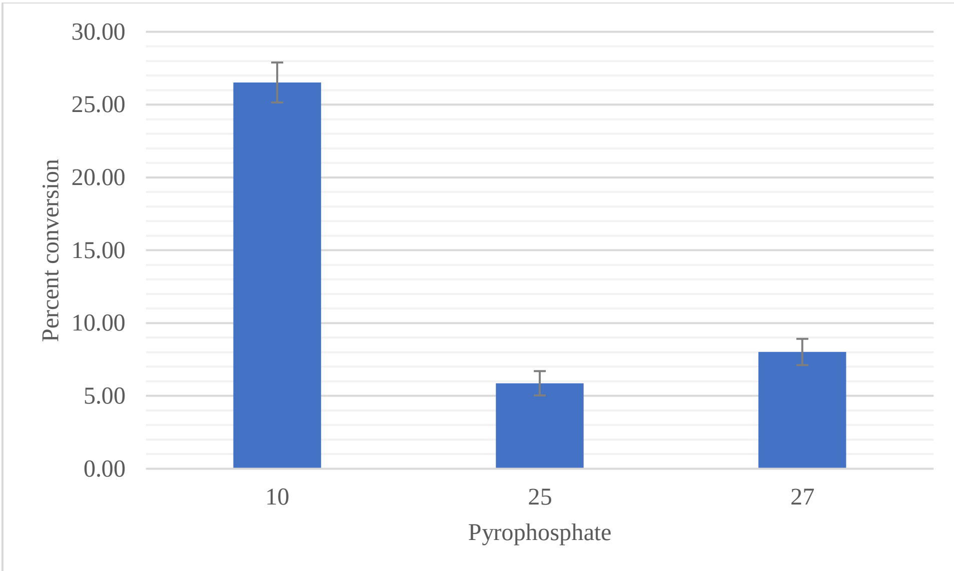

Figure 2.11. FgaPT2-catalyzed conversions with thiophene pyrophosphates compared to furfuryl pyrophosphate. Error bars represent the standard deviation of reactions in duplicate.

As mentioned above, the next two series were designed to answer several of the questions around FgaPT2 substrate limitations for linear alkene and alkynes. The alcohol versions of the hexenes were commercially available in homoallylic *cis* and *trans* forms, as was hex-4-ene in *trans* confirmation. Also the alcohol versions of propargyl and "propargyl" and "homopropargyl" hexyne and pentyne were commercially available. Once again, these alcohols could be readily converted to pyrophosphates using known synthetic methods.

For the series of alkenes, the reactions were setup and analyzed in the manner previously stated. Focusing on the hexenyl pyrophosphates tested because they were the only alkenic straight-chain pyrophosphates utilized by the enzyme, FgaPT2 was dramatically more active with the allylic pyrophosphates (**19** and **23**), and the only other detected product for this series was with *trans* homoallylic pyrophosphate (**29**) at a very low percent conversion (**Figure 2.12**).

Allylic butenyl, pentenyl, or heptenyl pyrophosphate were not tested, so a strong statement cannot be made about the length requirement for these substrates. However, there appears to be a strong preference for *trans* over *cis* (**19** vs. **23**) and also allylic over homoallylic (**23** vs. **29**).

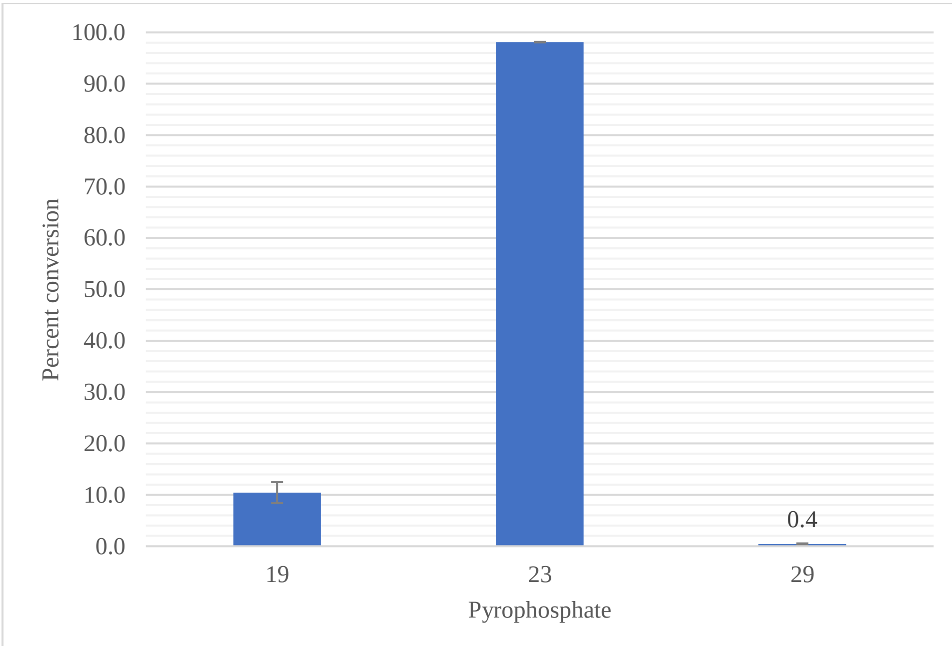

Figure 2.12. FgaPT2-catalyzed conversions with alkene series. Bars are labeled with percent conversion at the top, and the error bars represent the standard deviation of duplicate reactions. Bar is labeled with percent conversion for 29 for clarity.

For the series of alkynes, the reactions were setup and analyzed in the manner previously stated (**Figure 2.13**). The first part of this discussion will be divided into chain lengths—propargyl, butynyl, pentynyl, hexynyl, and heptynyl—to frame the discussion of potential chain length limitations. FgaPT2 was most active with the butynyl (**6** and **12**), followed by the pentynyl (**9**, **33**, **34**), and hexynyl (**13** and **32**) with propargyl (**35**) and heptynyl (**5**) not detected. The next part of the discussion will continue to divide into length of carbon chain but will focus on number of methylenes between triple bond and pyrophosphate: one, two, three, or four. There appears to be a preference for one methylene away over two, and there is lower activity the more methylenes away (**6** vs. **12** or **9** vs. **33** and **34**). However, there are a couple of examples where that trend does not follow: **33** (3 methylenes) had a higher conversion than **34** (2 methylenes); **13** (4 methylenes) had a higher conversion than **32** (1 methylene). This suggests there are cases when chain length and triple-bond proximity to pyrophosphate are not the only determinants of reactivity.

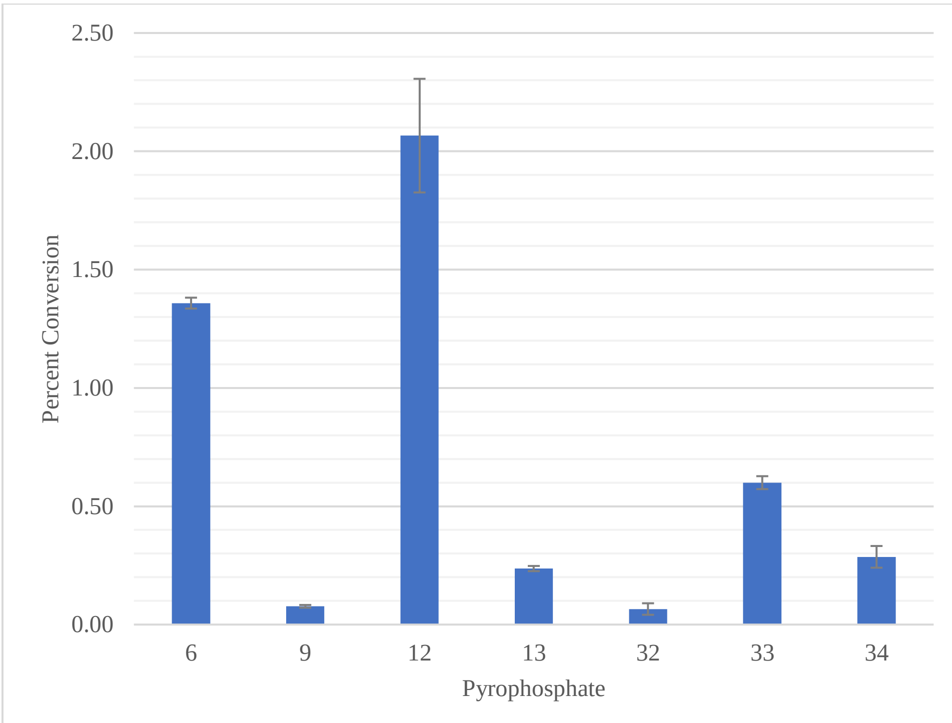

Figure 2.13. FgaPT2-catalyzed conversion with alkyne series. Error bars represent standard deviation of duplicates.

Data suggests multiple products for several of the FgaPT2 reactions. Reactions with **10**, **17**, **19**, **23**, **25**, and **27** have multiple product peaks in their HPLC chromatograms. MS data indicated that these are not regioisomers of the monoalkylated product but were di- and tri-alkylated product in addition to the monoalkylated, with the exception of reactions with **25** which contain mass ions consistent with the expected monoalkylated product and no di- or tri-alkylated. LR-LC-MS chromatograms for reactions with **1**, **3**, **4**, **10**, **17**, **19**, **23**, and **27** have mass ions consistent with multi-alkylated products. Multiprenylated products and regioisomers have been reported before in literature for several PTs.[76]

While surprising, the use of non-allylic substrates (albeit poorly) by FgaPT2 is supported by its structure and mechanism. FgaPT2 is part of a family of barrel-shaped enzymes whereby catalysis largely depends on positioning the substrates so the reacting carbons are positioned optimally for bond formation. The active-site residues serve to support catalysis with H-bonding, pi stacking, and hydrophobic and electrostatic interactions. The only residue implicated in reacting with the substrate is the base which deprotonates the arenium intermediate to rearomatize it. The working hypothesis from the FgaPT2 specificity studies is that the prenylation can proceed by either an associative or dissociative mechanism and which takes place is more dependent upon its ability to stabilize the (partial) positive charge of the intermediate. When the pyrophosphate is allylic, the carbocation produced by dissociation of the pyrophosphate could be stabilized through resonance. However, in cases where the carbocation could not be stabilized through resonance, the nucleophile attacks the carbon as the pyrophosphate leaves. This could explain why the enzyme is more active with allylic substrates and is less active with substrates as the pyrophosphate moved a methylene away, i.e. non-allylic. This hypothesis is being further investigated with isotope-labeling experiments and by structural determination of products to determine the nature of prenylation. A potential enzyme engineering method to further investigate this idea could be to modify the prenyl binding pocket to elongate the C-O bond and weaken it; this could be achieved by altering positive residues which hold the pyrophosphate or the hydrophobic ones that position the prenyl group so that they are a little farther away from each other than before. This could be used to increase activity with the non-allylic substrates.

A few of the FgaPT2 reactions with higher conversion have been successfully scaled up for structural determination of the isolated major product (**6**, **10**, **23**, and **27**). As of now, the determinations are tentative because they are only 1D ^{1}H-NMR experiments. Gratifyingly they are consistent with similar molecules from FgaPT2 reactions characterized by Shu-Ming Li's lab.[81] Focusing on the indole H's to determine its substitution, for **6** (**Figure 2.14**) and **23** (**Figure 2.14**) the splitting pattern and chemical shift suggest substitution at C5 or C6, and for **10** (**Figure 2.16**) and **27** (**Figure 2.17**), C4 or C7. Previously reported reaction products with FgaPT2 and non-natural pyrophosphates showed substitution at either C4 or C5 of the indole, so products with **6** and **23** are likely substituted at C5 and with **10** and **27**, at C4, but this will have to be confirmed with further NMR experiments. Confirming the structure of the prenyl moiety has been more difficult (especially for **6** and **23**) because many of its protons have expected chemical shifts which overlap with contaminants in the late alkyl and vinyl regions of the NMR. For **10** and **27**, the nature of prenylation could be more easily determined with more aromatic protons, and their splitting suggests "normal" prenylation with the carbon previously attached to the pyrophosphate forming the new bond to the indole acceptor because the splitting pattern and chemical shifts are consistent with substitution at C2 of the furan or thiophene like in the ^{1}H-NMR of the alkyl pyrophosphate starting material. Interestingly, there were also other less abundant peaks in the aromatic region for **10** and **27**, so there is potential for products other than the major that coeluted with the major in the purification. This will have to be determined by further optimization of the purification method.

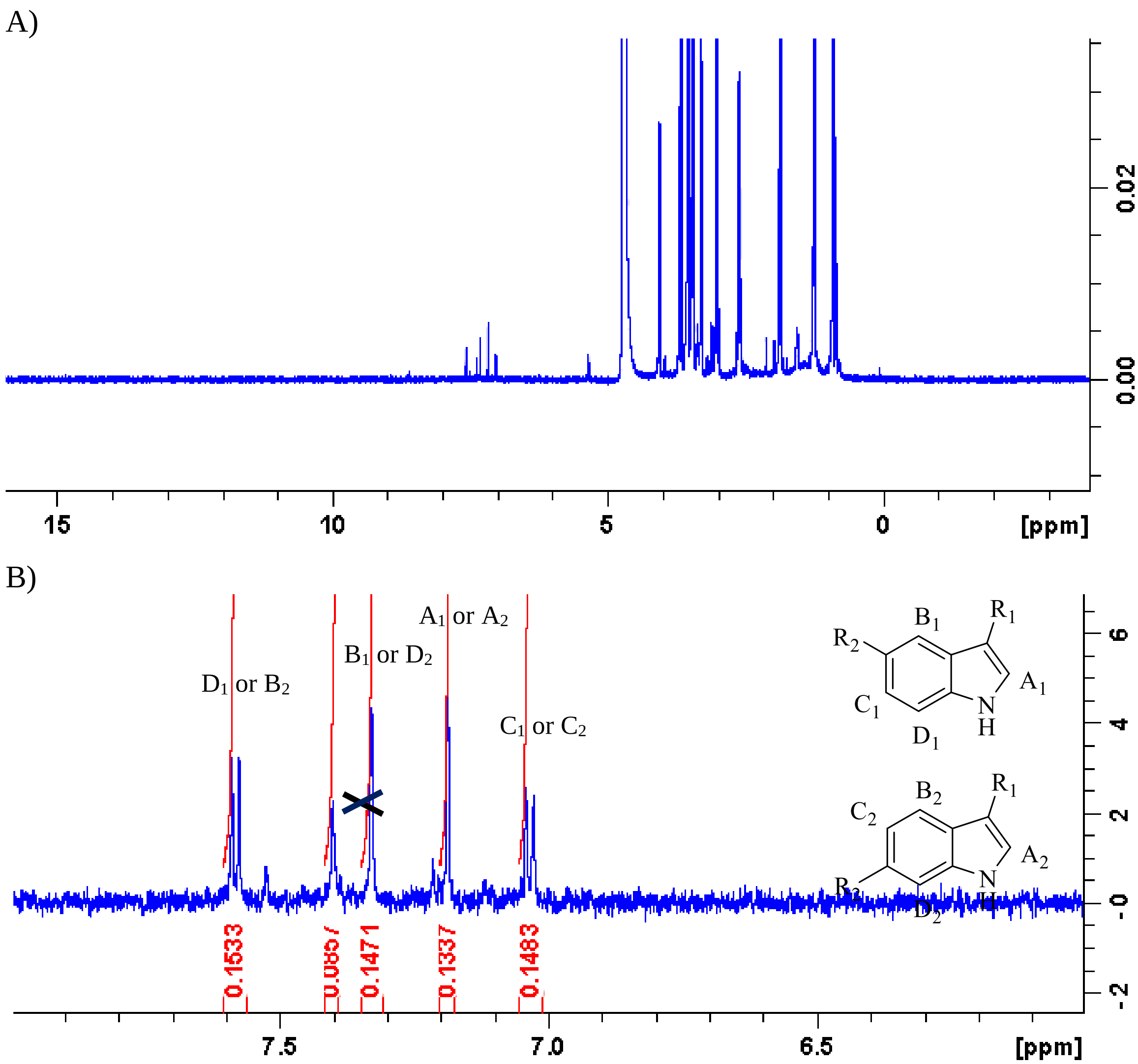

Figure 2.14. ^{1}H-NMR at 600 MHz in D_2O of the purified product with pyrophosphate **6**. A) Full spectrum, B) aromatic region of spectrum with integration of peaks and peak assignment. “x” indicates a peak that was ignored for analysis because it did not integrate to roughly the same peak area as the others, and therefore was assumed to be a contaminant.

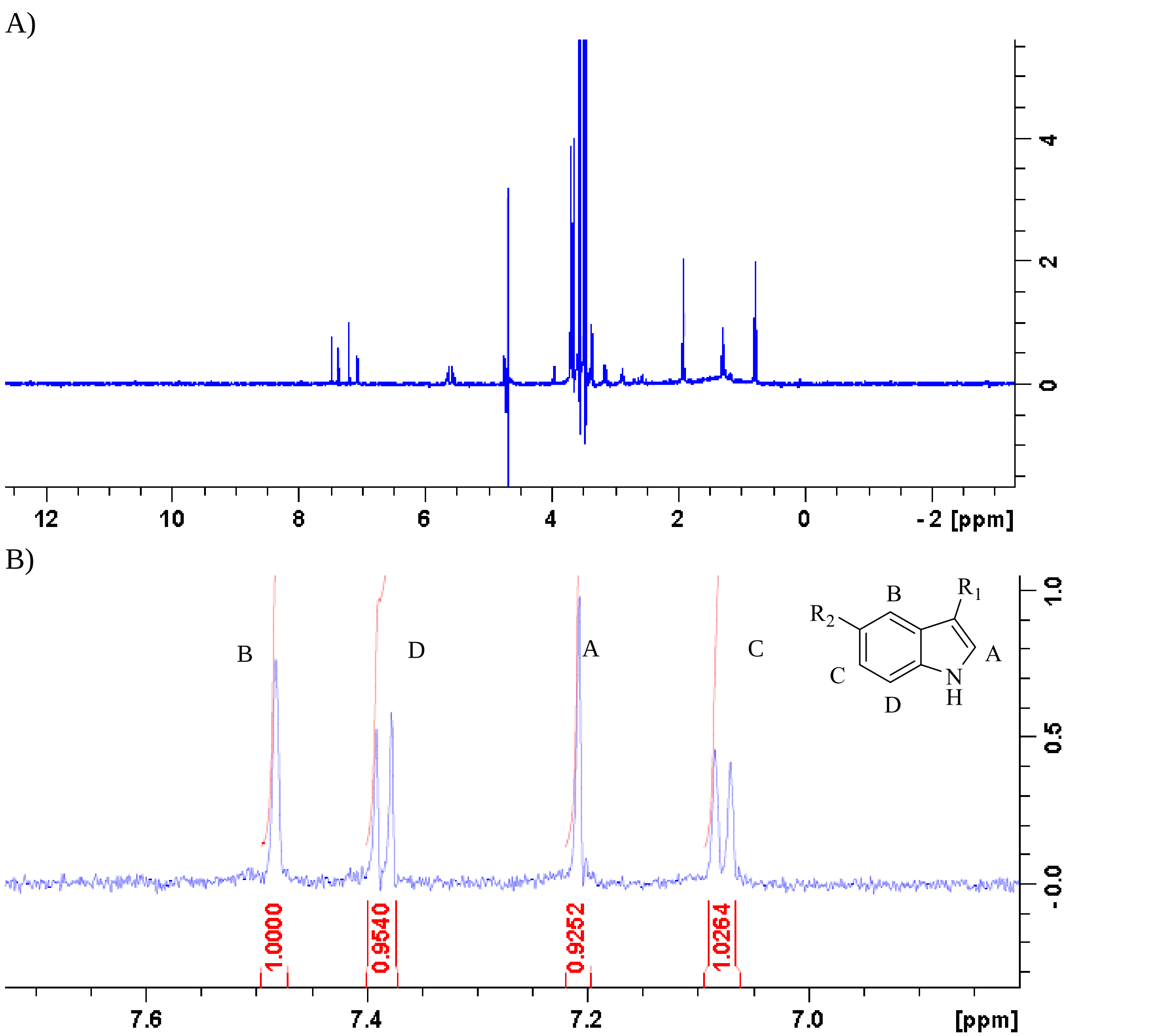

Figure 2.15. ^{1}H-NMR at 600 MHz in D_2O of the purified product with pyrophosphate **23**. A) Full spectrum, B) aromatic region of spectrum with integration of peaks and peak assignment.

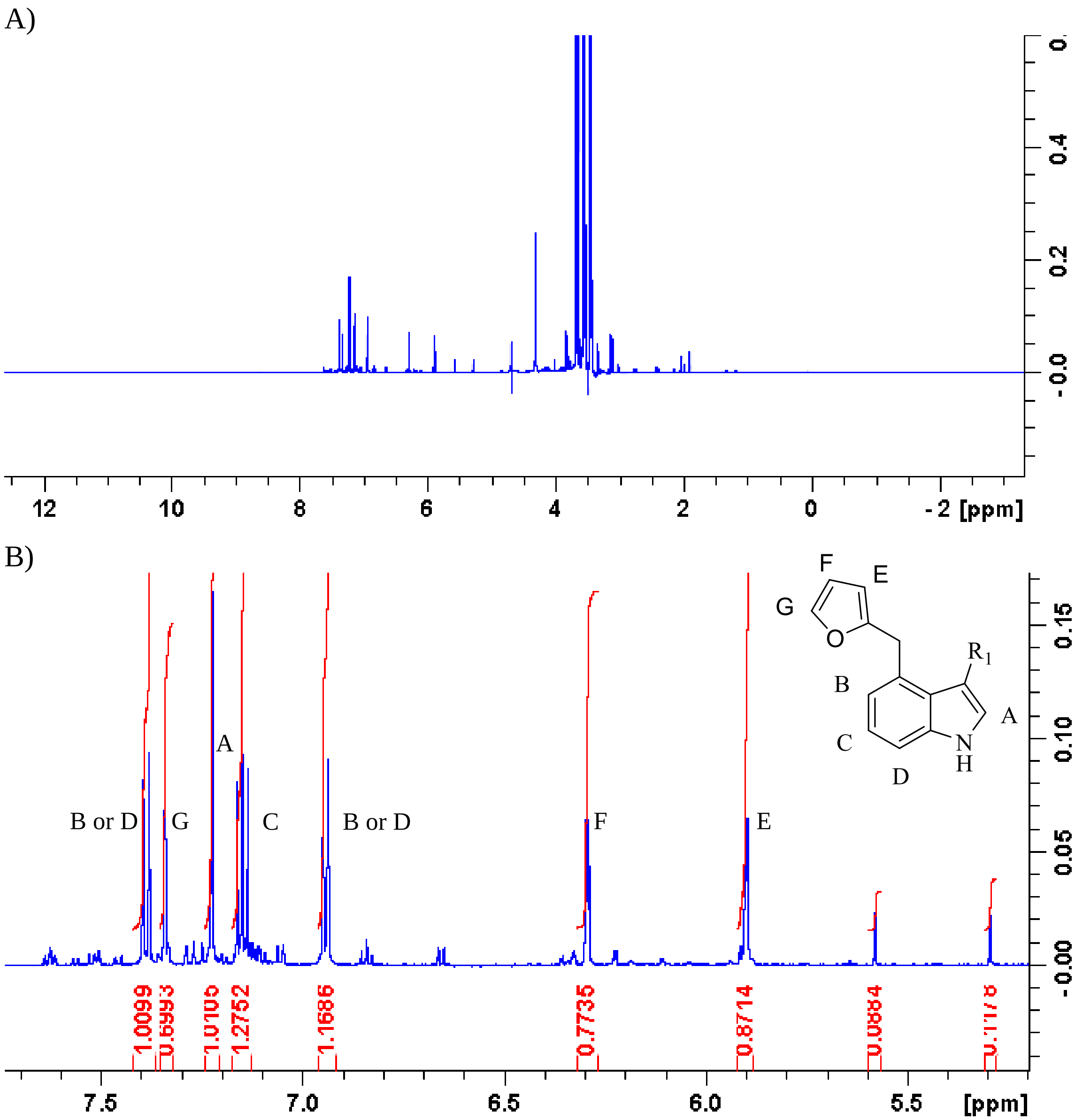

Figure 2.16. ^{1}H-NMR at 600 MHz in D_2O of the purified product with pyrophosphate **10**. A) Full spectrum, B) aromatic region of spectrum with integration of peaks and peak assignment.

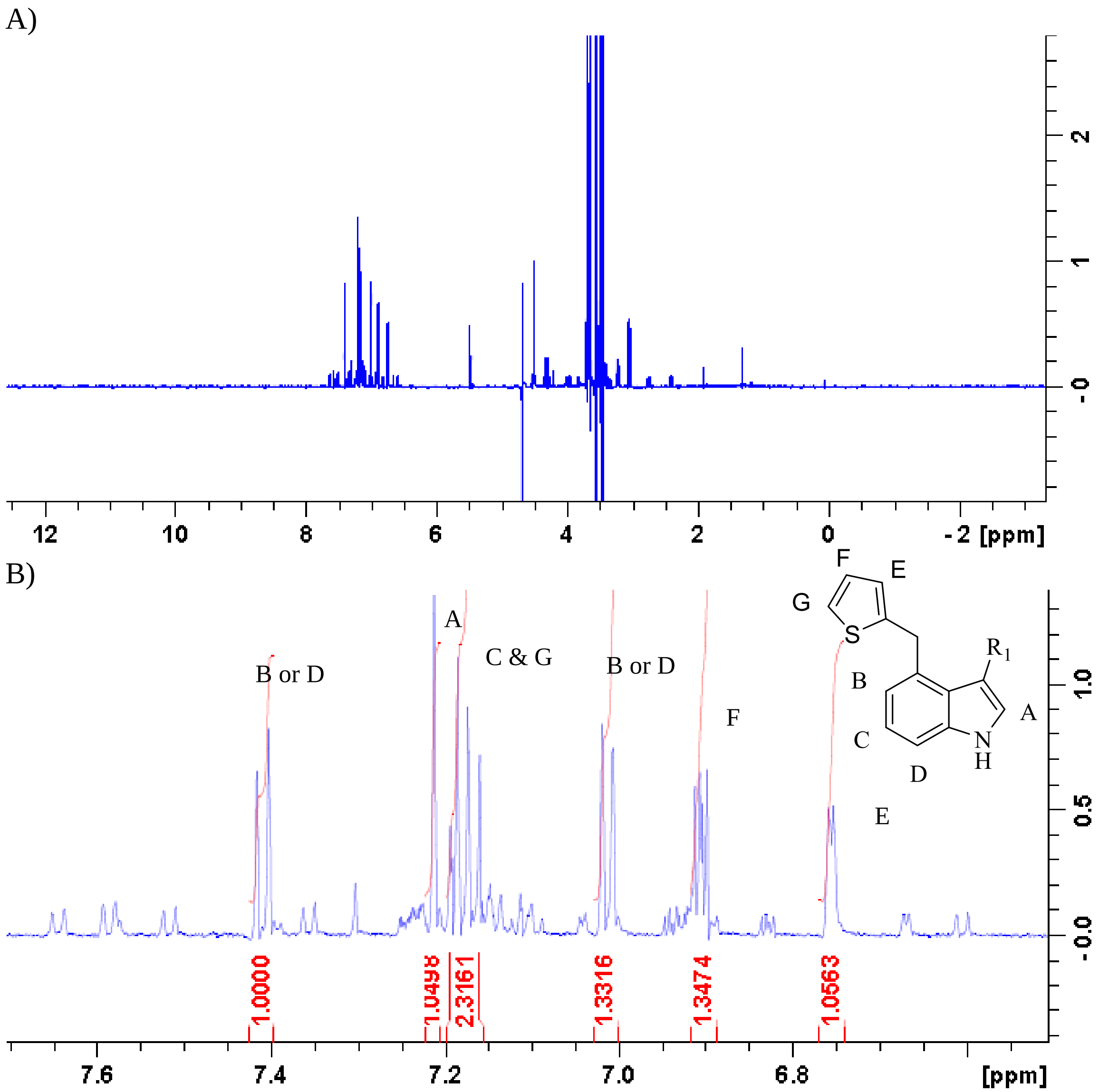

Figure 2.17. ^{1}H-NMR at 600 MHz in D_2O of the purified product with pyrophosphate **27**. A) Full spectrum, B) aromatic region of spectrum with integration of peaks and peak assignment.

In an effort to infer the alkylation position of the prenylation reactions, FgaPT2 reactions were setup with mono-substituted tryptophans methylated at positions 4, 5, 6, or 7 of the indole, using pyrophosphates which were most active with FgaPT2: **10**, **17**, **19**, and **23** (MS data in Appendix I). Product peak height in the MS chromatogram decreased dramatically as the methyl moved toward the natural prenylation position (activity: Trp >> 7-Me-Trp > 6-Me-Trp, 5-Me-Trp > 4-Me-Trp), suggesting that these prenylations were occurring at the previously reported 4 and/or 5 position of the indole, and the activity with even 7-Me-Trp was very low compared to Trp. This experiment was not without its limitations because substituted tryptophans were reported to have much lower activity with FgaPT2 by Shu-Ming Li's lab, proposed to be a result of the difference in its ability to bind the substituted substrate.[121]

2.3. Conclusion

Combining the *in vitro* promiscuity of PhoN and IPK (or previously studied mutants of IPK), a panel of natural and non-natural pyrophosphates could be synthesized enzymatically. While this could potentially be used as a shortcut to supplement natural production of terpenes, coupling these two enzymes provides a panel of pyrophosphates that could be used to produce new terpenes in organisms or to study the enzymes that make them. While there has been so much work on enzymatic synthesis of terpenes, it has been limited to natural starter and extender units (DMAPP and IPP), so there is still so much left to know. With FgaPT2 for instance, tryptophan was alkylated with a few unexpected alkyl pyrophosphates which were not allylic and a few non-natural allylic ones. The results herein suggest terpene biosynthesis needs to be further interrogated by testing other classes of aromatic prenyltransferases, prenylelongases, protein prenyltransferases, and terpene cyclases with non-natural alkyl pyrophosphates to determine which the substrate modifications that could be tolerated.

2.4. Methods

2.4.1. Plasmid construction for PhoN and FgaPT2

The codon-optimized sequence of *phoN*-Sf for expression in *E. coli* was synthesized by IDT (GI number 695261922). *PhoN* was PCR amplified using the following primers:

PhoN_BamHI_FWD, CTAGGATCCGATGAAACGTCAGCTGTT; and PhoN_NotI_Rev, CTAGGCGGCCGCTTATTTTTTCTGATTATT. The 50-µL PCR contained 5x Phire II buffer, 0.2 mM dNTPs, 0.5 µM of each primer, 1 µL Phire II DNA polymerase, and 20 ng of template DNA. The cycling parameters used were as follows: 1) 98 °C, 30 s; 2) 98 °C, 5 s; 3) 66 °C, 15 s; 4) 72 °C, 20 s; 5) repeat steps 2-4 thirty-four times; 6) 72 °C, 1 min; 7) 4 °C, hold. Following amplification, *phoN* was gel purified, restriction digested with *Bam*HI and *Not*I, and ligated into MCS1 of IPK-pETDuet and empty pETDuet. The plasmid was transformed into DH5α chemically competent *E. coli* and plated on an LB agar plate containing 100 µg/mL of ampicillin. The resultant colonies were sequenced to determine the presence of *phoN* using the primer pET-Upstream (ATGCGTCCGGCGTAGA).

Codon-optimized sequences of *fgaPT2* was synthesized by IDT (Genbank accession #: AAX08549.1). *FgaPT2* was PCR amplified by the following primers with the cut site underlined: FgaPT2_NdeI_FWD, ATACATATGAAAGCCGCAAACG; FgaPT2_HindIII_REV, TATAAGCTTATGCAGGCCGC. The reaction for amplification of FgaPT2 contained 5x Phire buffer, 0.2 mM dNTPs, 0.25 µM of each primer, 1 µL Phire II DNA polymerase, and 1 µL template DNA in 50 µL. The cycling parameters used for each were as follows: 1) 98 °C, 30 s; 2) 98 °C, 5 s; 3) 64 °C, 15 s; 4) 72 °C, 20 s; 5) repeat steps 2-4 thirty-four times; 6) 72 °C, 1 min; 7) 4 °C, hold. Following PCR amplification, the gene was restriction digested with *Hin*dIII and *Nde*I and ligated into pET-28a. The plasmid was then transformed into DH5α chemically competent *E. coli* and plated on LB agar plates containing 50 µg/mL of kanamycin. The resultant colonies were sequenced to determine the presence of *fgaPT2* using a primer corresponding to the T7 promoter.

2.4.2. PhoN expression, purification, and quantification

PhoN was transformed into chemically competent *E. coli* BL21(DE3) for protein expression. An overnight culture in 3 mL of LB broth of PhoN-pETDuet containing 100 μg/mL of ampicillin was grown at 37 °C with shaking at 270 rpm. A culture in 1 L of LB broth was inoculated with 1 mL of the overnight culture and grown at 37 °C with shaking at 250 rpm to an OD_{600} of 0.6. Once the desired OD_{600} was reached, the culture was cooled to 18 °C, and protein expression was induced by the addition of IPTG to an overall concentration of 1 mM. The culture was incubated at 18 °C with shaking at 200 rpm for an additional 16-20 h. The culture was spun down into a pellet which was stored at -20 °C until purification.

The cell pellets were thawed and resuspended in 20 mL of lysis buffer (250 mM sodium chloride, 50 mM sodium phosphate, 10 mM imidazole, pH 7.9). The cells were lysed by sonication and spun down. The cell lysate was then separated from the insoluble cell debris, and the His_6-tagged proteins were purified from the lysate using Ni beads on agarose using a low-imidazole buffer (50 mM Tris, 300 mM NaCl, 20 mM imidazole, pH 8.0) as the wash buffer and a high-imidazole buffer (50 mM Tris, 300 mM NaCl, 200 mM imidazole, pH 8.0) to isolate the protein. Then a 10-kDa spin filter was used to concentrate and buffer exchange the protein into storage buffer (50 mM Tris-HCl, 500 mM NaCl, 20% glycerol, pH 7.4). The concentration of protein was determined using a Bradford assay, and small aliquots of protein were stored at -80 °C until needed.

2.4.3 *In vitro* PhoN reactions

The *in vitro* reactions were run at pH 5.2 using a 5x 500-mM sodium acetate buffer and a panel of alcohols and phosphate donors. The 1reactions were run with 100 mM alcohol substrate, 50 mM ATP, and 2 µg of PhoN-Sf in 100 µL. The reaction was incubated at room temperature overnight and then quenched with an equal volume of cold methanol. The products were initially analyzed via low-resolution LC-MS (Shimadzu LC-MS 2020 with Kinetex 2.6 µm C18 50 x 2.10 mm; low-mass method, 3.5-min gradient of 0-100% acetonitrile with 0.1% formic acid), but then were further investigated and quantified using an alkyl-monophosphate internal standard of known concentration (either DMAP or cinnamyl pyrophosphate) using high-resolution LC-MS (*Thermo Scientific Dionex UltiMate 3000* LC system coupled to *Thermo Fisher Scientific Exactive Plus MS*; reverse phase C18 column (50 mm x 2.1 mm, 175 Å pore size, 1.9 µm particle size) at 35 °C; 0.500 mL/min with solvent A (H_2O with 0.1% formic acid) and solvent B (ACN with 0.1% formic acid); gradient of 5 % to 95 % B over 5 min followed by 3 min at 5 % B).

The internal standards were prepared with DMAP and cinnamyl-monophosphate synthesized by Sean Lund at a known stock concentration which was then serially diluted 1:1 to have concentrations from 0.315 mM to 0.0394 mM; this range was determined through previous experiments which determined the linear range of detection for cinnamyl monophosphate and DMAP. The standards and reactions were added together 1:1 and analyzed via HR-LC-MS using the same parameters outlined above; some reactions were further diluted so that the desired monophosphate detected was within the linear range as determined by the peak area of the extracted-ion chromatogram or XIC. Then a graph of the concentration vs. average XIC of each concentration of each monophosphate in triplicate was constructed, and the line of best fit used to convert XICs of the product monophosphates to concentration, correcting for any dilution required for analysis (calibration curve in Appendix I). The reactions were performed in duplicate, and their reported yields are the average of the calculated concentrations.

2.4.4. Pyrophosphate synthesis and characterization

Alkyl pyrophosphates were synthesized by a previously reported method for phosphorylating alcohols to mono-, di-, tri-, etc. phosphates (Reference), by either Sean Lund or the author, Rachael Hall. Briefly, 4 mmol alcohol were dissolved in 10 mL trichloroacetonitrile in a 50 mL plastic tube. The alcohol solution was treated with three 10-mL aliquots of freshly made triethylammonium phosphate (TEAP) solution (19 mL solution B, 12.5 mL solution A; solution B: 110 mL Et_3N, 100 mL MeCN; solution A: 25 mL H_3PO_4, 94 mL MeCN) with a 5-min incubation at 37 °C after each addition. Then 10 mL column mobile phase (6:2.5:0.5 IPA/NH_4OH/H_2O) were added to crash out some of the material that crashes upon column loading and would clog the column, and then the reaction was briefly spun down in a centrifuge. The supernatant was loaded onto a silica column with the above-mentioned mobile phase, and fractions analyzed via LR-LC-MS. Fractions containing the pyrophosphate were concentrated, lyophilized, and stored long-term as a solid and short-term as at 10 or 25 mM in water, both at -20 °C.

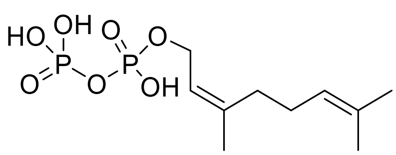

Neryl pyrophosphate (**1**); ^{1}H-NMR (D_2O, 600 MHz): 1.56 (s, 3H), 1.63 (s, 3H), 1.69 (s, 3H), 2.09 (m, 4H), 4.38 (t, 2H), 5.13 (t, 1H), 5.41 (t, 1H); ^{13}C-NMR (D_2O, 150 MHz): 16.95, 22.57, 24.82, 25.97, 31.21, 62.41 (d, *J*=5.86), 120.75 (d, *J*=8.68), 123.93, 133.92, 142.75; LR-LC-MS: $[M-H]^-$ = $[C_{10}H_{19}O_7P_2]^-$, calculated $[M-H]^-$ 313.05, experimental $[M-H]^-$ 312.85

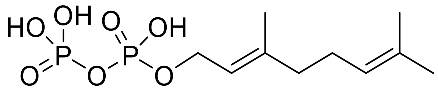

Geranyl pyrophosphate (**3**); ^{1}H-NMR (D_2O, 600 MHz): 1.54 (s, 3H), 1.60 (s, 3H), 1.64 (s, 3H), 2.02 (t, 2H), 2.07 (q, 2H), 4.39 (t, 2H), 5.14 (t, 1H), 5.40 (t, 1H); ^{13}C-NMR (D_2O, 150 MHz): 15.54 (d, *J*=4.31), 16.92, 62.69 (d, *J*=5.12), 119.76 (d, *J*=9.38), 124.11, 133.70, 142.78; LR-LC-MS: $[M\text{-}H]^-$ = $[C_{10}H_{19}O_7P_2]^-$, calculated $[M\text{-}H]^-$ 313.05, experimental $[M\text{-}H]^-$ 312.85

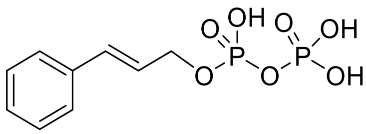

Pyrophosphate **4**; ^{1}H-NMR (D_2O, 600 MHz): 4.56 (m, 2H), 6.40 (dt; *J*=15.7, 6.2; 1H), 6.69 (dd; *J*=15.71, 5.4; 1H), 7.25 (t, *J*=7.4, 1H), 7.32 (t, *J*=7.4, 2H), 7.46 (d, *J*=7.4, 2H); ^{13}C-NMR (D_2O, 150 MHz): 66.49 (d, *J*=4.95), 125.88 (d, *J*=9.01), 126.62 (d, *J*=7.51), 128.05 (d, *J*=7.51), 132.06, 136.56 (d, *J*=9.01); LR-LC-MS: $[M\text{-}H]^-$ = $[C_9H_{11}O_7P_2]^-$, calculated $[M\text{-}H]^-$ 293.00, experimental $[M\text{-}H]^-$ 292.80

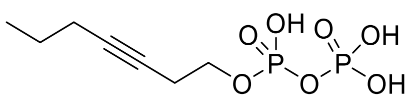

Pyrophosphate **5**; ^{1}H-NMR (D_2O, 600 MHz): 0.85 (t, 3H), 1.41 (m, 2H), 2.08 (t, 2H), 2.45 (t, 2H), 3.90 (q, 2H); ^{13}C-NMR (D_2O, 150 MHz): 12.74, 20.34 (d, *J*=7.58), 21.63, 64.49 (d, *J*=5.49), 77.41, 83.22; LR-LC-MS: $[M\text{-}H]^-$ = $[C_7H_{13}O_7P_2]^-$, calculated $[M\text{-}H]^-$ 271.00, experimental $[M\text{-}H]^-$ 270.85

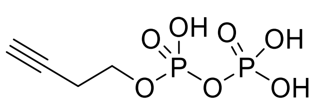

Pyrophosphate **6**; ^{1}H-NMR (D_2O, 600 MHz): 2.49 (m, 2H), 3.95 (m, 2H); ^{13}C-NMR (D_2O, 150 MHz): 20.09 (d, *J*=8.45), 63.70 (d, *J*=5.51), 70.40, 82.23; LR-LC-MS: $[M\text{-}H]^-$ = $[C_4H_7O_7P_2]^-$, calculated $[M\text{-}H]^-$ 228.95, experimental $[M\text{-}H]^-$ 228.90

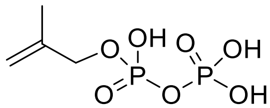

Pyrophosphate **7**; ^{1}H-NMR (D_2O, 600 MHz): 1.69 (s, 3H), 4.31 (d, 2H), 4.87 (s, 1H), 5.01 (s, 1H); ^{13}C-NMR (D_2O, 150 MHz): 18.30, 69.48 (d, *J*=4.99), 111.49, 142.23 (d, *J*=7.16); LR-LC-MS: $[M-H]^-$ = $[C_4H_9O_7P_2]^-$, calculated $[M-H]^-$ 231.00, experimental $[M-H]^-$ 230.90

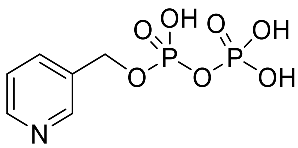

Pyrophosphate **8**; ^{1}H-NMR (D_2O, 600 MHz): 4.99 (d, *J*=7.14, 2H), 7.47 (dd; *J*=8.29, 5.53; 1H), 7.97 (d, *J*=7.37, 1H), 8.43 (d, *J*=5.53, 1H), 8.55 (br, 1H); ^{13}C-NMR (D_2O, 150 MHz): 64.91 (d, *J*=5.23), 124.50, 134.49 (d, *J*=7.66), 137.90, 146.65, 147.06; LR-LC-MS: $[M-H]^-$ = $[C_6H_8NO_7P_2]^-$, calculated $[M-H]^-$ 268.00, experimental $[M-H]^-$ 267.85

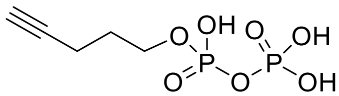

Pyrophosphate **9**; ^{1}H-NMR (D_2O, 600 MHz): 1.78 (m, 2H), 2.26 (m, 2H), 3.93 (q, 2H); ^{13}C-NMR (D_2O, 150 MHz): 14.21, 28.83 (d, *J*=6.87), 64.85 (d, *J*=5.38), 85.25; LR-LC-MS: $[M-H]^-$ = $[C_5H_9O_7P_2]^-$, calculated $[M-H]^-$ 243.00, experimental $[M-H]^-$ 242.90

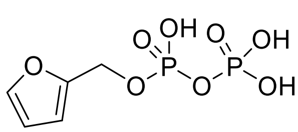

Pyrophosphate **10**; ^{1}H-NMR (D_2O, 600 MHz): 4.84 (d, 2H), 6.37 (t, 1H), 6.45 (d, 1H), 7.45 (s, 1H); ^{13}C-NMR (D_2O, 150 MHz): 59.53 (d, *J*=5.5), 109.89, 110.65, 143.55, 150.90 (d, *J*=8.3); LR-LC-MS: $[M-H]^-$ = $[C_5H_7O_8P_2]^-$, calculated $[M-H]^-$ 256.95, experimental $[M-H]^-$ 256.85

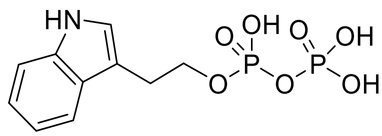

Pyrophosphate **11**; ^{1}H-NMR (D_2O, 600 MHz): 3.07 (t, 2H), 4.15 (q, *J*=7.19, 2H), 7.11 (t, *J*=8.14, 1H), 7.16 (t, *J*=7.49, 1H), 7.27 (s, 1H), 7.44 (d, *J*=8.14, 1H), 7.69 (d, *J*=7.49, 1H); ^{13}C-NMR (D_2O, 150 MHz): 25.88 (d, *J*=8.15), 66.00 (d, *J*=5.47), 111.18, 111.73, 118.74, 119.12, 121.80, 123.74, 126.91, 136.03; LR-LC-MS: $[M-H]^-$ = $[C_{10}H_{12}NO_7P_2]^-$, calculated $[M-H]^-$ 320.00, experimental $[M-H]^-$ 319.85

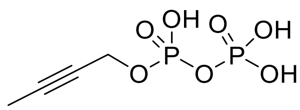

Pyrophosphate **12**; ^{1}H-NMR (D_2O, 600 MHz): 1.78 (m, 3H), 4.46 (m, 2H); ^{13}C-NMR (D_2O, 150 MHz): 2.61, 54.32 (d, *J*=4.9), 84.09; LR-LC-MS: $[M-H]^-$ = $[C_4H_7O_7P_2]^-$, calculated $[M-H]^-$ 228.95, experimental $[M-H]^-$ 228.85

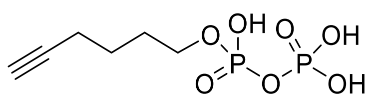

Pyrophosphate **13**; ^{1}H-NMR (D_2O, 600 MHz): 1.54 (m, 2H), 1.67 (m, 2H), 2.19 (td, 2H), 3.87 (q, 2H); ^{13}C-NMR (D_2O, 150 MHz): 17.27, 24.13, 28.99 (d, *J*=7.63), 65.68 (d, *J*=6.46), 69.20, 86.14; LR-LC-MS: $[M-H]^-$ = $[C_6H_{11}O_7P_2]^-$, calculated $[M-H]^-$ 257.00, experimental $[M-H]^-$ 256.85

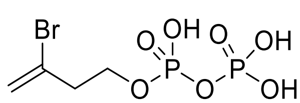

Pyrophosphate **15**; ^{1}H-NMR (D_2O, 600 MHz): 2.73 (t, 2H), 4.04 (m, 2H), 5.49 (d, 1H), 5.79 (s, 1H); ^{13}C-NMR (D_2O, 150 MHz): 41.63 (d, *J*=6.48), 63.40 (d, *J*=5.58), 119.19, 129.85; LR-LC-MS: $[M-H]^-$ = $[C_4H_8BrO_7P_2]^-$, calculated $[M-H]^-$ 308.90, 310.90; experimental $[M-H]^-$ 308.75, 310.75

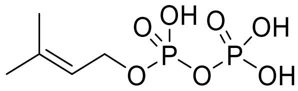

DMAPP (**17**); ^{1}H-NMR (D_2O, 600 MHz): 1.64 (s, 3H), 1.68 (s, 3H), 4.36 (t, *J*=6.81, 2H), 5.38 (tt; *J*=7.40, 1.48; 1H); ^{13}C-NMR (D_2O, 150 MHz): 17.22, 24.88, 62.60 (d, 5.97), 119. 72 (d, *J*=8.96), 139.93; LR-LC-MS: [M-H]$^-$ = [$C_5H_{11}O_7P_2$]$^-$, calculated [M-H]$^-$ 245.00, experimental [M-H]$^-$ 244.90

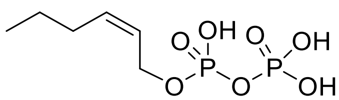

Pyrophosphate **19**; ^{1}H-NMR (D_2O, 600 MHz): 0.78 (t, 3H), 1.29 (m, 2), 2.01 (m, 1H), 4.46 (m, 2H), 5.55 (m, 2H), 5.61 (m, 1H); ^{13}C-NMR (D_2O, 150 MHz): 12.95, 22.08, 28.86, 61.88 (d, 5.86), 124.83 (d, *J*=6.57), 135.20 (d, *J*=6.57); LR-LC-MS: [M-H]$^-$ = [$C_6H_{13}O_7P_2$]$^-$, calculated [M-H]$^-$ 259.00, experimental [M-H]$^-$ 285.85

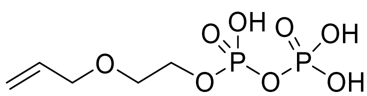

Pyrophosphate **20**; ^{1}H-NMR (D_2O, 600 MHz): 3.66 (t, 2H), 3.98 (m, 2H), 4.01 (d, 2H), 5.17 (d, *J*=10.53, 1H), 5.29 (dd; *J*=17.54, 1.75; 1H), 5.87 (m, 1H); ^{13}C-NMR (D_2O, 150 MHz): 64.72 (d, *J*=5.44), 69.41 (d, *J*=8.84), 71.73, 118.57, 133.56; LR-LC-MS: [M-H]$^-$ = [$C_5H_{11}O_8P_2$]$^-$, calculated [M-H]$^-$ 261.00, experimental [M-H]$^-$ 260.85

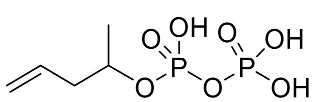

Pyrophosphate **21**; ^{1}H-NMR (D_2O, 600 MHz): 1.19 (d, 3H), 2.25 (m, 1H), 2.32 (m, 1H), 4.33 (m, 1H), 5.03 (dd; *J*=10.5, 1.2; 1H), 5.07 (dd; *J*=16.9, 2.1; 1H), 5.81 (m, 1H); ^{13}C-NMR (D_2O, 150 MHz): 20.31 (d, *J*=3.73), 41.24 (d, *J*=5.49), 73.39 (d, *J*=6.08), 117.47, 134.63; LR-LC-MS: [M-H]$^-$ = [$C_5H_{11}O_7P_2$]$^-$, calculated [M-H]$^-$ 245.00, experimental [M-H]$^-$ 244.85

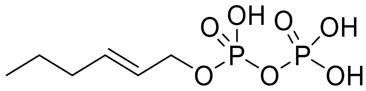

Pyrophosphate **23**; ^{1}H-NMR (D_2O, 600 MHz): 0.81 (t, 3H), 1.34 (m, 2H), 1.97, (m, 2H), 4.32 (m, 2H), 5.61 (m, 1H), 5.80 (m, 1H); ^{13}C-NMR (D_2O, 150 MHz): 12.96, 23.18 (d, *J*=4.47), 33.67, 69.56 (d, *J*=5.26), 125.42 (d, *J*=7.65), 136.10; LR-LC-MS: $[M-H]^-$ = $[C_6H_{13}O_7P_2]^-$, calculated $[M-H]^-$ 259.00, experimental $[M-H]^-$ 258.85

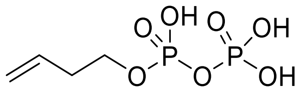

Pyrophosphate **24**; ^{1}H-NMR (D_2O, 600 MHz): 2.31 (q, 2H), 3.88 (q, 2H), 5.01 (d, *J*=10, 1H), 5.08 (d, *J*=17, 1H), 5.79 (m, 1H); ^{13}C-NMR (D_2O, 150 MHz): 34.24 (d, *J*=7.41), 65.35 (d, *J*=5.89), 116.82, 135.21; LR-LC-MS: $[M-H]^-$ = $[C_4H_9O_7P_2]^-$, calculated $[M-H]^-$ 231.00, experimental $[M-H]^-$ 230.90

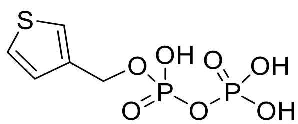

Pyrophosphate **25**; ^{1}H-NMR (D_2O, 600 MHz): 4.92 (d, 2H), 7.14 (d, 1H), 7.37 (t, 1H), 7.40 (br, 1H); ^{13}C-NMR (D_2O, 150 MHz): 63.04 (d, *J*=5.43), 123.98,126.73, 127.45, 138.52 (d, *J*=8.72); LR-LC-MS: $[M-H]^-$ = $[C_5H_7O_7P_2S]^-$, calculated $[M-H]^-$ 272.95, experimental $[M-H]^-$ 272.80

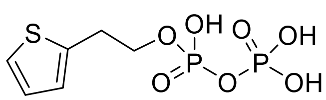

Pyrophosphate **26**; ^{1}H-NMR (D_2O, 600 MHz): 3.11 (t, 2H), 4.09 (q, 2H), 6.95 (m, 2H), 7.23 (dd, 1H); ^{13}C-NMR (D_2O, 150 MHz): 30.42 (d, *J*=7.82), 66.30 (d, *J*=5.55), 124.35, 125.72, 127.14, 141.11; LR-LC-MS: $[M-H]^-$ = $[C_6H_9O_7P_2S]^-$, calculated $[M-H]^-$ 286.95, experimental $[M-H]^-$ 286.85

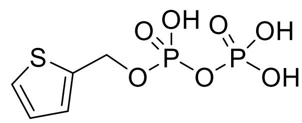

Pyrophosphate 2**7**; ^{1}H-NMR (D_2O, 600 MHz): 5.05 (d, J=7.19, 1H), 6.97 (dd; J=5.31,3.53; 1H), 7.11 (d, J=3.38, 1H), 7.38 (dd; J=4.66, 1.29; 2H); ^{13}C-NMR (D_2O, 150 MHz): 62.32 (d, J=5.36), 127.00, 127.11, 127.55, 139.84 (d, J=8.78); LR-LC-MS: $[M-H]^-$ = $[C_5H_7O_7P_2S]^-$, calculated $[M-H]^-$ 272.95, experimental $[M-H]^-$ 272.80

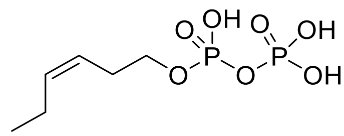

Pyrophosphate **28**; ^{1}H-NMR (D_2O, 600 MHz): 0.87 (t, 3H), 1.99 (m, 2H), 2.32 (q, 2H), 3.86 (q, 2H), 5.35 (m, 1H), 5.51 (m, 1H); ^{13}C-NMR (D_2O, 150 MHz): 13.54, 20.18, 28.02 (d, J=7.62), 65.81 (d, J=5.51), 124.65, 135.06; LR-LC-MS: $[M-H]^-$ = $[C_6H_{13}O_7P_2]^-$, calculated $[M-H]^-$ 259.00, experimental $[M-H]^-$ 258.80

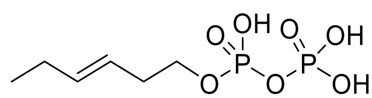

Pyrophosphate **29**; ^{1}H-NMR (D_2O, 600 MHz): 0.86 (t, 3H), 1.92 (m, 2H), 2.27 (q, 2H), 3.86 (q, 2H), 5.38 (m, 1H), 5.62 (m, 1H); ^{13}C-NMR (D_2O, 150 MHz):12.89, 25.06, 33.16 (d, J=7.66), 65.95 (d, J=7.10), 124.73, 135.48; LR-LC-MS: $[M-H]^-$ = $[C_6H_{13}O_7P_2]^-$, calculated $[M-H]^-$ 259.00, experimental $[M-H]^-$ 258.85

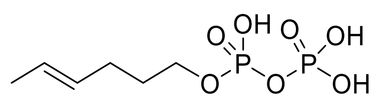

Pyrophosphate **30**; ^{1}H-NMR (D_2O, 600 MHz):1.57 (d, 3H), 1.61 (m, 2H), 1.99 (m, 2H), 3.86 (q, 2H), 5.49 (m, 2H); ^{13}C-NMR (D_2O, 150 MHz): 17.16, 28.00, 29.73 (d, J=7.82), 66.08 (d,

J=6.42), 126.13, 130.89; LR-LC-MS: $[M-H]^-$ = $[C_6H_{13}O_7P_2]^-$, calculated $[M-H]^-$ 259.00, experimental $[M-H]^-$ 258.85

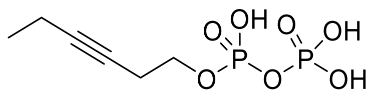

Pyrophosphate **31**; ^{1}H-NMR (D_2O, 600 MHz): 1.02 (t, 3H), 2.10 (m, 2H), 2.46 (m, 2H), 3.91 (q, 2H); ^{13}C-NMR (D_2O, 150 MHz): 11.65, 13.22, 20.35 (d, J=7.41), 64.21 (d, J=5.45), 76.77, 84.57; LR-LC-MS: $[M-H]^-$ = $[C_6H_{11}O_7P_2]^-$, calculated $[M-H]^-$ 257.00, experimental $[M-H]^-$ 256.85

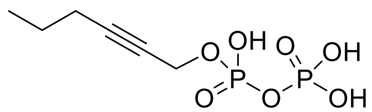

Pyrophosphate **32**; ^{1}H-NMR (D_2O, 600 MHz): 0.85 (t, 3H), 1.43 (m, 2H), 2.13 (tt; J=7.06, 2.45; 2H), 4.47 (dt; J=7.68, 2.31; 2H); ^{13}C-NMR (D_2O, 150 MHz): 12.75, 19.95, 21.30, 54.18 (d, J=4.61), 76.05 (d, J=10.68), 88.44; LR-LC-MS: $[M-H]^-$ = $[C_6H_{11}O_7P_2]^-$, calculated $[M-H]^-$ 257.00, experimental $[M-H]^-$ 256.85

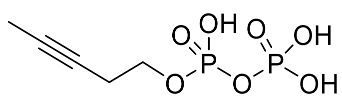

Pyrophosphate **33**; ^{1}H-NMR (D_2O, 600 MHz): 1.69 (t, 3H), 2.42 (m, 2H), 3.90 (q, 2H); ^{13}C-NMR (D_2O, 150 MHz): -0.004, 17.89 (d, J=8.01), 62.09 (d, J=6.65), 73.95, 76.12; LR-LC-MS: $[M-H]^-$ = $[C_5H_9O_7P_2]^-$, calculated $[M-H]^-$ 243.00, experimental $[M-H]^-$ 242.85

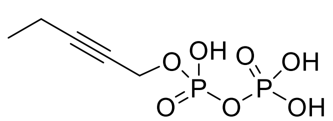

Pyrophosphate **34**; ^{1}H-NMR (D_2O, 600 MHz): 1.03 (t, 3H), 2.17 (qt; J=7.59, 2.31; 2H), 4.47 (dt; J=7.92, 2.31; 2H); ^{13}C-NMR (D_2O, 150 MHz): 11.72, 12.79, 54.36 (d, J=4.56), 75.06 (d,

J=11.24), 89.88; LR-LC-MS: $[M-H]^- = [C_5H_9O_7P_2]^-$, calculated $[M-H]^-$ 243.00, experimental $[M-H]^-$ 242.85

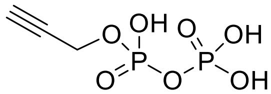

Pyrophosphate **35**; ^{1}H-NMR (D_2O, 600 MHz): 4.50 (dd, J=8.87, 2.22; 2H); ^{13}C-NMR (D_2O, 150 MHz): 53.65 (d, J=4.93), 75.38, 79.73 (d, 9.68); LR-LC-MS: $[M-H]^- = [C_3H_5O_7P_2]^-$, calculated $[M-H]^-$ 214.95, experimental $[M-H]^-$ 214.85

2.4.5. Expression and purification of FgaPT2

FgaPT2 was transformed into chemically competent Rossetta PLysS cells for expression. An overnight culture of these cells in 3 mL LB containing 50 μg/mL of kanamycin and 25 μg/mL of chloramphenicol was grown at 37 °C with shaking at 270 rpm. A culture in 1 L terrific broth containing 30 μg/mL of kanamycin and 35 μg/mL of chloramphenicol was inoculated with 2 mL of overnight culture and grown at 37 °C with shaking at 250 rpm to an OD_{600} of 0.6. Once OD was reached, the culture was cooled to 24 °C and induced by the addition of IPTG to 0.5 mM overall. Then the culture was incubated for 24 hours at 24 °C. The culture was pelleted and stored in two aliquots at -20 °C until purification.

Cell pellets overexpressing FgaPT2 were thawed and resuspended in 25 mL lysis buffer (250 mM sodium chloride, 50 mM sodium phosphate, 10 mM imidazole, pH 7.9). The cells were lysed by sonication and spun down. The cell lysate was then separated from the insoluble cell debris, and the His_6-tagged proteins were purified from the lysate using the Bio-Rad Profinia system and Bio-Scale Mini Nuvia IMAC Ni-Charged 5-mL columns. Following loading of the sample onto the column, the system washed first with 6 column volumes of 2x Native IMAC Wash 1 solution (1 M NaCl, 100 mM Tris, 10 mM imidazole, pH 8.0) and then with 6 column volumes of 2x Native IMAC Wash 2 solution (1 M NaCl, 100 mM Tris, 40 mM imidazole, pH 8.0). The sample was eluted in 3 column volumes of 2x Native IMAC Elution buffer (1 M NaCl, 100 mM Tris, 500 mM imidazole, pH 8.0). Then the eluent was concentrated and buffer exchanged into protein storage buffer (50 mM Tris-HCl, 500 mM NaCl, 20% glycerol, pH 7.4) using molecular-weight cutoff filters (50-kDa for FgaPT2). The concentration of protein was determined using a Bradford assay, and small aliquots of protein were stored at -80 °C until needed.

2.4.6 *In vitro* reactions to test specificity of FgaPT2

FgaPT2 reactions were run at 37 °C and pH 7.5 in 100 µL containing 50 mM Tris-HCl, 5 mM $CaCl_2$, 10% glycerol, 1 mM L-tryptophan, 3 mM pyrophosphate of interest, and 20 µg of FgaPT2. The reactions were run over night, quenched with equal volume of cold methanol, and spun down to remove the precipitated protein before analysis. For analytical-scale HPLC analysis, FgaPT2 reactions were followed at 269 nm using a Phenomenex Kinetex 5u EVO C18 column (250 x 4.6 mm; 100 Å) at a flow rate of 1 mL/min and a linear gradient of 20–70% acetonitrile in 0.1% aqueous trifluoroacetic acid over 20 min. For conversion calculations, all potential product peaks were summed, divided by the sum of product and leftover Trp, and multiplied by 100.

2.4.7. *In vitro* reactions of FgaPT2 for structural determination

FgaPT2 reactions were run at 37 °C and pH 7.5 in 10 mL containing 50 mM Tris-HCl, 5 mM $CaCl_2$, 10% glycerol, 1 mM L-tryptophan, 3 mM pyrophosphate of interest, and protein at a final concentration of 0.35 µg/mL. The reactions were run overnight with agitation at 175 rpm in a shaker, quenched with equal volume with cold methanol, and spun down to remove precipitate protein before analysis. For semi-prep HPLC separation, the supernatant of the reaction was concentrated to a few milliliters and injected 1 mL per run into the instrument. The reactions were followed at 269 nm using (Luna 5 µm C18(2) 100Å LC column 250 x 10 mm) at a flow rate of 2.5 mL/min and a linear gradient of 20–70% acetonitrile in 0.1% aqueous trifluoroacetic acid over 30 min, followed by 10 min at 100% acetonitrile and then 10 min at 20% acetonitrile.

NMR determination of products, focusing on aromatic regions:

Product with pyrophosphate **6**; ^{1}H-NMR (D_2O, 600 MHz): 7.03 (d, *J*=8.17, 1H), 7.18 (s, 1H), 7.33 (s, 1H), 7.58 (d, *J*=8.17, 1H)

Product with pyrophosphate **10**; ^{1}H-NMR (D_2O, 600 MHz): 5.9 (dd; *J*= 2.37, 1.24; 1H), 6.3 (dd; *J*=2.93, 1.76; 1H), 6.95 (d, *J*=7.16, 1H), 7.15 (t, *J*=8.02, 1H), 7.23 (s, 1H), 7.34 (d, *J*=1.74, 1H), 7.38 (d, *J*=8.28, 1H)

Product with pyrophosphate **23**; ^{1}H-NMR (D_2O, 600 MHz): 7.08 (d, *J*=8.09 1H), 7.21 (s, 1H), 7.38 (d, *J*=8.57, 1H), 7.48 (s, 1H)

Product with pyrophosphate **27**; ^{1}H-NMR (D_2O, 600 MHz): 6.75 (d, *J*=3.78, 1H), 6.91 (dd; *J*=5.04, 3.36; 1H), 7.02 (d, *J*= 7.14, 1H), 7.18 (m, 2H), 7.22 (s, 1H), 7.40 (d, *J*=7.98, 1H)

CHAPTER 3: Coupling of PhoN, IPK, and FgaPT2 to alkylate Trp

3.1. Introduction

A recent publication from our group describes the development of an alternative pathway to produce DMAPP and IPP by sequentially phosphorylating their alcohol counterparts, dimethylallyl alcohol (DMAA) or isopentenol (ISO), with PhoN-Sf and IPK respectively.[43] This method is analogous to precursor-directed biosynthesis in polyketides. This involves, as the name implies, using a synthetic precursor to provide a non-natural product; for example, using a fluoro-malonic acid instead of malonic acid would result in a fluorinated derivative of the final product. This process is something the Williams Lab has built a large body of work around, and two recent graduates, Drs. Samantha Meiser Carpenter and Edward Kalkreuter, contributed to a book chapter reviewing work using precursor-directed diversification.[95,96,130–135] A very important tool in this method are CoA ligases, which attach Coenzyme A to malonic acids and acyl groups so they can be used by the polyketide machinery. The Williams Lab has investigated MatB and several other CoA ligases which can prepare these substrates for use, and they have had much success enzymatically synthesizing several acyl and malonic-acid derivatives and using them for polyketide reactions.[133]

One could imagine applying a similar technique to diversify terpenes, now supplying alternative alkyl pyrophosphates which would then undergo the same transformations as DMAPP or IPP. For example, several aromatic prenyltransferases which prenylate aromatic amino acids have been shown to have activity with a variety of allylic pyrophosphates outside of the natural ones, DMAPP or geranyl pyrophosphate (GPP).[76] However, this knowledge has yet to be leveraged to produce a derivative of a “mature” natural product enzymatically in a cellular environment. An obvious obstacle is the lack of a method to supply these non-natural pyrophosphates to the cellular environment; this requires something analogous to malonic acids and CoA ligases—in this case, the use of cell-permeable alcohols and kinases to sequentially phosphorylate the alcohols to pyrophosphates within the cell.[43]

This method also has similar difficulties to precursor-directed diversification in polyketides *in vivo*. In the broadest sense, substrates are limited to those which can get into the cell in the first place. Beyond that, substrates are also limited by their ability to be processed by ALL of the enzymes in pathway. Each molecule (referring to the alcohol, monophosphate, and diphosphate iterations with the same R group as the same "molecule" in this sense) tested in Chapter 2 had different levels of success with PhoN, IPK, and FgaPT2, and thus would likely have different bottlenecks and would need different engineering and optimization to increase its final yield of alkylated Trp. Importantly, the cellular environment is much more complicated than this pathway alone and contains other molecules with which these enzymes are also active, so reactions besides the specific desired phosphorylations and alkylations can take place.

This chapter will discuss the use of this new pathway to produce lycopene and 4-dimethylallyltryptophan (4-DMAT) *in vivo* in *E. coli* and 4-DMAT *in vitro* also. In light of the promiscuity of wild-type PhoN-Sf, IPK, and FgaPT2 discussed in Chapter 2, the potential of this pathway to produce analogues of 4-DMAT enzymatically in *E. coli* will be evaluated. This chapter will also discuss investigation of known chain-length determining mutations of IPK and FgaPT2 to produce geranyl-tryptophan and the ability of the FgaPT2 mutant to process the other alkyl pyrophosphates tested with the wild-type in Chapter 2.

3.2. Results and Discussion

3.2.1. *In vivo* coupling of PhoN and IPK to produce lycopene

It was hypothesized that PhoN and IPK could be used together, feeding DMAA and ISO into the culture, to increase the production of terpenes *in vivo* in *E. coli*. This was investigated using a common reporter of cellular terpene production, carotenoids. Many varieties of a visual screen of carotenoid production were investigated (**Figure 3.1** for one example) and validated to confirm the increases in carotenoid production were dependent upon alcohol concentration and expression of both PhoN and IPK detected by SDS-PAGE analysis of cultures. However, instead of a simple visual screen, extraction and quantification were used, following absorbance at the λ max of the carotenoid of interest in the extraction solvent (refer to the recent Williams Lab publication in *ACS Synth Biol* for more information). In short, PhoN and IPK were able to work together in the prototype strain to phosphorylate DMAA and ISO to DMAPP and IPP, which was then used to produce lycopene at ~190 mg/L which is comparable to other engineered lycopene-producing strains of *E. coli*.[43]

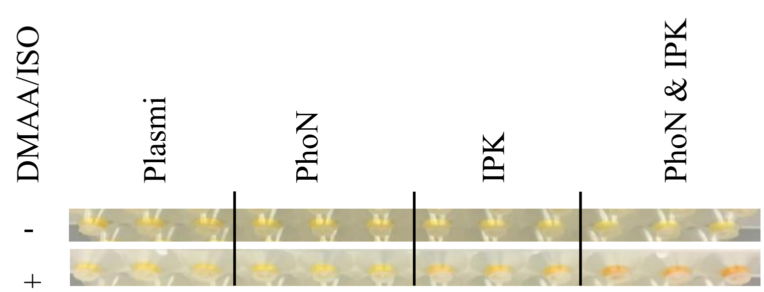

Figure 3.1. Deep-well screen for beta-carotene production. DMAA and ISO were fed into cultures of beta-carotene-producing *E. coli* expressing enzymes of interest to test for increased production.

3.2.2. Coupling of PhoN, IPK, and FgaPT2 *in vitro* and *in vivo*

Initial investigations of the PhoN-IPK *in vitro* were difficult, and no desired pyrophosphate could be detected (data not shown). The hypothesis is that PhoN as a phosphatase unproductively dephosphorylated the monophosphates and diphosphates produced by the pathway. To overcome this difficulty, the pathway was coupled to prenylation by FgaPT2 to use the pathway products before they could be dephosphorylated by PhoN. Using a combination of initial reaction conditions for all three enzymes when they were characterized individually, a reaction was setup to form DMAPP *in situ* from DMAA and then use it to prenylate L-Trp. Unfortunately, the conversion of this reaction was only 1.6 % as measured by HPLC. Next, it was hypothesized that this initial poor conversion could be optimized through combinatorial optimization of the reaction conditions. First the reaction buffer conditions were optimized for the three-enzyme system, altering the buffer, metal ion, and pH. The conditions which provided the highest percent conversion were used for the rest of the optimization. For optimizing concentration of substrates and enzymes, the "Design of Experiment" or DOE tools were used in the software program JMP to iteratively determine which of the six reaction components were important for yield, use that information to raise or lower the concentration of those components, and retest. To determine important components, the screening-design tool in JMP was used, which based on the parameters and replicates desired, to design a simple "+" or "-" set of experiments with the fewest amounts of experiments possible. In this case the "+" was a concentration higher than the original concentration used, and "-," lower. For example, the design tool produced 12 reactions to test to determine which of the six reaction components of interest had the biggest effect on the product formation, while if all possible high and low conditions were tested there would be 64 reactions (**Figure 3.2 A**). Then those concentrations can be placed into the grid along with the response, percent conversion in this case, to determine how changing a component changes the response, and thus determining which components are the most important for the overall conversion from alcohol to alkylated Trp (**Figure 3.2 B**). This analysis determined that variables "X2" and "X1" were important for "response," or in other words changes in concentration of component "X2" and "X1" had the biggest effect on percent conversion. Taking the analysis one step forward, lower values of "X2" and "X1" gave higher conversion, so the next step was to determine the optimum lower concentrations of "X2" and "X1."

A)

	X1	X2	X3	X4	X5	X6	Y
1	1	2.5	30	200	65	20	13.45
2	1	2.5	30	270	65	20	14.55
3	1	2.5	50	270	40	20	8.05
4	1	5	30	200	40	35	1.15
5	1	5	50	200	65	35	0.76
6	1	5	50	270	40	20	0.16
7	3	2.5	30	200	40	20	5
8	3	2.5	50	200	40	35	3.58
9	3	2.5	50	270	65	35	6.65
10	3	5	30	270	40	35	0.37
11	3	5	30	270	65	20	1.69
12	3	5	30	200	65	20	1

B)

Predictor	Contribution	Portion	Rank
X2	36.7277	0.3977	1
X1	20.7202	0.2244	2
X5	10.2946	0.1115	3
X6	9.7673	0.1058	4
X3	8.5754	0.0929	5
X4	6.2616	0.0678	6

Figure 3.2. DOE analysis to determine which reaction components are most important for percent conversion. A) Screening design produced by JMP filled in with concentration and percent conversion. B) Predictor analysis of the components.

To optimize the important reaction components, "response surface" analysis in JMP was used. This also had a similar experiment designer where parameters and replicates could be entered to produce a set of experiments to answer the research question. For example, if one wanted to optimize two reaction components to have the highest percent yield, the reaction components could be treated as x and y and the percent yield as z to produce a "response surface." For optimization using "central composite design," the two reaction components of interest were varied along a defined range, and the corresponding yields of those reactions were added to analyze for the optimal concentrations of those two components for the highest percent yield (**Figure 3.3**). Then, another screen was performed to determine the most important components under the new reaction conditions, and then those conditions optimized, over and over.

A)

	Pattern	X1	X2	Y
1	a0	0	82.5	0
2	−−	0.5	65	5.43
3	−+	0.5	100	5.89
4	0a	1.8	57.8	8.79
5	00	1.8	82.5	9.78
6	00	1.8	82.5	8.89
7	00	1.8	82.5	9.11
8	00	1.8	82.5	12.23
9	00	1.8	82.5	8.82
10	0A	1.8	107.2	8.74
11	+−	3	65	4.1
12	++	3	100	5.71
13	A0	3.5	82.5	4.17

B)

Solution

Variable	Critical Value
X1(0.5,3)	1.8484352
X2(65,100)	87.020684

Solution is a Maximum

Predicted Value at Solution 9.8038235

Canonical Curvature

Prediction Profiler

Figure 3.3. Surface-response analysis to optimize two reaction components for maximal yield. A) Individual experiment design produced by JMP filled in with concentration and percent conversion. B) Calculated concentrations of components which would give highest conversion

After a few iterations of DOE, a conversion of 80.1 % was obtained (**Table 3.1**). There were a few important lessons learned from the optimization. Concentrations of ATP and alcohol were very important. ATP was serving as a phosphate donor for two enzymes, so it was important to have an excess. However, ADP is an inhibitor of one of the enzymes, so it was also important not to produce too much ADP and inhibit IPK. Alcohol concentration generally needed to be high, potentially to increase the likelihood of alcohol cleaving the phosphate from PhoN rather than water. Through the series of iterations to increase percent conversion of Trp to alkylated Trp, all the reaction components were increased to different degrees except Trp. The specific information garnered from this optimization would not likely be useful outside of the simplified case of an *in vitro* reaction but could provide relative information on amount of each enzyme needed *in vivo*.

Table 3.1. *In situ* production of DMAPP from DMAA by PhoN and IPK followed by use by FgaPT**2.** Concentration of reaction components were optimized by DOE for higher percent conversion as detected by HPLC at 269 nm.

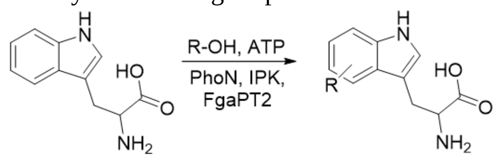

Component	Initial Conditions Concentration		Best Conditions Concentration	
Trp	1	mM	1	mM
ATP	2.5	mM	3.6	mM
R-OH	5	mM	70	mM
FgaPT2	200	ng/uL	350	ng/uL
IPK	20	ng/uL	50	ng/uL
PhoN	20	ng/uL	87	ng/uL
% Conversion	1.6		80.1	

The next task was to determine if PhoN and IPK could make DMAPP to be used by FgaPT2 *in vivo*. The pathway was first validated in the same manner as the lycopene screen to ensure all components were necessary for formation of product, 4-dimethylallyl tryptophan or 4-DMAT in this case (refer again to the recent Williams Lab paper for more information).[43] There is DMAPP in cells naturally, so there was low-level 4-DMAT formation in any strain overexpressing FgaPT2. However, there was an increase in 4-DMAT production by two orders of magnitude when the PhoN-IPK pathway and alcohol were added.[43]

The next step was to determine if analogues of alkyl pyrophosphates could be synthesized and utilized by a prenyltransferase *in vivo*. To this end, a small panel of alcohols was selected for *in vivo* testing, based on their ability to be processed by PhoN, IPK, and FgaPT2, using the data in Chapter 2. These cultures were setup and analyzed in the same manner as the ones to produce 4-DMAT. Following sample prep and HR-LC-MS, the successful production cultures (indicated by *m/z* consistent with the expected product) were ones with substrates most active with FgaPT2 in its individual characterization (**Figure 3.4**, raw data in Appendix I). Gratifyingly, those products (with **10**, **19**, and **23**) were not detected in any of the negative controls or in cross-checking the other production cultures. The XICs had abundances from 10^6 to 10^4, and comparing those abundances to ones from *in vitro* samples, the products were estimated to be from 250 to 50 nM in culture. The method of analysis was limited in that products with isomers of DMAPP could not be reliably detected because of FgaPT2's background activity with DMAPP in the cell.

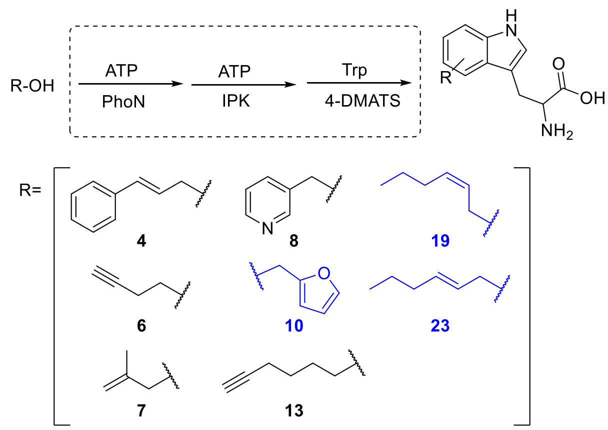

Figure 3.4. *In vivo* production of DMAPP from DMAA by PhoN and IPK and subsequent use by FgaPT2. Blue: mass ions were detected by HR-LC-MS consistent with the expected product. Alcohols of interest (5 mM) were fed into cultures expressing FgaPT2, PhoN, and IPK in *E. coli* Rosetta PLysS. Media and cell lysate were analyzed by HR-LC-MS searching for mass ion consistent with expected product. Experiments were performed in duplicate.

3.2.3. Manipulating the chain-length specificity of the PhoN-IPK-FgaPT2 pathway: modifications of FgaPT2 *in vitro*

Potential chain-length determining mutations were investigated for FgaPT2 based on the crystal structure and the proposed prenyl binding pocket. Selected residues along this pocket were chosen for saturation mutagenesis: M328, Y345, Y398, Y413, E89, and K174. Mutants were prepared using saturation-mutagenesis PCR with overlapping, NNK primers and transformed into *E. coli*. Purified plasmids from successful transformants were sequenced to determine the mutation and transformed into an expression strain of *E. coli*. Then the mutants were expressed and purified using IMAC. Purified mutants were tested in the same manner as wild-type FgaPT2 described in Chapter 2 with a subset of the panel of pyrophosphates (**1**, **3**, **4**, **10**, **14**, **17**, and/or **23**) to determine if the mutation reduced activity with DMAPP and increased activity with longer-chain pyrophosphates. It is important to note that the libraries of mutants were not screened exhaustively, were tested as they were sequence-confirmed and until a potential chain-length determining mutant was found, one with diminished DMAPP activity but increased activity with bigger alkyl pyrophosphates (the opposite of wild-type FgaPT2). The most promising mutant, M328G, was found to have reduced activity for DMAPP but retained activity with furfuryl pyrophosphate, so it was investigated further (data not shown because this mutant was retested with the full panel of pyrophosphates, **Figure 3.5**). While this work was in progress, Mai et al. published their work investigating a saturation library of FgaPT2 at M328 for chain-length determining mutations, and M328G was also one of their best mutations for reducing activity with DMAPP and increasing activity with GPP.[93]

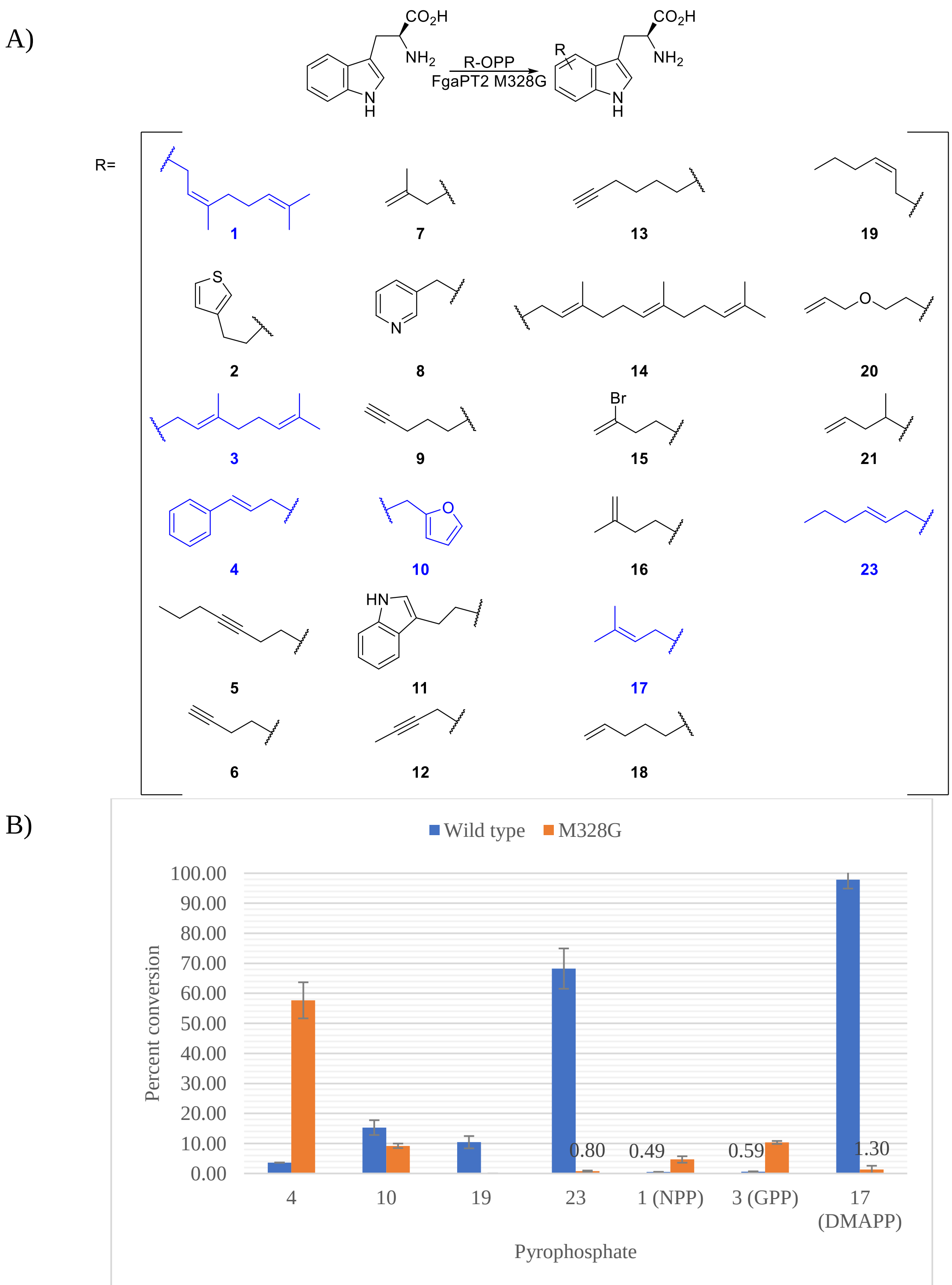

Figure 3.5. Reaction catalyzed by FgaPT2 M328G. A) Panel of pyrophosphates tested. Blue: products detected by HPLC and confirmed by LR-LC-MS with mass ions consistent with the expected product. B) Percent conversion of successful reactions in panel A catalyzed by FgaPT2 M328G compared to wild-type FgaPT2. Error bars are standard deviation of the mean of duplicate reactions. Bars <2% are labeled for clarity.

For FgaPT2 M328G, the enzyme was most active with allylic pyrophosphates again (**Figure 3.5 A**), but this time GPP and NPP are better substrates compared to wild-type while DMAPP was used less (**Figure 3.5 B**). The mutation also increased activity with cinnamyl pyrophosphate (**4**), as compared to wild-type FgaPT2. Interestingly this mutation seems to have opened up the prenyl binding site but not changed the preference for alkyl pyrophosphates with *trans* double bonds allylic to the pyrophosphate moiety.

3.2.4. Potential modifications to PhoN-IPK-FgaPT2 pathway: modification to both FgaPT2 and IPK *in vivo*

The next important question: could FgaPT2 M328G be used *in vivo* to produce geranylated Trp? Cultures were setup with wild-type or mutant FgaPT2 with PhoN-IPK Y70A-V130A-I140A (an IPK mutant previously engineered to accept GP) feeding in different concentrations of geraniol in DMSO: 0, 0.5, 2, 5, and 10 mM.[99] Unfortunately, geraniol is toxic to *E. coli*, so the cultures supplemented with ≥2 mM geraniol produced dramatically smaller cell pellets after culturing. In this case, all that was necessary for geranyl-Trp formation was FgaPT2 M328G because GPP is naturally found in *E. coli*, and therefore does not require the alternative pathway. However the samples were much noisier overall by HPLC than *in vitro* reactions, and there was not a peak above the noise consistent with the *in vitro* retention time to detect and quantify geranyl-Trp in any of the samples by HPLC. However a low-abundance mass ion consistent with geranyl-Trp was detected by LR-LC-MS in these samples (MS data in Appendix I), and ones expressing FgaPT2 M328G with low geraniol added had the highest peak heights for the extracted-ion chromatogram of *m/z* consistent with the desired product in LR-LC-MS. In the future, there are a few possibilities for overcoming geraniol toxicity in *E. coli*: engineering *E.*

coli to tolerate it, feeding in smaller chain alcohols which could be stitched together by a prenylelongase following phosphorylation by PhoN and IPK, or engineer enzymes to more efficiently use geraniol and its derivatives such that smaller amounts could be fed in.

3.3. Conclusion

In addition to production of natural pyrophosphates to make terpenes like lycopene or 4-DMAT, the PhoN-IPK pathway can produce non-natural pyrophosphates which can then be utilized by alkyl-pyrophosphate-utilizing enzymes to produce analogues of DMAT in the simple proof-of-concept laid out herein. There are several parts that can be optimized to produce more and/or detect more of the product, but it is very gratifying that non-natural analogues of DMAT were detected without optimization. In addition, the chain-length-determining mutant FgaPT2 M328G was also used *in vivo* to produce DMAT with a longer chain, now C10 instead of C5.

Now that activity of this pathway and coupling of it to other pathways have been demonstrated in these simple cases, it can be applied to more potentially relevant research questions: diversification of natural products made from alkyl pyrophosphates, interrogation of structure/activity relationships of modification to the prenyl groups of natural products, interrogation of mechanism and substrate tolerance of different types of alkyl-pyrophosphate-utilizing enzyme, etc. The alcohol-dependent hemiterpene pathway opens up *in vivo* investigation of terpenes and enzymes that use or produce them in a way it has never been before.

3.4. Methods

3.4.1. Plasmid construction

The codon-optimized sequence of *ipk* for heterologous expression in *E. coli* was synthesized by IDT (GI number 297343032). *IPK* was PCR amplified using the following primers with cut sites underlined: IPK_FWD_NdeI, GTAC<u>CATATG</u>ATAGATCCGTTCACCATGATCATCC; and IPK_REV_XhoI, GTAC<u>CTCGAG</u>TTAGCGAATCACGGTACC. The PCR contained 5x Phire II buffer, 0.2 mM dNTPs, 0.5 µM of each primer, 1 µL Phire II DNA polymerase, and 1 µL of template DNA in 50 µL. The cycling parameters used were as follows: 1) 98 °C, 30 s; 2) 98 °C, 5 s; 3) 63 °C, 15 s; 4) 72 °C, 20 s; 5) repeat steps 2-4 thirty-four times; 6) 72 °C, 1 min; 7) 4 °C, hold. Following amplification, IPK was restriction digested with *Nde*I and *Xho*I and ligated into multi-cloning site two (MCS2) of pETDuet-1 and PhoN-pETDuet. The plasmid was transformed into DH5α chemically competent *E. coli* and plated on an LB agar plate containing 100 µg/mL of ampicillin, and the resultant colonies were sequenced to determine the presence of *ipk* using the primer DuetUP2 (TTGTACACGGCCGCATAATC). For cloning into pET28a, the ipk gene was PCR amplified using the following primers (GTACCATATGGATCCGTTCACCATGATGATCC and GTACCTCGAGTTAGCGAATCACGGTACCGAT) and the same PCR conditions as described above. Following amplification, the product was purified by gel electrophoresis and was digested with *Nde*I and *Xho*I and ligated into similarly treated pET28a. The ligation mixture was then transformed into chemically competent *E. coli* DH5α and plated on LB agar containing 50 µg/mL kanamycin. Plasmid was prepared from a single colony and the gene sequence confirmed by DNA sequencing using T7 primers. IPK-pET28a was cloned by Sean Lund.

For *in vivo* experiments, *fgapt2* was cloned into pCDFDuet to avoid conflicts in origin of replication for pET28a and pETDuet. The gene was amplified using the same cycling parameters for cloning *fgapt2* into pET28a with the following primers: TATAGGATCCGATGAAAGCCGCAAACG and ATATAAGCTTATGCAGGCCGC. Following amplification, the product was purified by gel electrophoresis and was digested with *Bam*HI and *Hin*dII and ligated into similarly treated pCDFDuet. The ligation mixture was then transformed into chemically competent *E. coli* DH5α and plated on LB agar containing 100 μg/mL streptomycin. Purified DNA from a single transformant was submitted for DNA sequencing using the same primers to confirm PhoN cloning into MCS1 of pETDuet described in Chapter 2.

3.4.2. Plasmid mutagenesis

Several mutants of *fgaPT2* were made by saturation mutagenesis through PCR with NNK primers. The table below lists the primers and desired mutations using each primer (**Table 3.2**). The reactions contained 10x Ultra AD buffer, 0.2 mM dNTPs, 0.2 μM of each primer (M328X, Y345X, Y398X, Y413X, E89X, or K174X primer sets), 6% DMSO, 0.5 μL Pfu Ultra DNA polymerase, and 50 ng of template vector, FgaPT2-pET28a, in 50 μL. The following cycling parameters were used: 1) 95 °C, 2 min; 2) 95 °C, 50 s; 3) 60 °C, 50 s; 4) 68 °C, 10.5 min; 5) repeat steps 2-4 eighteen times; 6) 68 °C, 12 min; 7) 4 °C, hold. The M328G mutation was made in FgaPT2-pCDFDuet using the primers listed in **Table 3.2** and the same cycling parameters for saturation mutagenesis of FgaPT2-pET28a. *Ipk* was sequentially mutated to the triple mutant Y70A-V130A-I140A in IPK-pET28a, IPK-pETDuet, and PhoN-IPK-pETDuet using the same cycling parameters mentioned above. Following PCR amplification, reactions were *Dpn*I digested with the addition of 1 µL *Dpn*I and incubation at 37 °C for 3-4 h. After digestions, 10 µL of PCR were transformed in chemically competent *E. coli* DH5α. The transformations were plated on LB containing antibiotic of interest and grown at 37 °C overnight. Purified DNA from transformants was submitted for sequencing with the same primers used to confirm cloning into pET28a and into MCS2 of pETDuet. IPK single mutants were sequence confirmed and then used to produce double mutants, which were then sequence confirmed and used to produce triple mutants.

Table 3.2. Primers for site-directed mutagenesis.

Gene	Mutation	Forward primer	Reverse Primer
FgaPT2	M328X	GAGCGTTTACCGCTGNNKGCCAATTTTACCCTG	CAGGGTAAAATTGGCMNNCAGCGGTAAACGCTC
	Y345X	CCGGAACCGCAGGTGNNKTTTACAACCTTCGGC	GCCGAAGGTTGTAAAMNNCACCTGCGGTTCCGG
	Y398X	AACTATTTACATGCCNNKATCAGCTTTAGCTAT	ATAGCTAAAGCTGATMNNGGCATGTAAATAGTT
	Y413X	CCGTATCTGAGTGTGNNKCTGCAGAGCTTCGAA	TTCGAAGCTCTGCAGMNNCACACTCAGATACGG
	E89X	TACGGTACCCCGTTTNNKCTGAGCCTGAACTGC	GCAGTTCAGGCTCAGMNNAAACGGGGTACCGTA
	K174X	ATCCGCACCCAGAACNNKCTGGCACTGGACCTG	CAGGTCCAGTGCCAGMNNGTTCTGGGTGCGGAT
	M328G	GAGCGTTTACCGCTGGGCGCCAATTTTACCCTG	CAGGGTAAAATTGGCGCCCAGCGGTAAACGCTC
IPK	Y70A	CGTAGCAGCATCGGCGCGAGCATCGTGCATCGC	GCGATGCACGATGCTCGCGCCGATGCTGCTACG
	V73A	ATCGGCTACAGCATCGCGCATCGCGACATGGAA	TTCCATGTCGCGATGCGCGATGCTGTAGCCGAT
	V130A	GTGAGCTATGGCGACGCGTATATCAAGGACGAA	TTCGTCCTTGATATACGCGTCGCCATAGCTCAC
	I140A	GAACATAGCTATGGCGCGTACAGCGGCGACGAT	ATCGTCGCCGCTGTACGCGCCATAGCTATGTTC

3.4.3. Protein expression and purification

PhoN and FgaPT2 were expressed and purified as described in Chapter 2. Also FgaPT2 M328G was expressed and purified in the same manner as wild-type FgaPT2.

IPK-pET28a was transformed into chemically competent *E. coli* BL21(DE3) for protein expression. An overnight culture in 3 mL LB broth supplemented with kanamycin (50 µg/mL) was grown at 37 °C with shaking at 270 rpm. A culture in 1 L of LB broth was inoculated with 1 mL of the overnight culture and grown at 37 °C with shaking at 250 rpm to an OD_{600} of 0.6. The culture was cooled to 30 °C, and protein expression was induced by the addition of IPTG to a final concentration of 1 mM. The culture was incubated at 30 °C with shaking at 200 rpm for an additional 20 h. The culture was spun down into a pellet which was stored at -20 °C until purification. Cell pellets overexpressing IPK were treated in the same manner as FgaPT2 to purify IPK. Then resultant protein solution was concentrated and buffer exchanged into protein storage buffer (50 mM Tris-HCl, 500 mM NaCl, 20% glycerol, pH 7.4) using 10 kDa molecular-weight cutoff filters. The concentration of protein was determined using a Bradford assay and small aliquots of protein were stored at -80 °C until needed.

3.4.4. *In vitro* reactions

For reaction buffer optimization for PhoN, IPK, and FgaPT2 coupled reactions with DMAA, several components were varied: identity of buffer (Tris or phosphate), concentration of buffer (50 mM or 25 mM), pH (6.5, 7.0, 7.5, 8.0, 8.5), metal-ion identity (Mg^{2+} or Ca^{2+}), and metal-ion concentration (5 mM or 2.5 mM). With all the buffer condition combinations, eighty reactions were setup, each with different buffer conditions, but all containing 1 mM Trp, 2.5 mM ATP, 5 mM DMAA, 200 ng/µL FgaPT2, 20 ng/µL PhoN, and 10 ng/µL IPK in 100 µL. Reactions were incubated at 37 °C overnight and then quenched with equal volume methanol. The reactions were analyzed using the same HPLC parameters as wild-type FgaPT2 reactions, following at 269 nm. The buffer of the reaction with the highest percent yield of 4-DMAT was used for the rest of the optimization investigations.

The best reaction conditions for coupling PhoN, IPK, and FgaPT2 contained 25 mM Tris-HCl, 5 mM magnesium chloride, 1 mM L-tryptophan, 1.8 mM ATP, 30 mM DMAA, 270 ng/μL FgaPT2, 20 ng/μL IPK, and 87 ng/μL PhoN at pH 8.0 in a total volume of 50 μL. Reactions were run and analyzed under the same conditions as FgaPT2 reactions.

FgaPT2 M328G reactions were performed under the same conditions as wild-type described in Chapter 2, except with 350 ng/μL enzyme. They were also analyzed with the same HPLC conditions.

3.4.5. *In vivo* production

A 3 mL culture of *E. coli* Rosetta(DE3) pLysS pETDuet-PhoN-IPK+pCDFDuetFgaPT2 was grown overnight at 37 °C with shaking at 250 rpm in LB media containing ampicillin (100 μg/mL), chloramphenicol (35 μg/mL), and streptomycin (100 μg/mL). Cultures of strains excluding each of the enzymes were also setup as cultures. Aliquots (100 μL) of overnight culture were used to inoculate cultures in 10 mL of TB media containing the same antibiotics as before, and those cultures were grown at 30 °C for 6 h with shaking at 250 rpm until induction with 0.5 mM IPTG (final concentration) and addition to a final concentration of 5 mM DMAA and 5 mM ISO or an equal volume of DMSO, the solvent in which DMAA and ISO were dissolved. The cultures were grown for 48 h after induction. A portion of culture supernatant was reserved for analysis. The cell pellet was resuspended in 2 mL water, and 1 mL of suspension was lysed by a series of three free-thaws. The culture and lysate supernatant were diluted 1:1 in methanol before analysis by HPLC and HR-LC-MS using the same conditions used to analyze FgaPT2 *in vitro* reactions in Chapter 2. Cultures were prepared and assayed in duplicate.

For *in vivo* production of geranyl-Trp, production cultures were setup similarly to 4-DMAT producing cultures, except with pETDuet-PhoN-IPK Y70A-V130A-I140A in the place of wild-type plasmid and either pCDFDuet-FgaPT2 or pCDFDuet-FgaPT2 M328G with five different induction solutions containing IPTG to 0.5 mM and either 10, 5, 2, 0.5, or 0 mM geraniol upon addition to culture. Controlling for the solvent in which geraniol is dissolved, DMSO made up the difference in volume from diluting 1 M geraniol to the necessary concentration in the master mix, such that the condition with 0 mM geraniol has the same volume added as the one with 10 mM geraniol. Samples were prepared in the same manner as the above production cultures and analyzed by HPLC and LR-LC-MS.

CHAPTER 4: Probing the substrate promiscuity of CpaD and FtmPT1

4.1. Introduction

Terpenes and prenylated natural products are one of the most diverse families of natural products, despite having a common biosynthetic origin in the form of DMAPP and IPP. In prenylated natural products, the prenyl group is appended to a molecule of some other biosynthetic origin, a polyketide or cyclic peptide for example. Cyclic dipeptides (CDPs) are alkaloid natural products commonly produced by fungus, and they are commonly prenylated and further decorated to produce their final form. Focusing on tryptophan-containing CDPs, research suggests the prenyl group is important for their cytotoxic activity reported in several cancer cell lines.

The enzymes that prenylate tryptophan-containing CDPs are similar to enzymes that prenylate tryptophan, like FgaPT2 (discussed in Chapters 2 and 3). For example, CpaD, sharing 44% homology to FgaPT2, is a prenyltransferase involved in the biosynthesis of cyclopiazonic acid in *Aspergillus flavus*. CpaD catalyzes the prenylation of *cyclo*-acetoacetyl-L-tryptophan (cAATrp), the product of a hybrid PKS-NRPS called CpaS, at C4 of the indole ring (**Figure 4.1**).[136,137] CpaD has been characterized with regard to aromatic prenyl acceptor by Liu and Walsh at Harvard Medical School. CpaD would not accept free tryptophan to a high degree but would prenylate other peptides (linear and cyclic) containing tryptophan and other aromatic amino acids. The use of other natural prenyl donors (IPP, GPP, FPP, and GGPP) was also investigated, and no product was detected with any of these prenyl donors. [136]

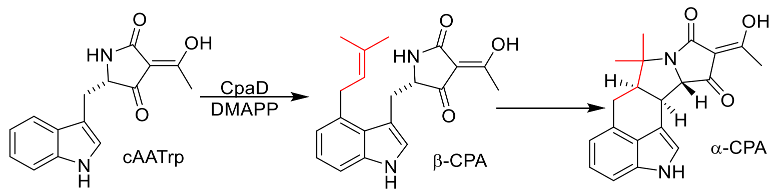

Figure 4.1. CpaD-catalyzed prenylation of cAATrp.

FtmPT1 is another prenyltransferase similar to FgaPT2 (36% homology) which utilizes cyclic dipeptides. FtmPT1 is used in the biosynthesis of the fumitremorgins to prenylate c-L-Trp-L-Pro (or brevianamide F) at C2 of the indole to produce tryprostatin B (**Figure 4.2**). FtmPT1 prefers DMAPP for the prenyl donor and will accept a variety of tryptophan-containing cyclic (di)peptides as an aromatic acceptor.[138] FtmPT1 has been successfully engineered to change its product distribution with a few simple mutations: Y205X or G115T to switch from C2 to C3 prenylation (normal for the former, reverse for the latter), Y205X and/or G115X to increase activity with hydroxynaphthalenes.[89,90,139–141] The substrate promiscuity with regard to the prenyl donor has been investigated very little for FtmPT1. Products were detected with butenyl and pentenyl allylic pyrophosphates similar to FgaPT2, but no other tests with non-natural alkyl pyrophosphates have been reported to date.[142] FtmPT1 has also been successfully engineered to accept GPP with an M364G mutation, similar to the FgaPT2 M328G mutant described in Chapter 3.[94]

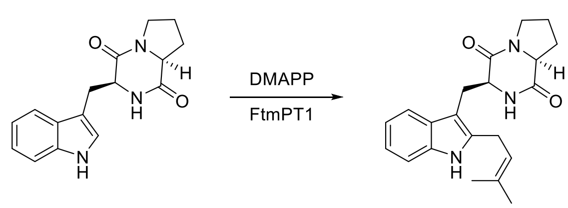

Figure 4.2. FtmPT1 catalyzes the prenylation of c-L-Trp-L-Pro at C2 of the indole ring.

This work will describe the substrate promiscuity of CpaD and FtmPT1 with three cyclic dipeptides (cWY, cWF, and cWG) and the panel of pyrophosphates used to characterize FgaPT2 in Chapter 2. The homologous, potentially chain-length determining mutant of each enzyme (I329G for CpaD and M364G for FtmPT1) will also be investigated with the panel of alkyl pyrophosphates similar to FgaPT2 M328G. In addition, preliminary experiments using CpaD and FtmPT1 with the PhoN-IPK pathway *in vivo* will also be described.

4.2. Results and discussion

A preliminary test was used to determine which of a panel of in-house prenyltransferases would be the best for this experiment. FgaPT2, BrePT, SirD, TyrPT, AtaPT, FtmPT1, CdpNPT, and CpaD were expressed in *E. coli* and purified using IMAC. Assays were setup with DMAPP and cWY, cWF, or cWG according to the published conditions for each enzyme, following via HPLC at 269 nm. Of the enzymes tested, FtmPT1 and CpaD were the only ones to accept each of the cyclic dipeptides tested to high degree with DMAPP, so they were used to examine the expanded alkyl pyrophosphate panel with each of the cyclic dipeptides.

4.2.1. Probing the substrate promiscuity of CpaD *in vitro*

CpaD was expressed in *E. coli* and purified using IMAC. Purified CpaD was tested with each of the cyclic dipeptides and the panel of alkyl pyrophosphates (**Figure 4.3**). The reactions were followed via HPLC and confirmed via LR-LC-MS (data in Appendix I). Comparing to the FgaPT2 specificity data presented in Chapter 2, these results are similar, and all of the substrates accepted by CpaD were accepted by FgaPT2. Focusing on the cyclic dipeptides, cWF was the better aromatic acceptor for every prenyl donor with the exception of **13**. For prenyl donors, most of the pyrophosphates accepted were allylic (**4**, **10**, **17**, **19**, **23**, **25**, and **27**). However, there were two exceptions: **13** which is essentially alkyl and **34** which is “propargyl” and thus analogous to an allylic pyrophosphate in methylenes between the double or triple bond and the pyrophosphate.

Applying similar comparisons to those in Chapter 2, a few trends can be seen in types of substrates preferred. First, comparing the furans and thiophenes (**10**, **25**, **26** and **27**), there is a slight preference for furan over thiophene, a preference for C2 substitution over C3, and a preference for benzylic over homobenzylic pyrophosphates. For proximity of pyrophosphate to double or triple bond, the same comparisons made for FgaPT2 cannot be applied here because products were not detected for substrates with more than one methylene between multiple bond and pyrophosphate with the exception of **13**, but there is a clear preference for allylic substrates. Comparing *cis* and *trans* isomers, there is a preference for *trans* over *cis* (**19** vs. **23**). For length of alkyl chain, medium (four to six linear carbons) alkyl chains were preferred over short (three linear carbons; **7** or **35**) or long (seven or eight linear carbons; **1**, **3**, or **5**).

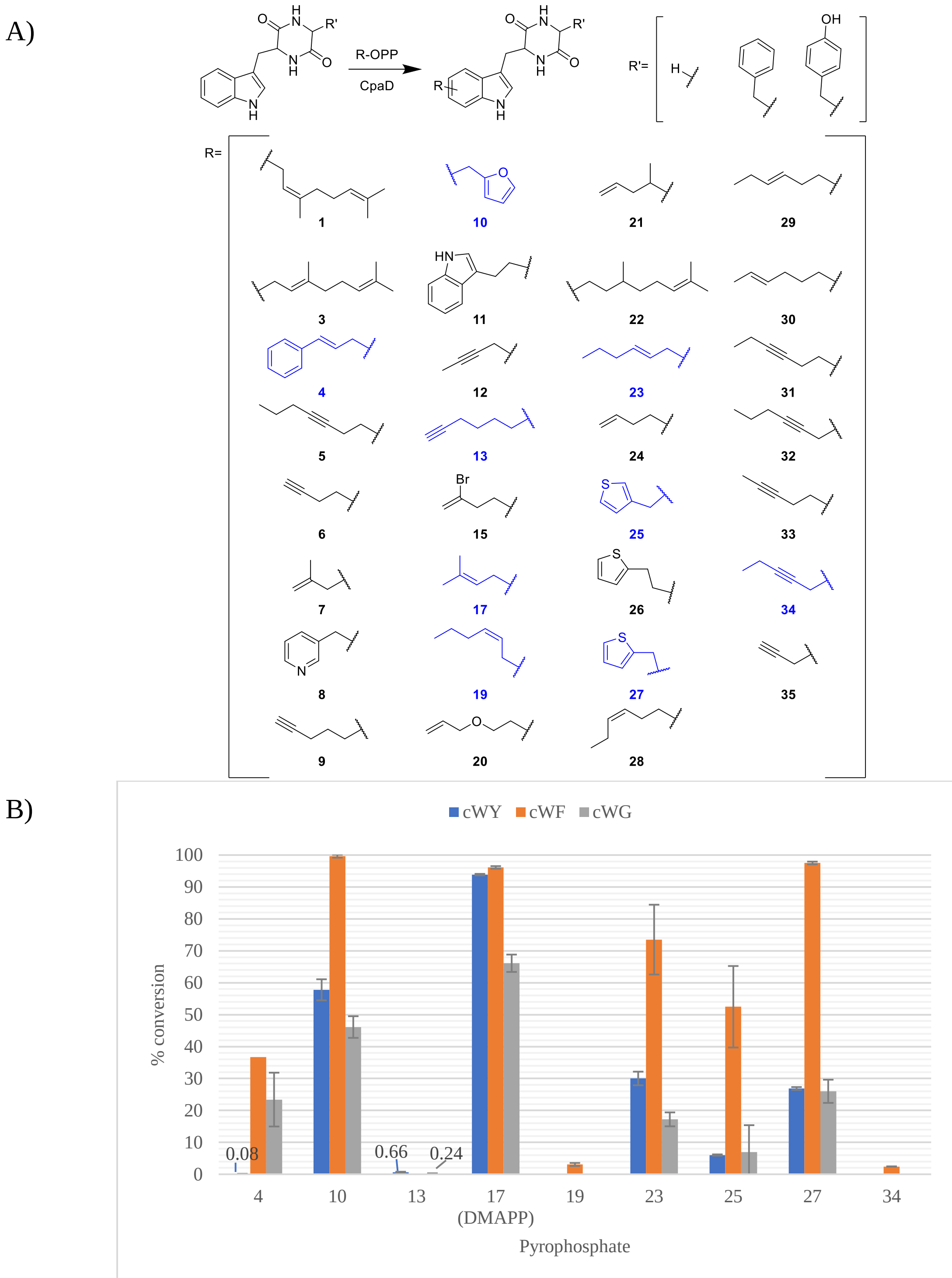

Figure 4.3. Reaction catalyzed by CpaD. A) CpaD was tested with three cyclic dipeptides and a panel of pyrophosphates. Blue: products detected by HPLC and confirmed by LR-LC-MS with mass ions consistent with the expected product with at least one of the cyclic dipeptides tested. B) Percent conversion with the pyrophosphates indicated in panel A. Data labels are provided for bars with <2 % for clarity. Error bars are the standard deviation of duplicates.

It is important to note that the conversions reported are calculated from the area of the peak of cyclic dipeptide left over and area of the new peak(s) in the product mixture. Multiple products could come from regioisomers produced by prenylation at different positions or multiple prenylations of the same molecule. Data indicates there may be multiple products for different alkyl pyrophosphates with each of the cyclic dipeptides. For cWY, reactions with **4**, **10**, **13**, and **27** suggest multiple products: **4** had multiple potential product peaks in HPLC; LR-LC-MS data for **4**, **10**, and **27** have mass ions consistent with the dialkylated product and **4** also suggesting trialkylated product; and LR-LC-MS data for **13** show three peaks consistent with mass ion of expected mono-alkylated product, suggesting three potential regioisomers. For cWF, reactions with **4**, **17**, **25**, and **34** suggest multiple products: **25** had multiple potential product peaks in HPLC; LR-LC-MS data for **17**, **25**, and **34** have mass ions consistent with di- and trialkylated products; and LR-LC-MS data for **4** show two peaks consistent with mass ion of expected mono-alkylated product, suggesting two regioisomers. For cWG, reactions with **4**, **25**, and **27** suggest multiple products: LR-LC-MS data for **4** and **27** have mass ions consistent with the di- and trialkylated products; LR-LC-MS data for **4** show two peaks for monoalkylated and two peaks for dialkylated suggesting two regioisomers for mono- and dialkylated products; and LR-LC-MS data for **25** show three peaks with mass ions consistent with the monoalkylated product, suggesting three regioisomers. Further NMR experiments are necessary to confirm the identity of these products.

4.2.3. Probing the substrate promiscuity of FtmPT1 *in vitro*

FtmPT1 was expressed in *E. coli* and purified using IMAC. Purified FtmPT1 was tested with each of the cyclic dipeptides and the panel of alkyl pyrophosphates (**Figure 4.4**). The reactions were followed via HPLC and confirmed via LR-LC-MS (data in Appendix I). Comparing to FgaPT2 specificity, all the prenyl donors accepted by FtmPT1 were also accepted by FgaPT2. In addition, comparing to CpaD specificity results, all prenyl donors accepted by FtmPT1 were also accepted by CpaD. For the cyclic dipeptides tested, similar to CpaD, cWF was a better aromatic acceptor for all of the prenyl donors tested except **13**. It is not surprising that most substrates accepted were allylic apart from **13**, which was also an exception mentioned in the two previous specificity discussions.

For prenyl donors, there are a few trends suggested from the accepted alkyl pyrophosphates. Comparing the furans and thiophenes (**10**, **25**, **26** and **27**), there is a slight preference for furan over thiophene (**10** vs. **27**), a preference for C2 substitution of the pyrophosphate over C3 (**25** vs. **27**), and a preference for benzylic over homobenzylic (**26** vs. **27**). For proximity of the pyrophosphate to the double or triple bond, there is a clear preference for allylic substrates, but unlike CpaD and FgaPT2, under the assay conditions no “propargyl” pyrophosphates were accepted. Also no products with homoallylic or homopropargyl were detected, so in this case the argument that the more methylenes the multiple bond and pyrophosphates are apart, the lower the activity with the pyrophosphate cannot be made, but it could still be the case, with products from pyrophosphates with two or three methylenes between the multiple bond and the pyrophosphate being too low to detect. Comparing *cis* and *trans* isomers **19** and **23**, there is a preference for *trans* over *cis*. In addition, there is a preference for medium chain length (4 to 6 linear carbons) over short (3 linear carbons) or long (7 or 8 linear carbons).

HPLC and LR-LC-MS data for FtmPT1 also suggest multiple products for a given alkyl pyrophosphate in the form of regioisomers and multi-prenylated products. For cWY, multiple products are suggested for reactions with **4**, **10**, **13**, **17**, **19**, **25**, and **27**: HPLC chromatograms of reactions with **17** had two product peaks and **10**, **23**, and **25** with three; LR-LC-MS data for **4** and **19** show two peaks with mass ions consistent with the mono-alkylated product, and three peaks for **13**; LR-LC-MS data for **4**, **10**, **17**, and **27** have mass ions consistent with the dialkylated product with **4** also having mass ions consistent with the trialkylated product. For cWF, reactions with **4**, **10**, **17**, **23**, **25**, and **27** suggest multiple products: HPLC chromatograms of reactions with **10**, **17**, and **23** show three products peaks and two for **4**, **25**, and **27**; LR-LC-MS data for **4**, **10** and **27** have mass ions consistent with dialkylated products; and LR-LC-MS data for **4** and **17** show two peaks with mass ions consistent with the monoalkylated product. For cWG, analysis of reactions with **4**, **10**, **17**, **23**, **25**, and **27** indicate multiple products: HPLC chromatograms of reactions with **17** and **23** showed two product peaks and **10** and **27**, three; LR-LC-MS data for **4**, **10**, **17**, and **27** have mass ions with di- and trialkylated products and for **25**, dialkylated product; and LR-LC-MS data for **4**, **10**, and **17** show two peaks with a mass ion consistent with the monoalkylated product and for **4**, two for the dialkylated product. The identity of these products needs to be confirmed with further NMR experiments.

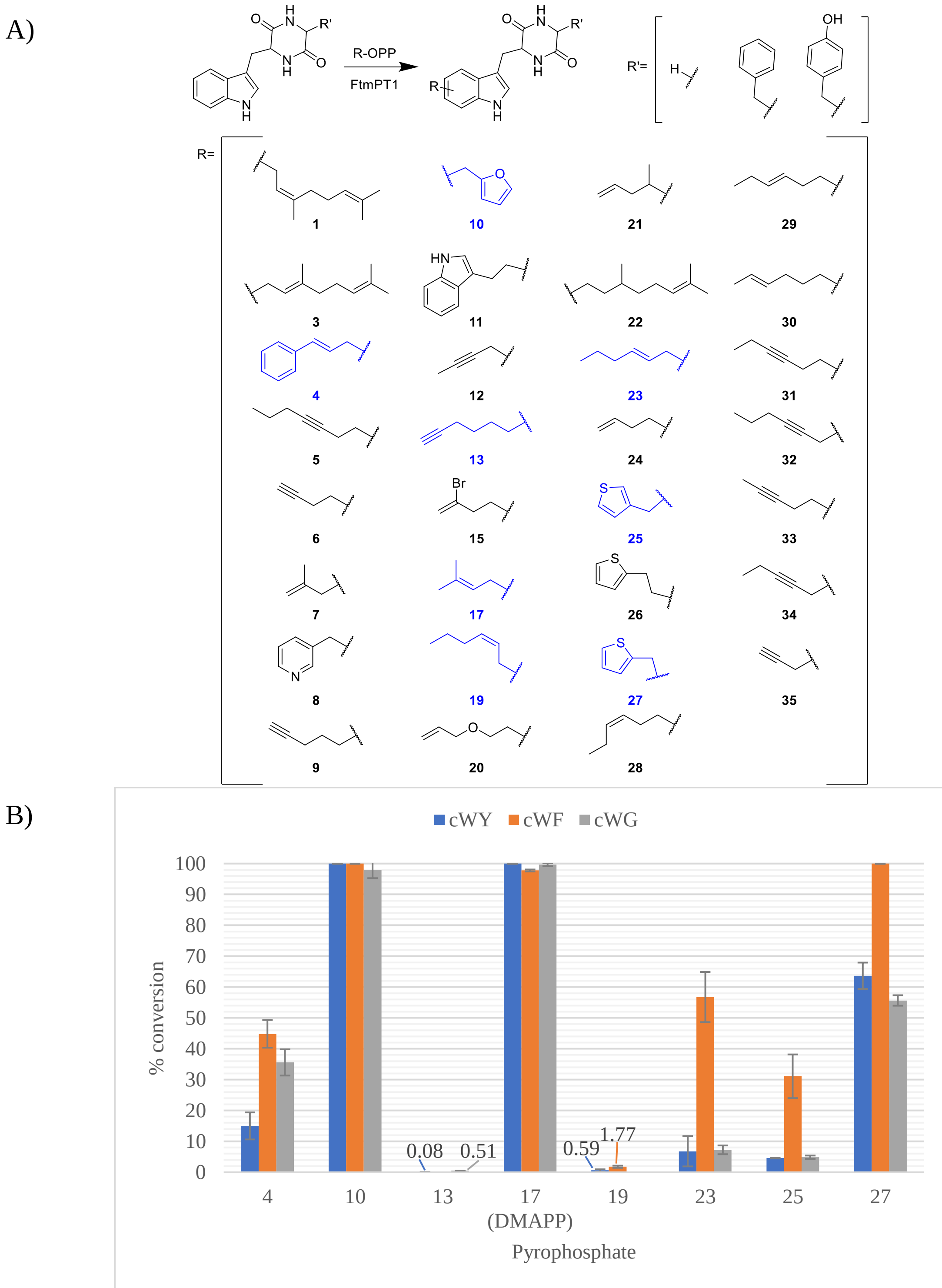

Figure 4.4. Reaction catalyzed by FtmPT1. A) FtmPT1 was tested with three cyclic dipeptides and a panel of alkyl pyrophosphates. Blue: products detected by HPLC and confirmed by LR-LC-MS with mass ions consistent with the expected product for at least one cyclic dipeptide. B) Percent conversion with the pyrophosphates indicated in panel A. Data labels are provided for bars with <2 % for clarity. Error bars are the standard deviation of duplicates.

4.2.4. Investigation of chain-length determining mutant in CpaD and FtmPT1

Because of the specificity switch afforded by FgaPT2 M328G, a mutation was made at the homologous residue in CpaD and FtmPT1. To determine the homologous residue, the amino acid sequence of FgaPT2 was aligned with those of CpaD and FtmPT1, and it was determined that M328 was homologous to I327 and M364 respectively. Those residues were switched to glycine using site-directed mutagenesis.

CpaD I329G was expressed in *E. coli* and purified using IMAC. Mutant reactions with purified enzyme were setup and analyzed in the same manner as the wild-type. Similar to FgaPT2 M328G, CpaD I329G had detectable activity with NPP and GPP and diminished activity with DMAPP, compared to the wild-type. Comparing cyclic dipeptides, the mutant was generally more active with cWF than the other cyclic dipeptides, like the wild-type. The mutant also continued to be more active with allylic pyrophosphates compared to non-allylic.

Comparing I329G to wildtype, the conversions were generally lower with the maximum under the assay conditions at 45 %. Activity was decreased for **17**, **10**, **23**, **25**, and **27**, while activity with **1**, **3**, **4**, and **22** was increased. Interestingly, product was detected for only cWF with **13** for the mutant, despite product detected for cWG and cWY with **13** but not cWF for wild-type. The most interesting addition is that of **22** or CPP which is a desaturated form of GPP (**3**) and NPP (**1**) making the pyrophosphate no longer allylic. Comparing **3** and **1** to **22**, activity with **22** is about a tenth of that with **1** and **3** with cWF.

Performing similar comparisons to the wild-type discussion, there are some trends that arise. Comparing furans to thiophenes (**10**, **25**, **26**, and **27**), those trends are the same as the wild-type: preference for furan over thiophene, for pyrophosphate at C2 over C3, and for benzylic over homobenzylic. All prenyl donors accepted were allylic with the exception of **13** and **22**. The most dramatic switch is long-chain alkyl pyrophosphates are preferred over medium or short with CpaD I 327G. Also the preference of *trans* over *cis* is present for **19** vs **23** but not with **1** vs **3**; however this could be due to the error in measurement of **1** and **3**.

CpaD I329G also had many instances of potential multiple products, in the form or regioisomers and multi-prenylated products. For cWY, data indicate reactions with **1**, **3**, **4**, **10**, **17**, **23**, and **27** have multiple products: HPLC chromatograms for 4 have two potential product peaks; LR-LC-MS data with **1**, **3**, **4**, **17**, **23**, and **27** have mass ions consistent with the dialkylated product and with **1** and **3**, also tri-alkylated product; LR-LC-MS data with **1**, **3**, **4**, and **10** show multiple peaks consistent with the mass ion of the monoalkylated product, and with **1** and **3**, multiple also for the dialkylated product. For cWF, analysis of reactions with **1**, **3**, **4**, **10**, **13**, **17**, **19**, **25**, and **27** suggest multiple products: HPLC chromatograms have multiple potential product peaks with **4** and **27**; LR-LC-MS data with **1**, **3**, **4**, **10**, **17**, **19**, **25**, and **27** have mass ions consistent with the dialkylated product and with **1**, **3**, **17**, and **25** also having ones consistent with trialkylated product; LR-LC-MS data shows multiple peaks consistent with the monoalkylated product with **1**, **3**, **4**, **13**, and **19** and multiple peaks for dialkylated product with **1**, **3**, **17**, **19**, **25**, and **27**. For cWG, reactions with **3**, **4**, **22**, **23**, and **27** have multiple products: LR-LC-MS data for **3**, **4**, **22**, and **27** have mass ions consistent with the dialkylated product and for **4** and **22**, the trialkylated product also; LR-LC-MS show multiple peaks consistent with the monoalkylated product with **4**, **23**, and **27** and multiple for the dialkylated product with **3**. Further NMR experiments are required to determine the identity of these products.

A)

B)

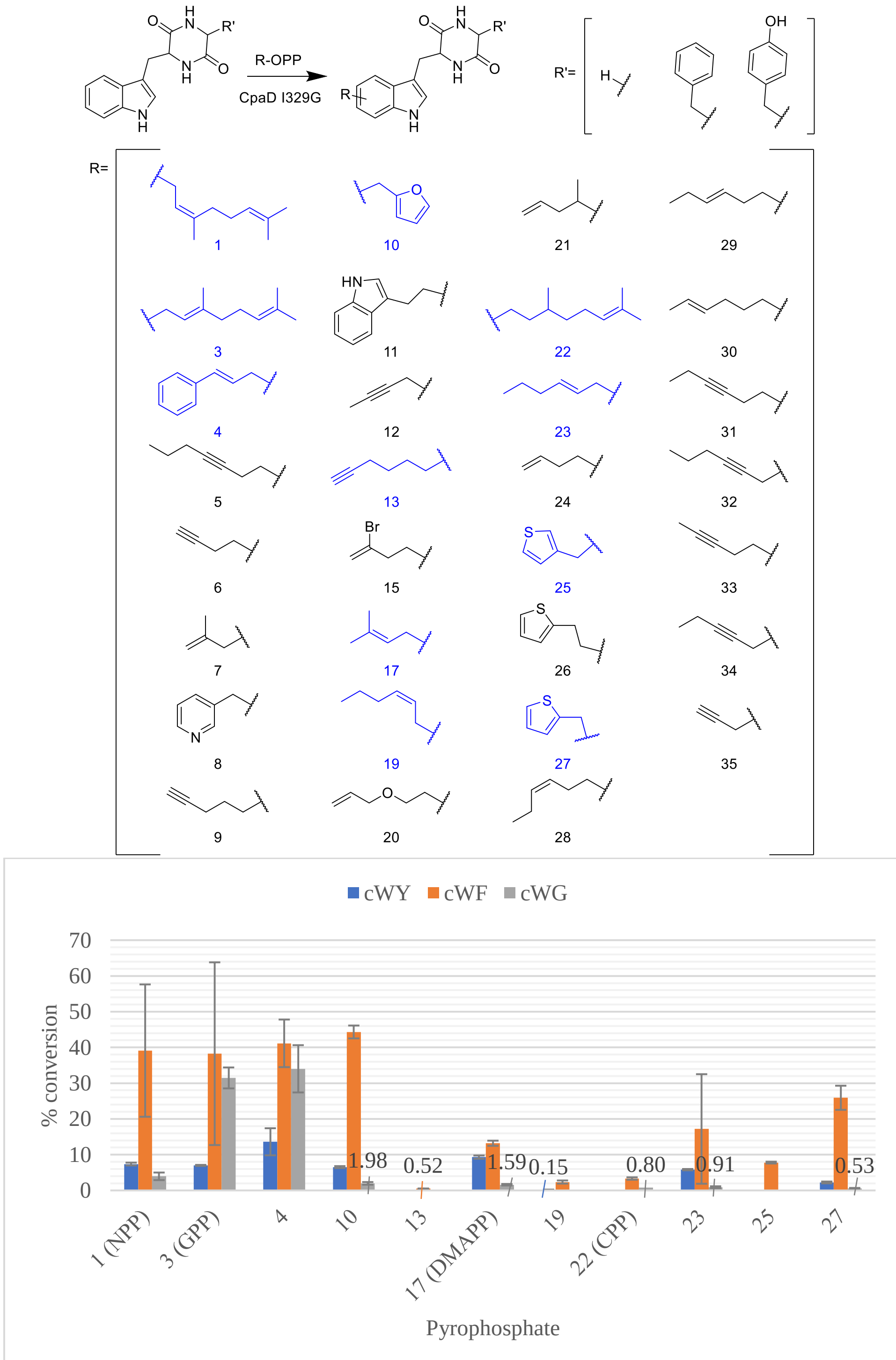

Figure 4.5. Reaction catalyzed by CpaD I329G. A) CpaD I329G was tested with three cyclic dipeptides and a panel of alkyl pyrophosphates. Blue: products detected by HPLC and confirmed by LR-LC-MS with mass ions consistent with the expected product with at least one of the cyclic dipeptides. B) Percent conversion with the pyrophosphates indicated in panel A. Data labels are provided for bars with <2 % for clarity. Error bars are the standard deviation of duplicates.

FtmPT1 M364G was expressed in *E. coli* and purified using IMAC. Mutant reactions with purified enzyme were setup and analyzed in the same manner as the wild-type. Similar to FgaPT2 M328G, FtmPT1 M364G had detectable activity with NPP and GPP, but this time activity with DMAPP was not dramatically diminished, compared to the wild-type FtmPT1. Comparing cyclic dipeptides, the mutant was generally more active with cWF than the other cyclic dipeptides, like the wild-type. The mutant also continued to be more active with allylic pyrophosphates compared to non-allylic.

Comparing M364G to wild-type, activity was not generally decreased, unlike CpaD I329G. With the mutant, activity with **1**, **3**, and **22** was now detectable. Also unlike CpaD I329G, many of the trends in activity decreases and increases for FtmPT1 M364G are not generalizable across all three cyclic dipeptides tested. For cWY, activity decreased with **10**, **25**, and **27** compared to the wild-type, while activity increased with **1**, **3**, **13**, **19**, and **22**. For cWF, activity decreased with **25**, and **27**, while activity increased with **1**, **3**, **4**, **13**, **19**, and **22**. For cWG, activity decreased with **4**, **10**, **17** and **27**, while activity increased with **1**, **3**, **19**, and **22**. The most interesting change is the addition of **22** or CPP which is a desaturated form of GPP (**3**) and NPP (**1**) making the pyrophosphate no longer allylic. Comparing **3** and **1** to **22**, activity with **22** is about a thirtieth of that with **1** and **3** with cWF.

Performing similar comparisons to the wild-type discussion, there are some trends that arise. Comparing furans to thiophenes (**10**, **25**, **26**, and **27**), those trends are the same as the wild-type: preference for furan over thiophene, for pyrophosphate at C2 over C3, and for benzylic over homobenzylic. All prenyl donors accepted were allylic with the exception of **13** and **22**. The most dramatic switch is the preference for long-chain alkyl pyrophosphates over medium or short with FtmPT1 M364G. In addition, the preference for *trans* over *cis* in the wild-type hardly exists in the mutant. For **1** vs. **3**, **1** has a higher conversion with nearly all of the cyclic dipeptides tested despite being the cis isomer of **3**. For **19** vs. **23**, the preference for *trans* over *cis* is much lower, with the percent conversion for **23** being 1.4 times large than **19**, compared to thirty times larger with the wild-type.

Specificity data for FtmPT1 M364G suggests multiple products for several single alkyl pyrophosphate reactions. For cWY, data indicates multiple potential products in reactions with **1**, **3**, **4**, **10**, **13**, **17**, **19**, **22**, **23**, and **27**: HPLC chromatograms of reactions with **1**, **3**, **10**, **17**, and **27** contained at least three potential product peaks; LR-LC-MS data showed mass ions consistent with dialkylated products with **1**, **3**, **4**, **10**, **17**, and **27**, and trialkylated with **1**, **3**, and **4**; LR-LC-MS data with **1**, **4**, **17**, **19**, and **23** have two peaks with mass ion consistent with monoalkylated product, and with **13** and **22**, three peaks. For cWF, data shows the potential for multiple products in reactions with **1**, **3**, **4**, **10**, **17**, **19**, **22**, **23**, **25**, and **27**: HPLC chromatograms had multiple potential product peaks for **1**, **3**, **4**, **10**, **17**, **19**, **22**, **23**, **25**, and **27**; LR-LC-MS data indicates mass ions consistent with the dialkylated product with **10**, **17**, and **27** with **17** also containing ones consistent with trialkylated product; LR-LC-MS data shows two peaks with mass ions consistent with the monoalkylated product for **10** and two with the dialkylated product for **27**. For cWG, data suggests multiple products for reactions with **1**, **3**, **4**, **10**, **17**, **19**, **22**, **23**, and **27**: HPLC chromatograms show multiple potential product peaks for **1**, **3**, **4**, **10**, **17**, **19**, **22**, **23**, and **27**; LR-LC-MS data shows mass ions consistent with the dialkylated product for **3**, **10**, **22**, and **27** and also trialkylated for 10; and LR-LC-MS data with **10** and **17** have two peaks consistent with mass ions consistent with the monoalkylated product.

A)

B)

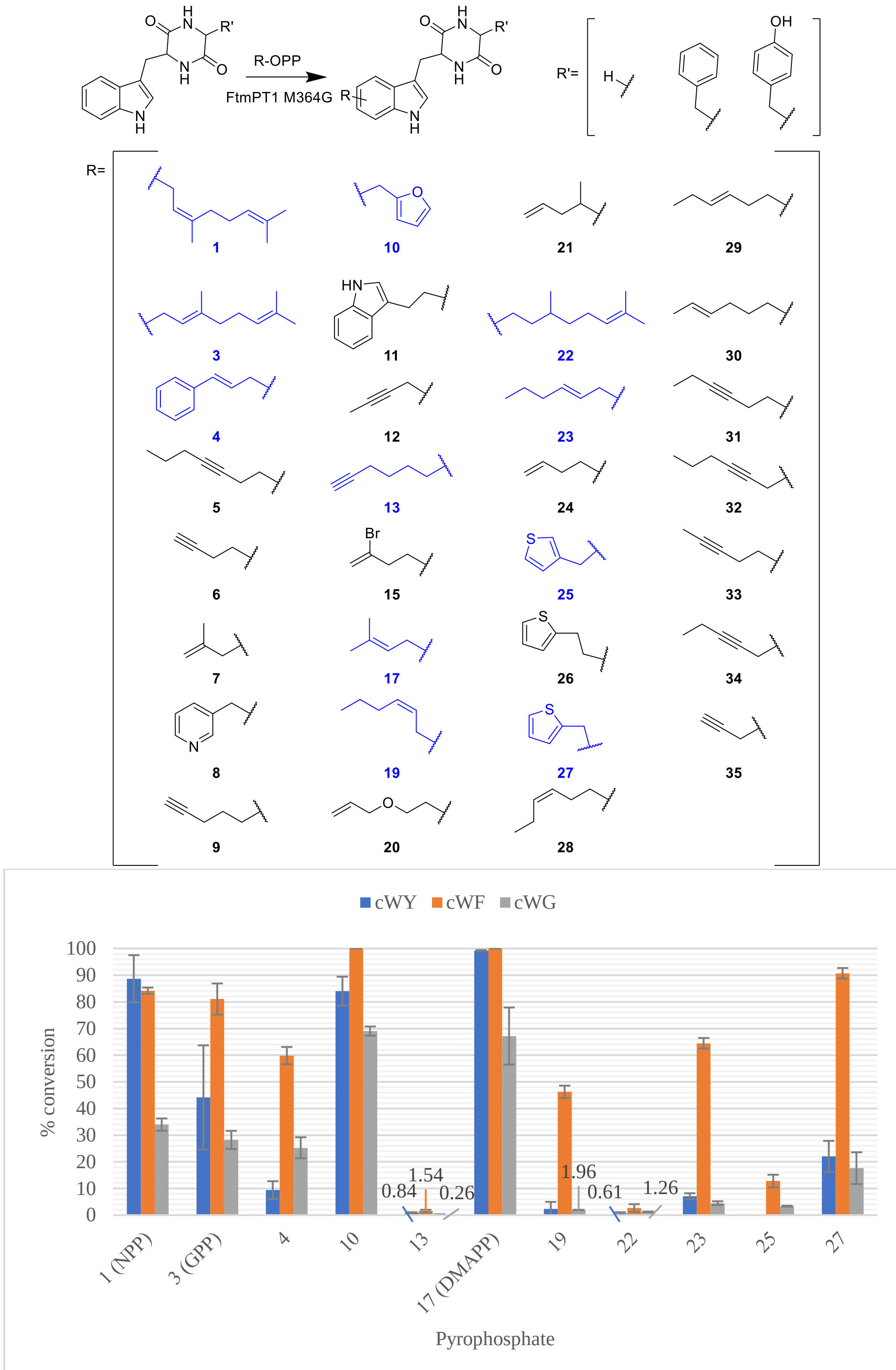

Figure 4.6. Reaction catalyzed by FtmPT1 M364G. A) FtmPT1 M364G was tested with three cyclic dipeptides and a panel of alkyl pyrophosphates. Blue: products detected by HPLC and confirmed by LR-LC-MS with mass ions consistent with the expected product with at least one of the cyclic dipeptides. B) Percent conversion with the pyrophosphates indicated in panel A. Data labels are provided for bars with <2 % for clarity. Error bars are the standard deviation of duplicates.

4.2.5. *In vivo* prenylation of cyclic dipeptides

Cultures in duplicate, expressing PhoN, IPK, and FtmPT1 or CpaD were setup feeding in DMAA and four different concentrations of cWY, cWF, or cWG (10, 5, 2.5, or 1 mM final concentration in culture) to determine if cyclic dipeptides could be prenylated *in vivo,* using 4-DMAT production cultures as a starting point for culture conditions and analysis. Once again, the noise in the HPLC traces of these *in vivo* reactions was much than that of the *in vitro* reactions, and a peak consistent in retention time for the cyclic-dipeptide prenylation product *in vitro* could not be reliably detected over the noise. However, a mass ion consistent with cyclic-dipeptide mono-prenylation product was detected in FtmPT1- and CpaD-expressing cultures in LR-LC-MS analysis (MS data in Appendix I).

4.3. Conclusion and implications

CpaD and FtmPT1 have similar activity to FgaPT2, preferring allylic alkyl pyrophosphates over any others supplied. Applying FgaPT2 M328G to CpaD and FtmPT1, the homologous mutation also increased activity with GPP and NPP. However, activity with DMAPP was not reduced in all cases. In addition, preliminary results indicate fed-in cyclic dipeptides can be prenylated *in vivo* in cultures expressing FtmPT1 and CpaD. This study lays the foundation for structure-activity studies of alkylated cyclic dipeptides which are active upon prenylation to determine how small changes in the alkyl group could change the biological activity of the molecule.

4.4. Methods

Pyrophosphates were synthesized and characterized by Sean Lund and the author Rachael Hall. The synthesis and characterization of those synthesized by Rachael Hall can be found in Chapter 2.

4.4.1. Plasmid construction

CpaD-pQTev was a gift from Dr. Xinyu Liu at University of Pittsburgh. FtmPT1-pET28a was synthesized and cloned by Twist Biosciences using *ftmPT1* (GenBank accession# AY861687) with *Nco*I and *Xho*I as cut sites.

For *in vivo* experiments with FtmPT1 and CpaD, their genes were cloned into in pCDFDuet using similar cycling parameters for cloning *fgapt2* into pCDFDuet using the following primer sets: for FtmPT1, TATACCATGGGCATGCCGCCGGC and TATAAAGCTTTTAATTCGGGAAACTCACATCG; for CpaD, TATAGAATTCGATGGAGATCTCCAAGAAAGC and TATAAAGCTTCTAAGGATTGTGGCCATCG. Both were cloned into MCS1, using *Nco*I and *Hin*dIII for FtmPT1 and *Eco*RI and *Hin*dIII for CpaD.

4.3.2. Plasmid mutagenesis

Mutations homologous to FgaPT2 M328G were made in CpaD and FtmPT1using site-directed mutagenesis with overlapping primers and the same cycling parameters described in Chapter 3 for mutagenizing FgaPT2. Primers to produce CpaD I329G were GAGCAGCTCCCCTTCGGCATAAATTTTACCTTG and CAAGGTAAAATTTATGCCGAAGGGGAGCTGCTC. Primers to produce FtmPT1 M364G were TTCGAAGCACCGATGGGCTTCCACTTCCATCTG and CAGATGGAAGTGGAAGCCCATCGGTGCTTCGAA.

4.4.3. Protein expression and purification

CpaD wild-type and mutant were transformed into chemically competent BL21(DE3) *E. coli* for expression. An overnight 3-mL culture of these cells containing 100 μg/mL of ampicillin in LB broth was grown at 37 °C with shaking at 270 rpm. A 1-L culture in LB containing 100 μg/mL of ampicillin was inoculated with 1 mL of overnight culture and grown at 37 °C with shaking at 250 rpm to an OD_{600} of 0.6. Once OD was reached, the culture was cooled to 16 °C and induced by the addition of IPTG to 0.25 mM overall. Then the culture was incubated for 12-16 hours with shaking at 200 rpm. The culture was pelleted and stored at -20 °C until purification. FtmPT1 was overexpressed in *E. coli* Rosetta PLysS in the same manner as FgaPT2 described in chapter 2 of this document.

Cell pellets overexpressing CpaD or FtmPT1 wild-type or mutant were purified in the same manner as FgaPT2 described in Chapter 2. Then the protein solutions were concentrated and buffer exchanged into storage buffer (50 mM Tris-HCl, 500 mM NaCl, 20% glycerol, pH 7.4) in 30-kDa spin filters. The concentration of protein was determined using a Bradford assay, and small aliquots of protein were stored at -80 °C until needed.

4.4.4. *In vitro* reactions

FtmPT1 reactions were setup with each cyclic dipeptide (1 mM) and the panel of pyrophosphates (3 mM) containing 50 mM Tris-HCl, 5 mM $MgCl_2$, and 100 ng/µL FtmPT1 wild-type or mutant at pH 7.5 in 100 µL. The reactions were incubated at 37 °C overnight and quenched with equal volume methanol. The reactions are then concentration and prepared for analysis using the same method as the final method for prepping FgaPT2 *in vitro* reactions for analysis. The product mixtures were analyzed by HPLC and confirmed by LR-LC-MS with mass ion consistent with expected product. The substrate (cyclic dipeptide) and product peak areas were determined by HPLC at a detection wavelength of 269 nm, and the percent conversion was calculated.

CpaD reactions were setup with each cyclic dipeptide (1 mM) and the panel of pyrophosphates (3 mM) containing 50 mM Tris-HCl, and 120 ng/µL CpaD wild-type or mutant at pH 7.5 in 100 µL. The reactions were incubated at 30 °C overnight and quenched with equal volume methanol. The reactions are then concentration and prepared for analysis using the same method as the final method for prepping FgaPT2 *in vitro* reactions for analysis. The product mixtures were analyzed by HPLC and confirmed by LR-LC-MS with mass ion consistent with expected product. The substrate (cyclic dipeptide) and product peak areas were determined by HPLC at a detection wavelength of 269 nm, and the conversion was calculated.

4.4.5. *In vivo* production

Production cultures were prepared in duplicate and run in the same manner as 4-DMAT producing cultures, switching FtmPT1- or CpaD-pCDFDuet for FgaPT2-pCDFDuet with twelve different induction solutions with IPTG to 0.5 mM, DMAA/ISO to 10 mM total, and cWG, cWF, or cWY to either 10, 5, 2.5, or 1 mM upon addition to culture. Samples were prepared for analysis in same manner as 4-DMAT cultures, and diluted lysate was analyzed via HPLC and LR-LC-MS.

CHAPTER 5: Future work and implications

There are several obvious places for work to be continued. As mentioned in previous chapters, the structures of products from FgaPT2, CpaD, and FtmPT1 reactions need to be further characterized to determine the nature of prenylation. Data suggest multiple products for several reactions, and further analysis is required to determine the product profile for each pyrophosphate for each enzyme and aromatic acceptor. Also there is the potential for optimization of the PhoN-IPK-PT pathways *in vivo* for increased product yield. There has been success in the simplest iteration, PhoN-IPK-FgaPT2, but culture conditions need to be optimized in the systems with other PTs or mutant IPK to improve yield. In addition, other forms of engineering, like RBS engineering, could be applied to optimize expression of enzymes of interest and flux through the pathway.

There are several possible continuations outside of these specific lines of questioning. Other kinases could be employed in alcohol-dependent hemiterpene pathway. Further experiments elucidating the mechanism of these PTs with non-allylic alkyl pyrophosphates. In addition, PTs outside of ABBA aromatic prenyl transferases, like reverse-prenylating PTs, UbiA-type PTs, protein PTs, or prenylelongases, could be interrogated regarding their alkyl pyrophosphate promiscuity also to determine their ability to utilize non-allylic alkyl pyrophosphates. Then the important question of whether changing small portions of the prenyl group can even change the biological activity of the molecule appreciably can be addressed with molecules which become biologically active upon prenylation.

For further work with the alcohol-dependent hemiterpene pathway, PhoN could be exchanged for another kinases or phosphatase with transphosphorylation activity. PhoN is quite promiscuous so many different alkyl monophosphates could be enzymatically synthesized.

However, PhoN can also use alkyl mono- and diphosphates as phosphate donors, depleting the molecules being synthesized in the first place. Depending on the goal, phosphorylating activity of the enzyme could outweigh its promiscuity. Two recent publications in this area used isozymes of PhoN from other species of bacteria or choline kinase in conjunction with IPK to phosphorylate DMAA and ISO to DMAPP and IPP *in vivo*.[42,43] Investigations are underway in the Williams lab to put PhoC G92D or ThiM in the place of PhoN. PhoC G92D is a mutant phosphatase which has been engineered for increased transphosphorylation activity over dephosphorylation activity and has been supplied by a collaborator, Dr. Melanie Hall at the University of Graz.[112] ThiM is a kinase involved in the biosynthesis of the cofactor thiamin in prokaryotes, phosphorylating 5-(2-hydroxyethyl)-4-methylthiazole, and it has been implicated as a kinase able to phosphorylate prenol in *E. coli*.[143] Other kinases listed in the recent Williams Lab publication are also being reinvestigated for activity which could produce non-natural mono- and diphosphates.[43]

The mechanisms of prenyltransferases have been investigated generally using their different methods: computational methods determining the energy required for proposed intermediates, using modified substrates which should alter the electronics of the reaction and comparing the changes in proxy reactions to the changes in enzymatic reactions to determine the reaction path, or using positional isotope exchange (PIX) which follows the “scrambling” of ^{18}O between a bridging and outside positions in a pyrophosphate group because ^{18}O-P bonds have different chemical shifts depending on bond order. All of these methods have their caveats but could be used to examine how a non-allylic alkyl pyrophosphate might be used by prenyltransferase, but most of the investigations into aromatic prenyltransferases specifically have used PIX.

Another obvious next step is to investigate the ability of small-molecule prenyltransferases generally (families of prenyltransferases outside of DMATS; prenylelongases and terpene synthases) to utilize non-natural pyrophosphate donors and then use these enzymes (along with studied ABBA PTs) to do any of the following: increase output of a natural small molecule, diversify a small molecule (fully terpene and hybrid) and potentially modulate its biologically activity or synthesize probes for the mechanism of downstream enzymes, or modulate/modify the activity of a protein by modifying its cofactor. Natural products which are partially terpene and partially some other family natural product are termed meroterpenes, and because of that have an inherent diversity in structure and biological activity. The other family of natural products could be anything from polyketide to amino-acid derived.

In general alkaloid-based drugs have been a target of biological synthesis and semi-synthesis because there are several FDA-approved drugs.[144] This method, using PhoN-IPK-PT, could be used to increase the yield of the prenylated indole portion of these alkaloids (specifically ones derived from tryptophan) with its natural pyrophosphate donor or to analogue with non-natural donors, using the PTs discussed in Chapters 2 and 4 or similar ones. Specifically focusing on cyclic peptides, many are prenylated, e.g. tryprostatins which are tryptophan-containing diketopiperazine natural products that are biologically active upon prenylation.[78,145] The work in Chapter 4 lays the foundation for determining the effects of small changes in the prenyl group on the biological activity of the molecule by assessing the biological activity of the prenylated, tryptophan-containing, cyclic dipeptides produced using CpaD, FtmPT1, and their mutants, but this could also be applied to other cyclic peptides and other PTs which act on them.

Outside of tryptophan-containing alkaloids, there are several other groups of natural products that could be similarly produced by increasing their natural pyrophosphate donor or diversified using non-natural alkyl pyrophosphate donors. Focusing on natural products derived from amino acids outside of peptides, novobiocin and chlorobiocin are coumarins derived from tyrosine. They are most known for their antibiotic activity but they and their analogues have a variety of other reported activities, and much of the work synthesizing and testing those analogues comes out of Brian Blagg's lab.[146–152] NovQ and CloQ are the PTs which append DMAPP onto 4-hydroxyphenyl pyruvic acid (4-HPPA) early in the biological synthesis of novobiocin and chlorobiocin, with the prenyl moiety ending up on the periphery of the molecule.[153] Many of the analogues with desirable biological activity are the result of changing or substituting the hydroxyphenyl ring originating from 4-HPPA, so further investigations of NovQ and CloQ could lead to desirable derivatives through full biological synthesis or semi-synthesis.[147,149,152]

Several meroterpenes are also derived from polyketides and fatty acids. Much work has been published recently on cannabinoids and production of their intermediates, final products, and derivatives using enzymes *in vitro* or *in vivo*.[48,154,155] Production and derivatization of the polyketide portion has been widely studied, determining which enzymes can make olivetolic acid (the polyketide precursor of cannabinoids) and what those enzymes can making using other starting materials.[156,157] The PT in this pathway appends GPP onto olivetolic acid to produce cannabigerolic acid acid, and much less is known about this transformation in terms of substrate promiscuity of the PT.[158] Because this PT is similar to others which prenylate small aromatic polyketides with longer chain pyrophosphates, NphB, a promiscuous aromatic geranyl-transferase from bacteria, has been used in *E.coli*, yeast, and in a cell-free system to produce cannabigerolic acid.[48,154,159] Very little is known about the alkyl pyrophosphate promiscuity of the enzyme from hemp extracts or NphB besides activity with NPP for hemp and an azido-analogue of GPP for NphB along with the preferred GPP.[158,160] Thus these enzymes are great candidates for further investigation with the panel of alkyl pyrophosphates described in Chapters 2 and 4 to determine the synthetic and derivatization potential of these enzymes for cannabinoid synthesis.

Many meroterpenoids are synthesized by prenylating the polyketide tetrahydroxynaphthalene (THN). In the biosynthesis of merochlorins, THN is prenylated by a PT called Mcl23 with isosesquilavandulyl diphosphate, an isomer of FPP, synthesized by prenylelongase Mcl22 from DMAPP and GPP.[58,161] Mcl23 and Mcl22 have not been investigated outside of their natural substrates to the author's knowledge, and because of that, this pathway has two potential places for further investigation and diversification with alkyl pyrophosphate donors. In the only published structure-activity study of merochlorins, Lopez-Perez et al. produced analogues of merochlorin A by changing small parts of the molecule based on the biological synthesis, and they had luck with an analogue shortening the carbon chain by one isoprene unit.[161] There is potential to access these and similar analogues with the investigation of Mcl23 and Mcl22.

Another common polyketide precursor is orsellinic acid. For example in the biosynthesis of daurichromenic acid, a meroterpenoid with anti-HIV activity, orsellenic acid is prenylated with FPP to produce grifolic acid which is then cyclized to the final product.[162] The PT in this pathway has not been identified but is thought to be similar to NphB. Gratifyingly, a mutant of NphB has been used to produce grifolic acid in *E. coli*.[159] Therefore further investigation of

NphB could enable diversification of not only cannabinoids but other natural products derived from small aromatic polyketides.

There is even potential for diversification of meroterpenoids from polyketides which take non-typical CoA-linked extender and starter units. In the first step of pyripyropene (a cholesterol medicine) biosynthesis, nicotinyl-CoA and two molecules of malonyl-CoA are condensed together to form a pyrone substituted with a pyridine, 4-hydroxy- 6-(3-pyridinyl)-2H-pyran-2-one or HPPO. Then HPPO is farnesylated by an enzyme termed pyr6. Then farnesyl-HPPO is oxidized, cyclized, and further decorated to produce pyripyropene A. The polyketide-synthase portion has been investigated a little with regard to starter-unit promiscuity and has accepted phenyl-CoA in the place of nicotinyl.[163] However there has not been any investigation into the substrate promiscuity of pyr6 with regard to alkyl pyrophosphate promiscuity. BASF has produced an analogue of pyripyropene A as an insecticide, named Afidopyropen™. The main differences are which hydroxyls are acylated and with what, so those changes are not something that would necessarily be installed using a PT. However it is gratifying to know that pyripyropene analogues are of interest to pharmaceutical companies, and pyr6 could be investigated with long-chain alkyl pyrophosphates to determine if analogues could be accessed biosynthetically.

Some important biological cofactors are synthesized via prenylation or a reaction with an allylic pyrophosphate leaving group. Prenylated cofactors and studying the synthesis of cofactors to make new ones or antibiotics. For instance, depending on the organism, thiamin pyrophosphate can be synthesized via a condensation of a pyrimidinyl pyrophosphate with a thiazole by an enzyme termed “ThiE.”[164] Some of the pyrophosphates used to examine the PTs in Chapters 2 and 4 could be used to interrogate ThiE, or the chemistry or biochemistry used to access those pyrophosphates be used to produce specific molecules to answer questions about the chemistry of thiamin pyrophosphate. In addition, flavin mononucleotide (FMN) is prenylated to serve as a cofactor for a family of reversible decarboxylases.[165] There are a few interesting points of investigation involving the PT responsible for FMN prenylation. First, depending on the organism, some are pyrophosphate-dependent but other are monophosphate dependent. The monophosphate-dependent PTs could be used to make rational mutations in pyrophosphate-dependent PTs to change them to monophosphate-dependent, and then only one alcohol phosphorylation step would be required to produce an alkyl group for use by a PT. Second, there PTs could be interrogated for their ability to use the panel of mono- or diphosphates described herein and the resultant alkylated FMN tested as cofactors for reactions. There is an interesting review paper that discusses the changes in chemistry between FMN and prenylated FMN or prFMN and how, “[the] ever-expanding range of distinct prFMN forms hints at the possibility of novel prFMN driven biochemistry yet to be discovered."[143] Thirdly, Wang et al. used an interesting screen of DMAA-phosphorylating activity to determine which enzyme already present in *E. coli* could phosphorylate DMAA, by coupling it to formation of the active form of prFMN in a protein and following the resultant color change.[165] A similar screen could be used to test candidate enzymes for their ability to phosphorylate DMAA.

Lastly, the chemistry used to access pyrophosphates in Chapters 2 and 4, could also be used to investigate protein prenyltransferases. Their proposed mechanism is associative rather than the dissociative one proposed for prenylelongases and some aromatic prenyltransferases, so it would be interesting to see how their substrate limitations vary. Considering the importance of prenylated proteins in human health, there are a few ways in which interrogation of the PTs involved could lead to more information about associated diseases. A new method for tagging prenylated proteins is to install long-chain pyrophosphates with terminal alkynes which can serve as Click handles for various visualization or pull-down methods.[166,167] There are even a few papers suggesting that certain diseases are caused by dysregulation of protein prenylation and that viruses and pathogens hijack host protein prenylation to better infect their host; they propose using PT inhibitors to combat these diseases.[168,169] More information about the mechanism of protein PTs could aid in design of inhibitors which could serve as human therapeutics.

In conclusion, there are many possibilities for continuation of this research. The alcohol-dependent hemiterpene pathway can be optimized or redesigned from the original prototype. The pyrophosphate-producing pathway or chemically synthesized pyrophosphates can be used to interrogate synthesis and structure-activity relationships of small-molecule terpenoids because specificity results herein suggest good synthetic potential for these enzymes. Even more broadly, these and similar pyrophosphates could be used to investigate proteins and cofactors which require prenylation for activity.

REFERENCES

(1) Maimone, T. J.; Baran, P. S. *Nat. Chem. Biol.* **2007**, *3* (7), 396.

(2) Moses, T.; Pollier, J. *New Phytol.* **2013**, *200*, 27.

(3) Gruchattka, E.; Hädicke, O.; Klamt, S.; Schütz, V.; Kayser, O. *Microb. Cell Fact.* **2013**, *12* (1), 84.

(4) Cunningham, F. X.; Sun, Z.; Chamovitz, D.; Hirschberg, J.; Gantt, E. *Plant Cell* **1994**, *6* (8), 1107.

(5) Furubayashi, M.; Ikezumi, M.; Kajiwara, J.; Iwasaki, M.; Fujii, A.; Li, N.; Saito, K.; Umeno, D. *PLoS One* **2014**, *9* (3).

(6) Nagel, R.; Schmidt, A.; Peters, R. J. *Planta* **2019**, *249* (1), 9.

(7) Tarshis, L. C.; Proteau, P. J.; Kellogg, B. a; Sacchettini, J. C.; Poulter, C. D. *Proc. Natl. Acad. Sci. U. S. A.* **1996**, *93* (26), 15018.

(8) Poulter, C. D.; Rilling, H. C. *Biochemistry* **1976**, *15* (5), 1079.

(9) Abdelmagid, W. M.; Adak, T.; Freeman, J. O.; Tanner, M. E. *Biochemistry* **2018**, *57* (38), 5591.

(10) Wheeler, C. J.; Croteau, R. *J. Biol. Chem.* **1987**, *262, No.17* (June), 8213.

(11) Tantillo, D. J. *Nat. Prod. Rep.* **2011**, *28* (6), 1035.

(12) Oldfield, E.; Lin, F.-Y. *Angew. Chem. Int. Ed. Engl.* **2012**, *51* (5), 1124.

(13) Yoshikuni, Y.; Ferrin, T. E.; Keasling, J. D. *Nature* **2006**, *440* (7087), 1078.

(14) Hare, S. R.; Tantillo, D. J. *Beilstein J. Org. Chem.* **2016**, *12*, 377.

(15) Xu, G.; Elkin, M.; Tantillo, D.; Newhouse, T.; Maimone, T. *Angew. Chemie Int. Ed.* **2017**.

(16) Tantillo, D. J. *Nat. Prod. Rep.* **2013**, *30* (8), 1079.

(17) Tantillo, D. J. *Angew. Chemie - Int. Ed.* **2017**, *56* (34), 10040.

(18) Wong, J.; Rios-Solis, L.; Keasling, J. D. In *Consequences of Microbial Interactions with Hydrocarbons, Oils, and Lipids: Production of Fuels and Chemicals*; Springer International Publishing: Cham, 2016; pp 1–24.

(19) Bian, G.; Deng, Z.; Liu, T. *Curr. Opin. Biotechnol.* **2017**, *48*, 234.

(20) Perez-Gil, J.; Rodriguez-Concepcion, M.; Vickers, C. E. In *Biogenesis of Fatty Acids, Lipids, and Membranes*; 2017; pp 1–22.

(21) Zhang, Y.; Nielsen, J.; Liu, Z. *FEMS Yeast Research*. December 1, 2017, pp 1–11.

(22) Niu, F.; Lu, Q.; Bu, Y.; Liu, J. *Synth. Syst. Biotechnol.* **2017**, *2* (3), 167.

(23) Zebec, Z.; Scrutton, N. S. *Adv. Biosyst.* **2018**, *2* (11), 1800056.

(24) Li, Y.; Wang, G. *J. Appl. Microbiol.* **2016**.

(25) Leavell, M. D.; McPhee, D. J.; Paddon, C. J. *Curr. Opin. Biotechnol.* **2016**, *37*, 114.

(26) Zebec, Z.; Wilkes, J.; Jervis, A. J.; Scrutton, N. S.; Takano, E.; Breitling, R. *Curr. Opin. Chem. Biol.* **2016**, *34*, 37.

(27) Vickers, C. E.; Williams, T. C.; Peng, B.; Cherry, J. *Curr. Opin. Chem. Biol.* **2017**, *40*, 47.

(28) Zhang, L.; Xiao, W.-H.; Wang, Y.; Yao, M.-D.; Jiang, G.-Z.; Zeng, B.-X.; Zhang, R.-S.; Yuan, Y.-J. *Biotechnol. Adv.* **2017**, *35* (8), 1022.

(29) Kemper, K.; Hirte, M.; Reinbold, M.; Fuchs, M.; Brück, T. *Beilstein J. Org. Chem.* **2017**, *13*, 845.

(30) Ward, V. C. A.; Chatzivasileiou, A. O.; Stephanopoulos, G. *FEMS Microbiol. Lett.* **2018**, *365* (10), 1.

(31) Lv, X.; Gu, J.; Wang, F.; Xie, W.; Liu, M.; Ye, L.; Yu, H. *Biotechnol. Bioeng.* **2016**, *113* (12), 2661.

(32) XIAO, Y.; GAO, T.; PENG, Q.; ZHANG, J.; SUN, D.; SONG, F. *J. Integr. Agric.* **2019**,

18 (3), 644.

(33) Englund, E.; Shabestary, K.; Hudson, E. P.; Lindberg, P. *Metab. Eng.* **2018**, *49*, 164.

(34) Yoon, S.-H.; Lee, Y.-M.; Kim, J.-E.; Lee, S.-H.; Lee, J.-H.; Kim, J.-Y.; Jung, K.-H.; Shin, Y.-C.; Keasling, J. D.; Kim, S.-W. *Biotechnol. Bioeng.* **2006**, *94* (6), 1025.

(35) Martin, V. J. J.; Pitera, D. J.; Withers, S. T.; Newman, J. D.; Keasling, J. D. *Nat. Biotechnol.* **2003**, *21* (7), 796.

(36) Pitera, D. J.; Paddon, C. J.; Newman, J. D.; Keasling, J. D. *Metab. Eng.* **2007**, *9* (2), 193.

(37) Kang, A.; Meadows, C. W.; Canu, N.; Keasling, J. D.; Lee, T. S. *Metab. Eng.* **2017**, *41* (April), 125.

(38) Alonso-Gutierrez, J.; Koma, D.; Hu, Q.; Yang, Y.; Chan, L. J. G.; Petzold, C. J.; Adams, P. D.; Vickers, C. E.; Nielsen, L. K.; Keasling, J. D.; Lee, T. S. *Biotechnol. Bioeng.* **2018**, *115* (4), 1000.

(39) Kirby, J.; Dietzel, K. L.; Wichmann, G.; Chan, R.; Antipov, E.; Moss, N.; Baidoo, E. E. K.; Jackson, P.; Gaucher, S. P.; Gottlieb, S.; LaBarge, J.; Mahatdejkul, T.; Hawkins, K. M.; Muley, S.; Newman, J. D.; Liu, P.; Keasling, J. D.; Zhao, L. *Metab. Eng.* **2016**, *38*, 494.

(40) Kwak, S.; Kim, S. R.; Xu, H.; Zhang, G.-C.; Lane, S.; Kim, H.; Jin, Y.-S. *Biotechnol. Bioeng.* **2017**, *114* (11), 2581.

(41) King, J. R.; Woolston, B. M.; Stephanopoulos, G. *ACS Synth. Biol.* **2017**, *6* (7), 1416.

(42) Chatzivasileiou, A. O.; Ward, V.; Edgar, S. M.; Stephanopoulos, G. *Proc. Natl. Acad. Sci.* **2019**, *116* (2), 506.

(43) Lund, S.; Hall, R.; Williams, G. J. *ACS Synth. Biol.* **2019**, *8* (2), 232.

(44) Korman, T. P.; Sahachartsiri, B.; Li, D.; Vinokur, J. M.; Eisenberg, D.; Bowie, J. U.

Protein Sci. **2014**, *23* (5), 576.

(45) Opgenorth, P. H.; Korman, T. P.; Bowie, J. U. *Nat. Chem. Biol.* **2016**, *12* (6), 393.

(46) Korman, T. P.; Opgenorth, P. H.; Bowie, J. U. *Nat. Commun.* **2017**, *8* (May), 15526.

(47) Opgenorth, P. H.; Korman, T. P.; Iancu, L.; Bowie, J. U. *Nat. Chem. Biol.* **2017**, *13* (9), 938.

(48) Valliere, M. A.; Korman, T. P.; Woodall, N. B.; Khitrov, G. A.; Taylor, R. E.; Baker, D.; Bowie, J. U. *Nat. Commun.* **2019**, *10* (1), 1.

(49) Dirkmann, M.; Nowack, J.; Schulz, F. *ChemBioChem* **2018**, *19* (20), 2146.

(50) Edgar, S.; Li, F.; Qiao, K.; Weng, J.; Stephanopoulos, G. *ACS Synth. Biol.* **2017**, *6* (2), 201.

(51) Eslami, H.; Mohtashami, S. K.; Basmanj, M. T.; Rahati, M.; Rahimi, H. *J. Mol. Model.* **2017**, *23* (7), 202.

(52) Muangphrom, P.; Seki, H.; Muranaka, T. *Biotarget* **2017**, *1*, 19.

(53) Abdallah, I. I.; van Merkerk, R.; Klumpenaar, E.; Quax, W. J. *Sci. Rep.* **2018**, *8* (1), 9961.

(54) Tang, X.; Demiray, M.; Wirth, T.; Allemann, R. K. *Bioorg. Med. Chem.* **2018**, *26* (7), 1314.

(55) Vattekkatte, A.; Garms, S.; Brandt, W.; Boland, W. *Org. Biomol. Chem.* **2018**, *16* (3), 348.

(56) Xu, J.; Ai, Y.; Wang, J.; Xu, J.; Zhang, Y.; Yang, D. *Phytochemistry* **2017**, *137*, 34.

(57) Bian, G.; Han, Y.; Hou, A.; Yuan, Y.; Liu, X.; Deng, Z.; Liu, T. *Metab. Eng.* **2017**, *42*, 1.

(58) Teufel, R. In *Methods in Enzymology*; Elsevier Inc., 2018; pp 425–439.

(59) Ignea, C.; Pontini, M.; Motawia, M. S.; Maffei, M. E.; Makris, A. M.; Kampranis, S. C. *Nat. Chem. Biol.* **2018**, *14* (12), 1090.

(60) Ramamoorthy, G.; Phan, R. M.; Poulter, C. D. *J. Org. Chem.* **2016**, *81* (12), 5093.

(61) Kudoh, T.; Park, C. S.; Lefurgy, S. T.; Sun, M.; Michels, T.; Leyh, T. S.; Silverman, R. B. *Bioorganic Med. Chem.* **2010**, *18* (3), 1124.

(62) Lefurgy, S. T.; Rodriguez, S. B.; Park, C. S.; Cahill, S.; Silverman, R. B.; Leyh, T. S. *J. Biol. Chem.* **2010**, *285* (27), 20654.

(63) Clarke, S. *Annu. Rev. Biochem.* **1992**, *61*, 355.

(64) Wang, B. H.; Ternai, B.; Polyat, G. *Phytochemistry* **1997**, *44* (5), 787.

(65) Murakami, a; Gao, G.; Omura, M.; Yano, M.; Ito, C.; Furukawa, H.; Takahashi, D.; Koshimizu, K.; Ohigashi, H. *Bioorg. Med. Chem. Lett.* **2000**, *10*, 59.

(66) Maitrejean, M.; Comte, G.; Barron, D.; El Kirat, K.; Conseil, G.; Di Pietro, a. *Bioorg. Med. Chem. Lett.* **2000**, *10*, 157.

(67) Rouger, C.; Derbré, S.; Richomme, P. *Phytochem. Rev.* **2018**, *440*, 1.

(68) Saleh, O.; Haagen, Y.; Seeger, K.; Heide, L. *Phytochemistry* **2009**, *70*, 1728.

(69) Borodina, I.; Nielsen, J. *Biotechnol. J.* **2014**, *9* (5), 609.

(70) Li, S. M. *Phytochemistry* **2009**, *70*, 1746.

(71) Li, S.-M. *Nat. Prod. Rep.* **2010**, *27*, 57.

(72) Yu, X.; Li, S.-M. *Methods Enzymol.* **2012**, *516*, 259.

(73) Heide, L. *Curr. Opin. Chem. Biol.* **2009**, *13* (2), 171.

(74) Kumano, T.; Richard, S. B.; Noel, J. P.; Nishiyama, M.; Kuzuyama, T. *Bioorg. Med. Chem.* **2008**, *16* (17), 8117.

(75) Winkelblech, J.; Li, S.-M. *Chembiochem a Eur. J. Chem. Biol.* **2014**, *15* (7), 1030.

(76) Fan, A.; Winkelblech, J.; Li, S. M. *Appl. Microbiol. Biotechnol.* **2015**, *99* (18), 7399.

(77) Chen, R.; Gao, B.; Liu, X.; Ruan, F.; Zhang, Y.; Lou, J.; Feng, K.; Wunsch, C.; Li, S.-M.;

Dai, J.; Sun, F. *Nat. Chem. Biol.* **2016**, *13* (2), 226.

(78) Elshahawi, S. I.; Cao, H.; Shaaban, K. A.; Ponomareva, L. V; Subramanian, T.; Farman, M. L.; Spielmann, H. P.; Phillips, G. N.; Thorson, J. S.; Singh, S. *Nat. Chem. Biol.* **2017**, *13* (4), 366.

(79) Tello, M.; Kuzuyama, T.; Heide, L.; Noel, J. P.; Richard, S. B. *Cell. Mol. Life Sci.* **2008**, *65* (10), 1459.

(80) Liebhold, M.; Xie, X.; Li, S. M. *Org. Lett.* **2013**, *15*, 3062.

(81) Liebhold, M.; Xie, X.; Li, S. M. *Org. Lett.* **2012**, *14* (18), 4882.

(82) Liebhold, M.; Xie, X.; Li, S. M. *Org. Lett.* **2013**, *15* (3), 3062.

(83) Winkelblech, J.; Liebhold, M.; Gunera, J.; Xie, X.; Kolb, P.; Li, S. M. *Adv. Synth. Catal.* **2015**, *357* (5), 975.

(84) Bandari, C.; Scull, E. M.; Masterson, J. M.; Tran, R. H. Q.; Foster, S. B.; Nicholas, K. M.; Singh, S. *ChemBioChem* **2017**, *18* (23), 2323.

(85) Fan, A.; Zocher, G.; Stec, E.; Stehle, T.; Li, S. M. *J. Biol. Chem.* **2015**, *290* (3), 1364.

(86) Jost, M.; Zocher, G.; Tarcz, S.; Matuschek, M.; Xie, X.; Li, S. M.; Stehle, T. *J. Am. Chem. Soc.* **2010**, *132* (50), 17849.

(87) Zheng, L.; Mai, P.; Fan, A.; Li, S.-M. *Org. Biomol. Chem.* **2018**, *16* (36), 6688.

(88) Fan, A.; Li, S.-M. *Appl. Microbiol. Biotechnol.* **2016**, *100* (12), 5389.

(89) Zhao, W.; Fan, A.; Tarcz, S.; Zhou, K.; Yin, W.-B.; Liu, X.-Q.; Li, S.-M. *Appl. Microbiol. Biotechnol.* **2017**, *101* (5), 1989.

(90) Zhou, K.; Zhao, W.; Liu, X.-Q.; Li, S.-M. *Appl. Microbiol. Biotechnol.* **2016**, *100* (23), 9943.

(91) Chen, R.; Gao, B.; Liu, X.; Ruan, F.; Zhang, Y.; Lou, J.; Feng, K.; Wunsch, C.; Li, S.-M.;

Dai, J.; Sun, F. *Nat. Chem. Biol.* **2017**, *13* (2), 226.

(92) Estrada, P.; Morita, M.; Hao, Y.; Schmidt, E. W.; Nair, S. K. *J. Am. Chem. Soc.* **2018**, *140* (26), 8124.

(93) Mai, P.; Zocher, G.; Stehle, T.; Li, S.-M. *Org. Biomol. Chem.* **2018**, *16* (40), 7461.

(94) Liao, G.; Mai, P.; Fan, J.; Zocher, G.; Stehle, T.; Li, S.-M. *Org. Lett.* **2018**, *20* (22), 7201.

(95) Kalkreuter, E.; Carpenter, S. M.; Williams, G. J. In *Chemical and Biological Synthesis: Enabling Approaches for Understanding Biology*; 2018; pp 275–312.

(96) Kalkreuter, E.; Williams, G. J.; Van Wezel, G.; Wright, G. *Curr. Opin. Microbiol.* **2018**, *45*, 140.

(97) van Dijk, J. W. A.; Wang, C. C. C. *Org. Lett.* **2018**, *20* (17), 5082.

(98) Chen, M.; Poulter, C. D. *Biochemistry* **2010**, *49* (1), 207.

(99) Mabanglo, M. F.; Pan, J. J.; Shakya, B.; Poulter, C. D. *ACS Chem. Biol.* **2012**, *7* (7), 1241.

(100) Dellas, N.; Noel, J. P. *ACS Chem. Biol.* **2010**, *5* (6), 589.

(101) Lund, S. R. Accessing non-natural terpenes via synthetic biology, 2017.

(102) Lund, S.; Courtney, T.; Williams, G. J. *ChemRxiv* **2019**.

(103) Liu, Y.; Yan, Z.; Lu, X.; Xiao, D.; Jiang, H. *Sci. Rep.* **2016**, *6*.

(104) Fitzpatrick, a. H.; Bhandari, J.; Crowell, D. N. *Plant J.* **2011**, *66*, 1078.

(105) Uchiya, K. I.; Tohsuji, M.; Nikai, T.; Sugihara, H.; Sasakawa, C. *J. Bacteriol.* **1996**, *178* (15), 4548.

(106) Tanaka, N.; Hasan, Z.; Hartog, A. F.; van Herk, T.; Wever, R.; Sanders, R.-J. *Org. Biomol. Chem.* **2003**, *1* (16), 2833.

(107) Van Herk, T.; Hartog, A. F.; Van Der Burg, A. M.; Wever, R. *Adv. Synth. Catal.* **2005**, *347* (7–8), 1155.

(108) Van Herk, T.; Hartog, A. F.; Schoemaker, H. E.; Wever, R. *J. Org. Chem.* **2006**, *71* (16), 6244.

(109) Makde, R. D.; Dikshit, K.; Kumar, V. *Biomol. Eng.* **2006**, *23* (5), 247.

(110) van Herk, T.; Hartog, A. F.; Babich, L.; Schoemaker, H. E.; Wever, R. *ChemBioChem* **2009**, *10*, 2230.

(111) Babich, L.; Hartog, A. F.; Van Der Horst, M. a.; Wever, R. *Chem. - A Eur. J.* **2012**, *18* (21), 6604.

(112) Tasnádi, G.; Zechner, M.; Hall, M.; Baldenius, K.; Ditrich, K.; Faber, K. *Biotechnol. Bioeng.* **2017**, *114* (10), 2187.

(113) Tasnádi, G.; Lukesch, M.; Zechner, M.; Jud, W.; Hall, M.; Ditrich, K.; Baldenius, K.; Hartog, A. F.; Wever, R.; Faber, K. *European J. Org. Chem.* **2016**, *2016* (1), 45.

(114) Makde, R. D.; Mahajan, S. K.; Kumar, V. *Biochemistry* **2007**, *46* (8), 2079.

(115) Tasnádi, G.; Jud, W.; Hall, M.; Baldenius, K.; Ditrich, K.; Faber, K. *Adv. Synth. Catal.* **2018**, *360* (12), 2394.

(116) Mihara, Y.; Utagawa, T.; Yamada, H.; Asano, Y. *Appl. Environ. Microbiol.* **2000**, *66* (7), 2811.

(117) Unsöld, I. a.; Li, S. M. *Microbiology* **2005**, *151*, 1499.

(118) Liebhold, M.; Li, S. M. *Org. Lett.* **2013**, *15* (22), 5834.

(119) Yu, X.; Yang, A.; Lin, W.; Li, S. M. *Tetrahedron Lett.* **2012**, *53* (50), 6861.

(120) Steffan, N.; Li, S. M. *Arch. Microbiol.* **2009**, *191*, 461.

(121) Steffan, N.; Unsöld, I. a.; Li, S. M. *ChemBioChem* **2007**, *8*, 1298.

(122) Elshahawi, S. I.; Cao, H.; Shaaban, K. A.; Ponomareva, L. V; Subramanian, T.; Farman, M. L.; Spielmann, H. P.; Phillips, G. N.; Thorson, J. S.; Singh, S. *Nat. Chem. Biol.* **2017**,

13 (4), 366.

(123) Fan, A.; Zocher, G.; Stec, E.; Stehle, T.; Li, S.-M. *J. Biol. Chem.* **2015**, *290* (3), 1364.

(124) Tanner, M. E. *Nat. Prod. Rep.* **2015**, *32* (1), 88.

(125) Luk, L. Y. P.; Tanner, M. E. *J. Am. Chem. Soc.* **2009**, *131* (39), 13932.

(126) Metzger, U.; Keller, S.; Stevenson, C. E. M.; Heide, L.; Lawson, D. M. *J. Mol. Biol.* **2010**, *404* (4), 611.

(127) Bayse, C. A.; Merz, K. M. *Biochemistry* **2014**, *53* (30), 5034.

(128) Yang, Y.; Miao, Y.; Wang, B.; Cui, G.; Merz, K. M. *Biochemistry* **2012**, *51* (12), 2606.

(129) Schuller, J. M.; Zocher, G.; Liebhold, M.; Xie, X.; Stahl, M.; Li, S. M.; Stehle, T. *J. Mol. Biol.* **2012**, *422* (1), 87.

(130) Kalkreuter, E.; CroweTipton, J. M.; Lowell, A. N.; Sherman, D. H.; Williams, G. J. *J. Am. Chem. Soc.* **2019**, *141* (5), 1961.

(131) Carpenter, S. M.; Williams, G. J. *ACS Chem. Biol.* **2018**, *13* (12), 3361.

(132) Koryakina, I.; McArthur, J. *ACS Chem. Biol.* **2012**, *8* (1), 200.

(133) Koryakina, I.; Williams, G. *ChemBioChem* **2011**, *12* (15), 2289.

(134) Koryakina, I.; McArthur, J. *Org. Biomol. Chem.* **2013**, *11* (27), 4449.

(135) Koryakina, I.; Kasey, C.; McArthur, J. B.; Lowell, A. N.; Chemler, J. A.; Li, S.; Hansen, D. A.; Sherman, D. H.; Williams, G. J. *ACS Chem. Biol.* **2017**, *12* (1), 114.

(136) Liu, X.; Walsh, C. T. *Biochemistry* **2009**, *48* (46), 11032.

(137) Liu, X.; Walsh, C. T. *Biochemistry* **2009**, *48*, 8746.

(138) Grundmann, A. *Microbiology* **2005**, *151* (7), 2199.

(139) Wollinsky, B.; Ludwig, L.; Xie, X.; Li, S.-M. *Org. Biomol. Chem.* **2012**, *10*, 9262.

(140) Pan, L. L.; Song, L. F.; Miao, Y.; Yang, Y.; Merz, K. M. *Biochemistry* **2017**, *56* (24),

2995.

(141) Mai, P.; Coby, L.; Li, S. *Appl. Microbiol. Biotechnol.* **2019**, *103* (9), 3773.

(142) Liebhold, M.; Xie, X.; Li, S. M. *Org. Lett.* **2013**, *15* (12), 3062.

(143) Leys, D. *Curr. Opin. Chem. Biol.* **2018**, *47*, 117.

(144) Ehrenworth, A. M.; Peralta-Yahya, P. *Nat. Chem. Biol.* **2017**, *13* (3), 249.

(145) Ma, Y.-M.; Liang, X.-A.; Kong, Y.; Jia, B. *J. Agric. Food Chem.* **2016**, *64* (35), 6659.

(146) Donnelly, A.; Blagg, B. *Curr. Med. Chem.* **2008**, *15* (26), 2702.

(147) Davis, R. E.; Zhang, Z.; Blagg, B. S. J. *Medchemcomm* **2017**, *8* (3), 593.

(148) Ghosh, S.; Liu, Y.; Garg, G.; Anyika, M.; McPherson, N. T.; Ma, J.; Dobrowsky, R. T.; Blagg, B. S. J. *ACS Med. Chem. Lett.* **2016**, *7* (8), 813.

(149) Burlison, J. A.; Neckers, L.; Smith, A. B.; Maxwell, A.; Blagg, B. S. J. *J. Am. Chem. Soc.* **2006**, *128* (48), 15529.

(150) Yu, X. M.; Shen, G.; Neckers, L.; Blake, H.; Holzbeierlein, J.; Cronk, B.; Blagg, B. S. J. *J. Am. Chem. Soc.* **2005**, *127* (37), 12778.

(151) Byrd, K. M.; Subramanian, C.; Sanchez, J.; Motiwala, H. F.; Liu, W.; Cohen, M. S.; Holzbeierlein, J.; Blagg, B. S. J. *Chem. - A Eur. J.* **2016**, *22* (20), 6921.

(152) Hall, J. A.; Seedarala, S.; Zhao, H.; Garg, G.; Ghosh, S.; Blagg, B. S. J. *J. Med. Chem.* **2016**, *59* (3), 925.

(153) Eustáquio, A. S.; Gust, B.; Galm, U.; Chater, K. F.; Heide, L.; Eusta, A. S.; Li, S. *Appl. Environ. Microbiol.* **2005**, *71* (5), 2452.

(154) Zirpel, B.; Degenhardt, F.; Martin, C.; Kayser, O.; Stehle, F. *J. Biotechnol.* **2017**.

(155) Luo, X.; Reiter, M. A.; D'Espaux, L.; Wong, J.; Denby, C. M.; Lechner, A.; Zhang, Y.; Grzybowski, A. T.; Harth, S.; Lin, W.; Lee, H.; Yu, C.; Shin, J.; Deng, K.; Benites, V. T.;

Wang, G.; Baidoo, E. E. K.; Chen, Y.; Dev, I.; Petzold, C. J.; Keasling, J. D. *Nature* **2019**, *567* (7746), 123.

(156) Flores-Sanchez, I. J.; Verpoorte, R. *Plant Cell Physiol.* **2008**, *49* (12), 1767.

(157) Abe, I.; Watanabe, T.; Noguchi, H. *Phytochemistry* **2004**, *65* (17), 2447.

(158) Fellermeier, M.; Zenk, M. H. *FEBS Lett.* **1998**, *427* (2), 283.

(159) Qian, S.; Clomburg, J. M.; Gonzalez, R. *Biotechnol. Bioeng.* **2019**, *116* (5), 1116.

(160) Xiao, Y.; Machacek, M.; Lee, K.; Kuzuyama, T.; Liu, P. *Mol. Biosyst.* **2009**, *5* (9), 913.

(161) López-Pérez, B.; Pepper, H. P.; Ma, R.; Fawcett, B. J.; Pehere, A. D.; Wei, Q.; Ji, Z.; Polyak, S. W.; Dai, H.; Song, F.; Abell, A. D.; Zhang, L.; George, J. H. *ChemMedChem* **2017**, *12* (23), 1969.

(162) Saeki, H.; Hara, R.; Takahashi, H.; Iijima, M.; Munakata, R.; Kenmoku, H.; Fuku, K.; Sekihara, A.; Yasuno, Y.; Shinada, T.; Ueda, D.; Nishi, T.; Sato, T.; Asakawa, Y.; Kurosaki, F.; Yazaki, K.; Taura, F. *Plant Physiol.* **2018**, *178* (2), 535.

(163) Itoh, T.; Tokunaga, K.; Matsuda, Y.; Fujii, I.; Abe, I.; Ebizuka, Y.; Kushiro, T. *Nat. Chem.* **2010**, *2* (10), 858.

(164) Jurgenson, C. T.; Begley, T. P.; Ealick, S. E. *Annu. Rev. Biochem.* **2009**, *78* (1), 569.

(165) Wang, P.; Khusnutdinova, A. N.; Luo, F.; Xiao, J.; Nemr, K.; Flick, R.; Brown, G.; Mahadevan, R.; Edwards, E. A.; Yakunin, A. F. *Cell Chem. Biol.* **2018**, *25* (5), 560.

(166) Suazo, K. F.; Schaber, C.; Palsuledesai, C. C.; Odom John, A. R.; Distefano, M. D. *Sci. Rep.* **2016**, *6* (1), 38615.

(167) Palsuledesai, C. C.; Ochocki, J. D.; Kuhns, M. M.; Wang, Y.-C.; Warmka, J. K.; Chernick, D. S.; Wattenberg, E. V; Li, L.; Arriaga, E. A.; Distefano, M. D. *ACS Chem. Biol.* **2016**, *11* (10), 2820.

(168) Marakasova, E. S.; Eisenhaber, B.; Maurer-Stroh, S.; Eisenhaber, F.; Baranova, A. *BioEssays* **2017**, *39* (10), 1700014.

(169) Jeong, A.; Suazo, K. F.; Wood, W. G.; Distefano, M. D.; Li, L. *Crit. Rev. Biochem. Mol. Biol.* **2018**, *53* (3), 279.

APPENDIX

APPENDIX A: Supplementary information

A.1. PhoN *in vitro*

Table A.1. Sample data from a replicate of PhoN. Reactions analyzed via HR-LC-MS with addition of an internal standard for yield calculation.

	Product				Standard			
OH#	Theo M-H	Exp M-H	Rt	EIC	Theo M-H	Exp M-H	EIC	Rt
1	233.0948	233.0945	3.89	1.29E+08	165.0317	165.0319	7.69E+07	0.77
2	206.9881	206.9884	1.25	1.98E+07	165.0317	165.032	1.92E+07	0.78
3	233.0948	233.0945	3.95	7.17E+07	165.0317	165.0319	2.41E+07	0.77
4	213.0317	213.032	2.9	5.42E+07	165.0317	165.032	1.42E+07	0.77
5	191.0473	191.0477	2.45	1.32E+07	165.0317	165.0319	2.87E+07	0.78
7	151.016	151.0163	0.48	7.46E+07	213.0317	213.0319	5.44E+07	2.84
8	188.0113	188.0118	0.39	1.49E+07	165.0317	165.032	3.26E+07	0.8
9	163.016	163.0164	0.47	6.87E+07	213.0317	213.032	3.61E+07	2.88
10	176.9953	176.9957	0.48	5.22E+07	213.0317	213.032	2.25E+07	2.85
11	240.0426	240.0429	2.5	5.24E+07	165.0317	165.0319	1.82E+07	0.76
12	149.0004	149.0007	0.44	9.81E+06	213.0317	213.032	1.21E+07	2.87
13	177.0317	177.0321	0.76	1.52E+06	213.0317	213.0323	1.10E+06	2.89
14	301.1569	301.1573	5.02	8.00E+06	165.0317	165.032	1.07E+07	0.77
15	228.9265	228.9269	0.85	1.81E+07	165.0317	165.032	6.52E+07	0.78
16	165.0317	165.0319	0.74	6.87E+07	213.0317	213.0321	3.63E+07	2.88
17	165.0317	165.032	0.76	7.27E+07	213.0317	213.0322	2.29E+07	2.89
6	149.0004	149.0009	0.4	8.44E+06	213.0317	213.0322	1.33E+07	2.87
18	165.0317	165.032	0.78	6.85E+07	213.0317	213.0321	4.83E+07	2.87
19	179.0473	179.0478	2.24	4.02E+07	213.0317	213.0321	3.40E+07	2.89
20	181.0266	181.0273	0.51	4.03E+07	165.0317	165.0321	3.67E+07	0.8
21	165.0317	165.0322	0.74	1.81E+06	213.0317	213.0323	4.79E+06	2.87
23	179.0473	179.0478	2.42	6.06E+07	213.0317	213.0322	1.25E+07	2.88
23	235.1099	235.1103	4.11	3.76E+07	165.0317	165.0321	2.37E+07	0.78

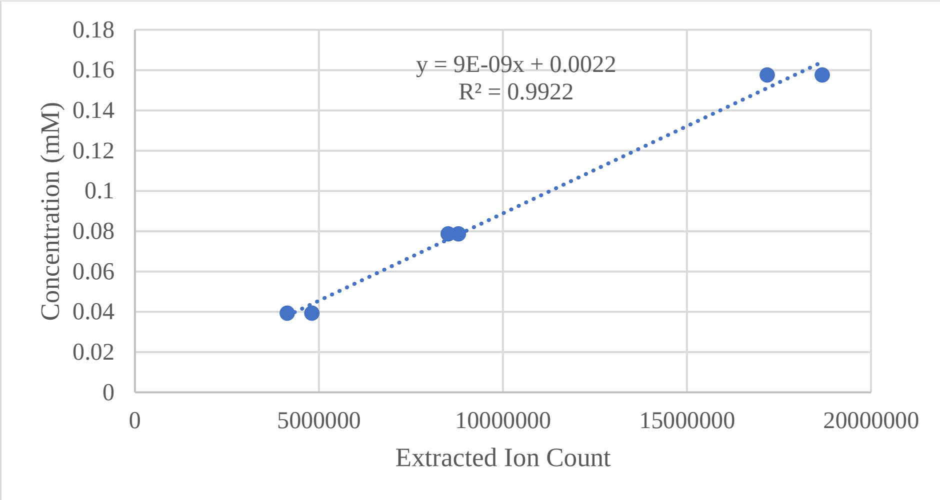

Figure A.1. Calibration curve to interconvert extracted ion count and concentration and calculate PhoN reaction yields. Data points are the average of three replicates at each concentration of monophosphates 17 and 4.

A.2. FgaPT2 *in vivo* and *in vitro*

Table A.2. HR-LC-MS analysis of FgaPT2 reactions *in vitro*. "--" = not detected.

	Product				
PP#	Calc M+H	Exp M+H	delta ppm	EIC	Rt (min)
24	259.1441	259.1446	-1.92943	1.93E+05	4.86, 5.06
21	273.1598	273.1601	-1.09826	2.91E+04	5.15, 5.27
15	337.0546	337.0551	-1.48344	3.00E+03	5.39
	339.0546	339.0536	2.949377	6.91E+03	5.4
9	271.1441	271.1447	-2.21285	1.25E+04	4.44, 5.08, 5.89
7	259.1441	259.1441	0	3.57E+07	4.99
18	273.1598	273.1602	-1.46434	6.66E+04	4.57, 5.27, 5.41
19	287.1754	287.1747	2.437535	1.55E+09	5.63
23	287.1754	287.1748	2.089315	2.48E+09	5.66
6	257.1285	257.1279	2.333464	2.55E+07	4.96
4	321.1598	321.1598	0	7.21E+03	5.44, 5.63
5	299.1754	--	--	5.47E+03	--
2	315.1162	--	--	0.00E+00	--
10	285.1234	285.1229	1.753627	5.84E+08	4.75, 4.90
12	257.1285	257.128	1.944553	4.41E+07	4.69
8	296.1394	296.1392	0.675358	5.33E+07	0.74
13	285.1598	285.1598	0	2.60E+06	5.28, 5.45
20	289.1547	289.1542	1.729178	5.93E+05	7.23
11	348.1707	--	--	4.39E+03	--
17	273.1598	273.1591	2.562603	2.40E+09	5.26

Table A.3. LR-LC-MS analysis of FgaPT2 reactions, sample replicate. "--" = not detected.

	PP-H				Trp+H				Prod+H			
PP #	Calc	Exp	peak height	Rt (min)	Calc	Exp	peak height	Rt (min)	Calc	Exp	peak height	Rt (min)
1	313.06	312.95	6.10E+06	1.6	205.10	205.05	6.00E+05	0.43	341.22	341.15	2.50E+05	1.75
3	313.06	312.95	6.10E+06	1.65	205.10	205.05	3.90E+05	0.4	341.22	341.15	2.60E+05	1.8
4	293.00	292.90	2.90E+06	0.55	205.10	205.10	5.70E+05	0.43	321.16	321.10	5.00E+05	1.55
5	271.01	270.90	4.30E+06	0.45	205.10	205.10	6.00E+05	0.43	299.18	--	--	--
6	228.97	228.90	3.40E+05	0.43	205.10	205.05	7.00E+05	0.43	257.13	257.05	2.50E+05	1.3
7	230.98	230.90	1.25E+06	0.43	205.10	205.05	5.00E+05	0.43	259.14	--	--	--
8	267.98	267.90	1.30E+05	0.35	205.10	205.10	4.20E+05	0.43	296.14	296.10	2.00E+04	0.35
9	242.98	242.90	8.20E+05	0.43	205.10	205.10	7.50E+05	0.43	271.14	271.10	1.90E+04	1.2
10	256.96	256.90	6.00E+05	0.45	205.10	205.05	7.00E+05	0.45	285.12	285.10	3.80E+06	1.25
11	320.01	319.95	1.65E+06	0.65	205.10	205.10	4.50E+05	0.5	348.17	--	--	--
12	228.97	228.90	2.20E+05	0.43	205.10	205.05	3.30E+05	0.43	257.13	257.10	6.00E+04	1.23
13	257.00	256.90	1.15E+06	0.45	205.10	205.05	4.50E+05	0.43	285.16	285.15	1.00E+05	1.5
15	308.89	308.80	1.80E+05	0.5	205.10	205.05	5.80E+05	0.43	337.06	--	--	--
17	245.00	244.90	1.30E+06	0.45	205.10	205.00	4.20E+04	1.43	273.16	273.10	6.50E+06	1.43
19	259.01	258.95	2.00E+06	0.5	205.10	205.10	4.50E+05	0.43	287.18	287.15	1.45E+06	1.6
20	260.99	260.95	1.75E+06	0.43	205.10	205.05	4.00E+05	0.43	289.16	289.20	1.35E+04	1.25
21	245.00	244.90	8.40E+05	0.47	205.10	205.05	6.00E+05	0.43	273.16	--	--	--
22	315.08	314.95	7.00E+06	1.65	205.10	205.05	6.40E+05	0.43	343.24	--	--	--
23	259.01	258.90	5.00E+05	0.6	205.10	--	--	--	287.18	287.10	3.30E+06	1.6

Table A.3 (continued)

24	230.98	230.90	1.00E+06	0.37	205.10	205.05	8.40E+05	0.45	259.14	--	--	--
25	272.94	272.85	6.30E+05	0.43	205.10	205.10	2.60E+05	0.47	301.11	301.05	7.70E+05	1.4
26	286.95	286.90	1.85E+06	0.43	205.10	205.10	3.00E+05	0.43	315.12	--	--	--
27	272.94	272.85	1.10E+06	0.43	205.10	205.10	3.50E+05	0.43	301.11	301.05	1.30E+06	1.33
28	259.01	259.00	1.00E+06	0.5	205.10	205.10	4.00E+05	0.43	287.18	287.15	1.30E+04	1.6
29	259.01	258.95	2.70E+06	0.45	205.10	205.05	4.00E+05	0.47	287.18	287.10	3.50E+05	1.6
30	259.01	258.95	4.30E+06	0.5	205.10	205.05	1.00E+06	0.5	287.18	--	--	--
31	257.00	256.90	1.40E+06	0.45	205.10	205.05	6.50E+05	0.43	285.16	--	--	--
32	257.00	256.90	2.20E+06	0.43	205.10	205.05	6.50E+05	0.43	285.16	285.10	5.00E+04	1.45
33	242.98	242.85	1.60E+06	0.45	205.10	205.10	5.50E+05	0.45	271.14	271.20	2.35E+04	1.23
34	242.98	242.90	1.80E+06	0.43	205.10	205.05	9.00E+05	0.45	271.14	271.10	6.50E+04, 4.00E+04	1.35, 1.2
35	214.96	214.90	3.60E+05	0.4	205.10	205.05	7.40E+05	0.45	243.12	--	--	--

Table A.4. LR-LC-MS analysis of FgaPT2 reactions sample replicate, looking for multiple prenylations. "--" indicates not detected, "x" means outside of mass range for particular LR-LC-MS run.

	+2 alkyl, M+H				+3alkyl, M+H			
PP#	Calc	Exp	peak height	Rt (min)	Calc	Exp	peak height	Rt (min)
1	477.35	477.35	3.50E+04	1.77	613.47	x	x	x
3	477.35	477.30	4.20E+04	1.77	613.47	x	x	x
4	437.22	437.15	6.00E+04	2.07	553.29	x	x	x
5	393.25	393.25	3.00E+04	1.63	487.33	--	--	--
6	309.16	--	--	--	361.19	--	--	--
7	313.19	--	--	--	367.24	--	--	--
8	387.18	--	--	--	478.22	478.20	1.50E+04	2.07
9	337.19	--	--	--	403.24	--	--	--
10	365.15	365.10	3.70E+04	1.53	445.18	--	--	--
11	491.24	--	--	--	634.32	x	x	x

Table A.4 (continued)

12	309.16	--	--	--	361.19	--	--	--
13	365.22	--	--	--	445.29	--	--	--
15	469.01	--	--	--	600.97	x	x	x
17	341.22	341.20	3.45E+05	1.77	409.29	409.55	5.00E+04	1.37
19	369.25	369.05	1.90E+04	0.33	451.33	451.15	2.40E+04	1.7
20	373.21	--	--	--	457.27	--	--	--
21	341.22	--	--	--	409.29	409.10	2.60E+04	0.4
22	481.38	--	--	--	619.52	x	x	x
23	369.25	369.05	2.50E+04	0.35	451.33	451.20	1.90E+04	1.7
24	313.19	313.15	1.55E+04	2.6	367.24	--	--	--
25	397.12	--	--	--	493.12	--	--	--
26	425.14	--	--	--	535.15	x	x	x
27	397.12	397.10	1.60E+04, 1.10E+04	0.43, 1.67	493.12	493.05	1.15E+04	0.45
28	369.25	--	--	--	451.33	451.25	1.10E+04, 1.65E+05	1.7, 1.93
29	369.25	--	--	--	451.33	451.15	1.25E+04	1.7
30	369.25	--	--	--	451.33	451.20	2.10E+04	1.7
31	365.22	--	--	--	445.29	--	--	--
32	365.22	--	--	--	445.29	--	--	--
33	337.19	--	--	--	403.24	--	--	--
34	337.19	--	--	--	403.24		1.40E+04, 2.30E+04	0.3, 1.9
35	281.15	--	--	--	319.18	--	--	--

Table A.5. LR-LC-MS analysis of FgaPT2-catalyzed alkylations of Trp and Me-Trp. “--” = not detected.

Aromatic acceptor	Calc M+H	peak height	PP#	Prod M+H	peak height
Trp	205	850000	19	287.18	850000
	205	--	23	287.18	3500000
	205	9000	10	285.12	150000
	205	20000	17	273.16	5500000
4-Me-Trp	219	400000	19	301.2	--
	219	500000	23	301.2	--
	219	400000	10	299.15	--
	219	370000	17	287.19	20000
5-Me-Trp	219	2200000	19	301.2	--
	219	1000000	23	301.2	15000
	219	1200000	10	299.15	--
	219	850000	17	287.19	40000
6-Me-Trp	219	1600000	19	301.2	--
	219	900000	23	301.2	--
	219	800000	10	299.15	--
	219	720000	17	287.19	31000
7-Me-Trp	219	1800000	19	301.2	15000
	219	850000	23	301.2	12500
	219	600000	10	299.15	--
	219	1350000	17	287.19	30000

Table A.6. HR-LC-MS analysis of cultures expressing PhoN, IPK, and FgaPT2 with alcohol fed in. These examples are only of ones which were successful, with background DMAT production included.

	Product				
R group	Calc M+H	Exp M+H	delta ppm	EIC	Rt
10	285.1234	285.1228	2.104352	6.47E+06	4.76, 4.93
23	271.1441	271.1439	0.737615	1.94E+04	6.66,7.47, 8.18
19	287.1754	287.1747	2.437535	4.23E+05	5.72
17 (background DMAT)	273.1598	273.1597	0.366086	4.56E+06	5.31
	273.1598	273.1606	-2.92869	2.59E+06	5.31
	273.1598	273.1608	-3.66086	3.66E+05	5.31

A.3. FgaPT2 M328G *in vitro* and *in vivo*

Table A.7. LR-LC-MS analysis of FgapT2 M328G *in vitro* reactions. “--” = not detected.

	PP-H				Trp+H				Prod+H			
PP #	Calc	Exp	peak height	Rt (min)	Calc	Exp	peak height	Rt (min)	Calc	Exp	peak height	Rt (min)
1	313.06	--	--	--	205.10	205.20	4.90E+05	0.43	341.22	341.20	7.40E+05	1.8
3	313.06	--	--	--	205.10	205.20	5.00E+05	0.43	341.22	341.25	2.85E+06	1.83
4	293.00	--	--	--	205.10	205.15	5.00E+05	0.43	321.16	321.15	2.70E+05	1.55
5	271.01		3.20E+04	0.35	205.10	205.15	4.60E+05	0.43	299.18	--	--	--
6	228.97	--	--	--	205.10	205.15	5.10E+05	0.43	257.13	--	--	--
7	230.98	--	--	--	205.10	205.15	4.30E+05	0.43	259.14	259.20	1.60E+04	0.5
8	267.98	--	--	--	205.10	205.15	5.00E+05	0.45	296.14	296.20	2.50E+04	1.85
9	242.98	--	--	--	205.10	205.15	6.00E+05	0.43	271.14	271.15	1.50E+04	1.23
10	256.96	--	--	--	205.10	205.05	8.80E+05	0.45	285.12	285.10	1.00E+06	1.27
11	320.01	--	--	--	205.10	205.15	1.40E+06	0.45	348.17	348.15	1.60E+04	1.23
12	228.97	--	--	--	205.10	205.15	5.30E+05	0.45	257.13	--	--	--
13	257.00	--	--	--	205.10	205.15	4.30E+05	0.43	285.16	285.15	1.65E+04	1.45
15	308.89	309.00	2.00E+04	2.85	205.10	205.15	4.40E+05	0.45	337.06	--	--	--
17	245.00	--	--	--	205.10	205.15	6.70E+05	0.43	273.16	273.20	1.26E+05, 1.20E+04	1.43, 1.85
19	259.01	--	--	--	205.10	205.15	8.00E+05	0.45	287.18	287.15	2.00E+04	1.6
20	260.99		1.75E+04	0.4	205.10	205.15	5.00E+05	0.43	289.16	289.15	1.25E+04	1.23
21	245.00	--	--	--	205.10	205.15	4.50E+05	0.43	273.16	--	--	--

Table A.7 (continued)

22	315.08	--	--	--	205.10	205.20	5.50E+05	0.43	343.24	343.30	2.00E+04	1.9
23	259.01	--	--	--	205.10	205.15	5.50E+05	0.45	287.18	287.20	2.00E+05	1.6
24	230.98	--	--	--	205.10	205.15	8.80E+05	0.45	259.14	--	--	--
25	272.94		1.80E+04	0.35	205.10	205.15	4.40E+05	0.43	301.11	301.10	5.00E+04	1.4
26	286.95	--	--	--	205.10	205.15	6.30E+05	0.45	315.12	--	--	--
27	272.94		1.90E+04	0.35	205.10	205.15	5.20E+05	0.43	301.11	301.10	3.60E+05	1.37
28	259.01	--	--	--	205.10	205.15	4.90E+05	0.43	287.18	--	--	--
29	259.01	--	--	--	205.10	205.15	1.30E+06	0.45	287.18	--	--	--
30	259.01	--	--	--	205.10	205.15	5.40E+05	0.43	287.18	--	--	--
31	257.00	--	--	--	205.10	205.15	6.80E+05	0.43	285.16	--	--	--
32	257.00	--	--	--	205.10	205.15	4.50E+05	0.43	285.16	--	--	--
33	242.98	--	--	--	205.10	205.15	5.60E+05	0.43	271.14	271.05	3.45E+04	1.2
34	242.98	--	--	--	205.10	205.15	1.30E+06	0.45	271.14	271.05	1.44E+05	1.17
35	214.96	--	--	--	205.10	205.20	5.90E+05	0.43	243.12	--	--	--

Table A.8. LR-LC-MS analysis of FgapT2 M328G reactions *in vitro*, looking for multiple prenylations. "--" = not detected.

	+2 alkyl, [M+H]				+3alkyl, [M+H]			
PP#	Calc	Exp	peak height	Rt (min)	Calc	Exp	peak height	Rt (min)
1	477.35	--	--	--	613.47	--	--	--
3	477.35	--	--	--	613.47	--	--	--
4	437.22	437.20	3.90E+04	2.07	553.29	--	--	--
5	393.25	393.15	2.10E+04	1.65	487.33	--	--	--
6	309.16	--	--	--	361.19	--	--	--
7	313.19	--	--	--	367.24	--	--	--
8	387.18	--	--	--	478.22	--	--	--
9	337.19	--	--	--	403.24	--	--	--
10	365.15	--	--	--	445.18	--	--	--
11	491.24	--	--	--	634.32	--	--	--
12	309.16	--	--	--	361.19	--	--	--
13	365.22	--	--	--	445.29	--	--	--
15	469.01	--	--	--	600.97	--	--	--
17	341.22	341.20	1.00E+04	1.8	409.29	409.20	1.00E+05	0.43
19	369.25	--	--	--	451.33	--	--	--
20	373.21	--	--	--	457.27	--	--	--
21	341.22	--	--	--	409.29	409.15	5.00E+04	0.43
22	481.38	--	--	--	619.52	--	--	--
23	369.25	--	--	--	451.33	--	--	--
24	313.19	--	--	--	367.24	--	--	--
25	397.12	--	--	--	493.12	--	--	--
26	425.14	--	--	--	535.15	--	--	--
27	397.12	--	--	--	493.12	--	--	--
28	369.25	369.05	1.20E+04	0.4	451.33	--	--	--
29	369.25	--	--	--	451.33	--	--	--
30	369.25	369.05	1.40E+04	0.43	451.33	--	--	--
31	365.22	--	--	--	445.29	--	--	--
32	365.22	--	--	--	445.29	--	--	--
33	337.19	--	--	--	403.24	--	--	--
34	337.19	--	--	--	403.24	--	--	--
35	281.15	--	--	--	319.18	--	--	--

Table A.9. LR-LC-MS analysis of PhoN-IPK mut with FgaPT2 wild-type and M328G mutations with geraniol *in vivo*. "--" = not detected; M = media, L = lysate; f = PhoN-IPK mut with FgaPT2, fmg = PhoN-IPK mut with FgaPT2 M328G; 11, 12 = DMSO; 21, 22 = 0.5 mM geraniol added to culture; 31, 32 = 2 mM geraniol added to culture; data not corrected for optical density of culture.

		PP-H			Trp+H			Prod+H		
sample		Calc mass	peak height	Rt	Calc mass	peak height	Rt	Calc mass	peak height	Rt
M	f11	313.05	--	--	205.10	240000	0.45	341.20	26000	1.6
	f12	313.05	--	--	205.10	190000	0.43	341.20	100000	1.6
	f21	313.05	--	--	205.10	150000	0.43	341.20	80000	1.57
	f22	313.05	--	--	205.10	225000	0.43	341.20	50000	1.57
	f31	313.05	--	--	205.10	185000	0.43	341.20	60000	1.57
	f32	313.05	--	--	205.10	200000	0.43	341.20	45000	1.57
	fmg11	313.05	--	--	205.10	165000	0.43	341.20	85000, 110000	1.53, 1.6
	fmg12	313.05	--	--	205.10	200000	0.43	341.20	30000	1.57
	fgm21	313.05	--	--	205.10	185000	0.43	341.20	45000	1.57
	fmg22	313.05	--	--	205.10	170000	0.43	341.20	80000	1.57
	fmg31	313.05	--	--	205.10	260000	0.45	341.20	50000	1.57
	fmg32	313.05	--	--	205.10	245000	0.43	341.20	50000	1.57
L	f11	313.05	--	--	205.10	94000	0.4	341.20	74000	1.57
	f12	313.05	--	--	205.10	108000	0.4	341.20	82000	1.57
	f21	313.05	--	--	205.10	76000	0.4	341.20	78000	1.57
	f22	313.05	38000	1.53	205.10	90000	0.45	341.20	45000	1.57
	f31	313.05	--	--	205.10	64000	0.4	341.20	54000, 58000	1.55, 1.65
	f32	313.05	--	--	205.10	66000	0.4	341.20	63000, 28000	1.57, 2.07
	fmg11	313.05	--	--	205.10	70000	0.4	341.20	93000	1.57
	fmg12	313.05	--	--	205.10	82000	0.4	341.20	72000	1.57
	fgm21	313.05	--	--	205.10	140000	0.45	341.20	75000	1.57
	fmg22	313.05	--	--	205.10	82000	0.43	341.20	102000	1.57
	fmg31	313.05	--	--	205.10	90000	0.4	341.20	76000	1.57
	fmg32	313.05	--	--	205.10	95000	0.43	341.20	52000	1.57

A.4. CpaD *in vitro* and *in vivo*

Table A.10. LR-LC-MS analysis of CpaD *in vitro* reactions with cWY. Cdp = cyclic dipeptide. *for PP15 rxn, not 1:1 for 482 or 614, so not likely actually product. "--" = not detected.

	PP-H				cdp+H				Prod+H			
PP#	Calc	Exp	peak height	Rt (min)	Calc	Exp	peak height	Rt (min)	Calc	Exp	peak height	Rt (min)
1	313.06	312.85	9.80E+06	1.35	350.15	350.10	7.30E+05	1.3	486.28	486.20	6.50E+04	1.35
3	313.06	312.90	9.50E+06	1.4	350.15	350.10	7.00E+05	1.3	486.28	486.20	6.00E+04	1.4
4	293.00	292.80	7.10E+06	0.55 smear	350.15	350.10	6.90E+05	1.3	466.21	466.20	3.50E+05	1.3
5	271.01	270.85	7.40E+06	0.5	350.15	350.15	6.00E+05	1.32	444.23	--	--	--
6	228.97	228.90	1.60E+06	0.45	350.15	350.10	8.50E+05	1.27	402.18	402.30	1.30E+04	2.1
7	230.98	230.90	5.00E+06	0.4	350.15	350.15	8.00E+05	1.3	404.20	--	--	--
8	267.98	267.85	1.50E+06	0.32	350.15	350.10	6.50E+05	1.27	441.19	--	--	--
9	242.98	242.85	4.50E+06	0.43	350.15	350.15	8.00E+05	1.3	416.20	416.15	4.80E+04	2.05
10	256.96	256.85	2.25E+06	0.45	350.15	350.15	2.50E+05	1.3	430.18	430.15	2.10E+06	1.6
11	320.01	319.85	7.20E+06	0.5 smear	350.15	350.10	7.00E+05	1.3	493.22	493.10	2.75E+04, 1.50E+04	1.6, 2.35
12	228.97	228.90	5.80E+05	0.43	350.15	350.15	6.70E+05	1.27	402.18	--	--	--
13	257.00	256.85	4.70E+06	0.45	350.15	350.10	8.00E+05	1.32	430.21	430.15	6.20E+04, 6.50E+04, 4.80E+04	1.3, 1.8, 2,15
15	308.89	308.80	2.50E+06	0.5	350.15	350.15	6.50E+05	1.27	482.11	482.40*	2.40E+04	2.5

Table A.10 (continued)

17	245.00	244.90	3.90E+06	0.43	350.15	350.05	5.60E+04, 9.50E+04	1.3, 1.77	418.21	418.15	3.50E+06	1.77
19	259.01	258.85	6.70E+06	0.5	350.15	350.15	6.00E+05	1.3	432.23	432.30	1.50E+06	1.9
20	260.99	260.85	4.70E+06	0.43	350.15	350.10	7.00E+05	1.3	434.21	434.30	3.50E+04	1.9
21	245.00	244.85	4.30E+06	0.43	350.15	350.20	6.00E+05	1.3	418.21	418.30	1.30E+04	2.35
22	315.08	314.90	1.04E+07	1.35	350.15	350.10	1.90E+05	1.3	488.29	488.25	5.00E+04	2.05
23	259.01	258.90	5.70E+06	0.55	350.15	350.15	4.50E+05	1.3	432.23	432.30	2.00E+06	1.9
24	230.98	230.90	3.75E+06	0.4	350.15	350.10	7.50E+05	1.3	404.20	--	--	--
25	272.94	272.85	4.30E+06	0.43	350.15	350.10	7.00E+05	1.3	446.16	446.15	2.15E+05	1.7
26	286.95	286.80	5.70E+06	0.45	350.15	350.10	8.00E+05	1.3	460.17	460.20	7.00E+05	2.05
27	272.94	272.80	4.70E+06	0.43	350.15	350.10	7.00E+05	1.3	446.16	446.10	1.20E+06	1.7
28	259.01	258.85	6.30E+06	0.45	350.15	350.10	7.00E+05	1.3	432.23	432.30	2.00E+06	1.9
29	259.01	258.85	6.70E+06	0.45	350.15	350.10	7.00E+05	1.32	432.23	432.30	1.80E+06	1.9
30	259.01	258.85	7.00E+06	0.45	350.15	350.10	7.00E+05	1.3	432.23	432.30	1.80E+06	1.9
31	257.00	256.85	5.90E+06	0.5	350.15	350.10	8.00E+05	1.27	430.21	430.15	5.80E+04, 3.80E+04	1.27, 2.13
32	257.00	256.80	6.30E+06	0.45	350.15	350.10	7.00E+05	1.3	430.21	430.10	4.70E+04, 3.80E+04	1.3, 2.13
33	242.98	242.90	4.00E+06	0.4	350.15	350.10	7.00E+05	1.3	416.20	416.15	5.10E+04	2.05

Table A.10 (continued)

34	242.98	242.85	4.70E+06	0.4	350.15	350.10	6.00E+05	1.3	416.20	416.15	3.10E+04, 2.30E+04, 6.20E+04	1.27, 1.65, 2.05
35	214.96	214.85	1.16E+06	0.43	350.15	350.10	7.40E+05	1.3	388.18	388.20	5.80E+04	1.57

Table A.11. LR-LC-MS analysis of CpaD reactions with cWY, looking for multiple prenylations. "--" = not detected. *for PP15 rxn, not 1:1 for 482 or 614, so not likely actually product.

	+2 alkyl, [M+H]				+3alkyl, [M+H]			
PP#	Calc	Exp	peak height	Rt (min)	Calc	Exp	peak height	Rt (min)
1	622.40	--	--	--	758.53	--	--	--
3	622.40	--	--	--	758.53	--	--	--
4	582.28	582.30	1.00E+05	1.3	698.34	698.50	6.00E+04	3.05
5	538.31	538.25	4.00E+04	2.05	632.38	632.95	2.50E+04	0.5
6	454.21	454.20	3.10E+04	1.65	506.24	--	--	--
7	458.24	--	--	--	512.29	512.45	2.15E+05	2.45
8	532.23	--	--	--	623.28	623.35	1.25E+04	2.4
9	482.24	482.40	2.50E+04	0.55	548.29	--	--	--
10	510.20	510.15	4.50E+04	1.6	590.23	--	--	--
11	636.30	--	--	--	779.37	--	--	--
12	454.21	454.20	6.40E+04	1.63	506.24	506.35	7.00E+04	1.65
13	510.28	--	--	--	590.34	--	--	--
15	614.06	614.40*	2.65E+04	2.5	746.02	745.85	2.40E+04	0.5
17	486.28	--	--	--	554.34	x	x	x
19	514.31	--	--	--	596.38	--	--	--
20	518.26	--	--	--	602.32	--	--	--
21	486.28	--	--	--	554.34	--	--	--
22	626.43	--	--	--	764.57	--	--	--
23	514.31	--	--	--	596.38	--	--	--
24	458.24	458.25	1.70E+04	1.95	512.29	512.40	6.00E+04	2.45
25	542.17	--	--	--	638.18	637.90	2.50E+04	0.37
26	570.19	570.40	4.00E+04	2.5	680.21	679.80	1.40E+04	2.9
27	542.17	542.10	2.75E+04	1.7	638.18	--	--	--
28	514.31	514.30	2.25E+04	2.05	596.38	--	--	--
29	514.31	514.30	2.20E+04	2.05	596.38	--	--	--
30	514.31	514.35	2.20E+04	2.05	596.38	--	--	--
31	510.28	--	--	--	590.34	--	--	--

Table A.11 (continued)

32	510.28	--	--	--	590.34		5.00E+04	2.4
33	482.24	482.30	3.70E+04	2.5	548.29	--	--	--
34	482.24	482.35	3.10E+04	2.5	548.29	548.30	1.50E+04	2.6
35	426.20	--	--	--	464.23	--	--	--

Table A.12. LR-LC-MS analysis of CpaD reactions with cWF *in vitro*. "--" = not detected.

	PP-H				cdp+H				Prod+H			
PP#	Calc	Exp	peak height	Rt (min)	Calc	Exp	peak height	Rt (min)	Calc	Exp	peak height	Rt (min)
1	313.06	312.90	8.50E+06	1.6 smear	334.40	334.10	4.90E+05	1.55	470.52	470.25	2.20E+05	1.55
3	313.06	312.85	9.50E+06	smear	334.40	334.15	1.08E+06	1.55	470.52	470.25	1.00E+06	1.55
4	293.00	292.85	7.20E+06	0.55	334.40	334.15	7.00E+05	1.55	450.46	450.20	8.80E+04, 3.20E+04	1.55, 1.85
5	271.01	270.85	7.80E+06	0.5	334.40	334.10	1.20E+06	1.55	428.48	--	--	--
6	228.97	228.90	1.30E+06	0.43	334.40	334.15	1.28E+06	1.53	386.43	--	--	--
7	230.98	230.90	5.10E+05	0.4	334.40	334.15	1.20E+06	1.55	388.45	388.25	2.60E+04	1.15
8	267.98	267.85	1.60E+06	0.4	334.40	334.15	1.35E+06	1.55	425.44	425.20	1.18E+05	1.2
9	242.98	242.90	4.10E+06	0.4	334.40	334.10	1.20E+06	1.55	400.45	--	--	--
10	256.96	256.85	2.30E+06	0.43	334.40	334.10	3.50E+04	1.27	414.42	414.15	1.60E+06	1.8
11	320.01	319.85	7.60E+06	0.5	334.40	334.10	1.30E+07	1.55	477.47	--	--	--
12	228.97	228.85	1.60E+06	0.43	334.40	334.10	9.00E+05	1.55	386.43	386.15	1.75E+04	1.75
13	257.00	256.85	5.40E+06	0.43	334.40	334.15	1.00E+06	1.55	414.46	414.20	1.12E+05	2.03
15	308.89	308.75	1.44E+06	0.4	334.40	334.10	1.30E+06	1.53	466.36	--	--	--
17	245.00	244.85	4.90E+06	0.4	334.40	334.15	3.30E+04	1.55	402.46	402.20	6.00E+05	1.94

Table A.12 (continued)

19	259.01	258.90	6.50E+06	0.45	334.40	334.15	1.10E+06	1.55	416.48	416.20	1.90E+05	2.07
20	260.99	260.85	5.60E+06	0.45	334.40	334.10	1.00E+06	1.55	418.46	--	--	--
21	245.00	244.85	5.70E+06	0.45	334.40	334.10	1.00E+06	1.55	402.46	--	--	--
22	315.08	314.90	9.30E+06	1.6 smear	334.40	334.10	1.00E+06	1.6 smear	472.54	--	--	--
23	259.01	258.85	6.80E+06	0.5	334.40	334.15	6.00E+04	1.53	416.48	416.20	1.80E+05	2.07
24	230.98	230.90	5.00E+06	0.4	334.40	334.10	1.10E+06	1.55	388.45	--	--	--
25	272.94	272.80	4.30E+06	0.45	334.40	334.15	4.00E+05	1.55	430.41	430.10	1.00E+06	1.88
26	286.95	286.80	6.50E+06	0.45	334.40	334.15	7.00E+05	1.55	444.42	--	--	--
27	272.94	272.80	4.80E+06	0.45	334.40	--	--	--	430.41	430.10	1.00E+06	1.88
28	259.01	258.85	7.80E+06	0.45	334.40	334.15	1.20E+06	1.55	416.48	416.20	5.60E+04	2.05
29	259.01	258.85	7.40E+06	0.5	334.40	334.10	1.20E+06	1.55	416.48	416.20	9.00E+04	2.08
30	259.01	258.85	7.10E+06	0.45	334.40	334.15	7.00E+05	1.55	416.48	416.20	5.20E+04	2.05
31	257.00	256.85	5.30E+06	0.45	334.40	334.10	7.00E+05	1.55	414.46	414.20	3.20E+04	1.55
32	257.00	256.85	6.50E+06	0.5	334.40	334.10	9.00E+05	1.55	414.46	414.20	4.20E+04, 2.40E+04	1.95, 1.55
33	242.98	242.85	5.00E+06	0.4	334.40	334.10	1.20E+06	1.55	400.45	--	--	--
34	242.98	242.85	5.50E+06	0.4	334.40	334.15	1.00E+06	1.55	400.45	400.20	1.22E+05	1.88
35	214.96	214.85	9.00E+05	0.4	334.40	334.15	1.30E+06	1.55	372.43	372.20	2.65E+05, 2.10E+04, 1.80E+04	1.8, 2.1, 2.35

Table A.13. LR-LC-MS analysis of CpaD reactions with cWF, looking for multiple prenylations. “--” = not detected. “x” means outside of mass range for particular LC-MS run.

	+2 alkyl, [M+H]				+3alkyl, [M+H]			
PP#	Calc	Exp	peak height	Rt (min)	Calc	Exp	peak height	Rt (min)
1	606.65	606.40	1.00E+05	1.55	742.77	742.60	2.50E+04	1.55
3	606.65	606.40	6.80E+04	1.55	742.77	742.50	1.50E+05	1.55
4	566.52	--	--	--	682.59	--	--	--
5	522.56	--	--	--	616.63	--	--	--
6	438.46	--	--	--	490.49	--	--	--
7	442.49	--	--	--	496.54	496.45	2.70E+04	2.45
8	516.48	--	--	--	607.53	--	--	--
9	466.49	466.10	6.50E+04	0.35	532.54	x	x	x
10	494.45	--	--	--	574.48	--	--	--
11	620.55	--	--	--	763.62	764.05	3.50E+05	0.5
12	438.46	438.35	3.25E+04	2.5	490.49	490.80	1.90E+04	0.33
13	494.52	--	--	--	574.59	--	--	--
15	598.31	x	x	x	730.27	x	x	x
17	470.52	470.10	5.10E+04	1.35	538.59	538.30	3.00E+04	2.05
19	498.56	--	--	--	580.63	580.30	4.00E+04, 6.00E+04	1.7, 1.95
20	502.51	--	--	--	586.57	--	--	--
21	470.52	--	--	--	538.59	x	x	x
22	610.68	--	--	--	748.82	--	--	--
23	498.56	--	--	--	580.63	--	--	--
24	442.49	--	--	--	496.54	--	--	--
25	526.42	526.40	3.50E+04	2.5	622.43	622.30	1.50E+04	2.4
26	554.44	--	--	--	664.46	664.85	6.80E+04	0.35
27	526.42	--	--	--	622.43	--	--	--
28	498.56	498.15	5.30E+04	1.65	580.63	--	--	--
29	498.56	498.00	3.40E+04	0.95	580.63	--	--	--
30	498.56	--	--	--	580.63	--	--	--
31	494.52	--	--	--	574.59	--	--	--
32	494.52	--	--	--	574.59	--	--	--
33	466.49	466.05	3.00E+04	0.27	532.54	532.95	9.20E+04	0.35
34	466.49	466.10	4.50E+04	0.3	532.54	532.95	9.50E+04	0.37
35	410.45	--	--	--	448.48	--	--	--

Table A.14. LR-LC-MS analysis of CpaD reactions with cWG *in vitro*. “--” = not detected.

	PP-H				cdp+H				Prod+H			
PP	Calc	Exp	peak height	Rt (min)	Calc	Exp	peak height	Rt (min)	Calc	Exp	peak height	Rt (min)
1	313.06	312.85	9.50E+06	1.4	244.37	244.10	2.70E+04	0.63	380.50	--	--	--
3	313.06	312.85	9.50E+06	1.45	244.37	244.10	3.70E+04	0.65	380.50	--	--	--
4	293.00	292.80	8.30E+06	0.55	244.37	244.10	1.50E+05	0.73	360.44	360.10	4.50E+05, 5.00E+04	0.73, 1.65
5	271.01	271.85	8.40E+06	0.45	244.37	244.10	5.50E+04	0.7	338.45	--	--	--
6	228.97	228.90	1.55E+06	0.43	244.37	244.10	5.20E+04	0.7	296.40	296.15	2.50E+04	1.45
7	230.98	230.90	5.60E+06	0.4	244.37	244.10	9.70E+04	0.75	298.42	298.20	1.80E+04	1.85
8	267.98	267.85	1.55E+06	0.33	244.37	244.10	7.30E+04	0.7	335.41	335.95	5.00E+04	0.33
9	242.98	242.85	5.30E+06	0.43	244.37	244.10	2.40E+05	0.73	310.42	--	--	--
10	256.96	256.85	3.00E+06	0.43	244.37	244.10	3.70E+04	0.65	324.40	324.10	1.15E+06	1.5
11	320.01	319.85	7.70E+06	0.45	244.37	244.10	4.60E+04	0.67	387.45	--	--	--
12	228.97	228.90	9.80E+05	0.43	244.37	244.10	4.40E+04	0.65	296.40	296.10	2.10E+04, 1.80E+04	1.45, 1.25
13	257.00	256.85	6.30E+06	0.45	244.37	244.10	2.10E+05	0.73	324.44	324.15	3.10E+04, 1.90E+04, 2.10E+04	0.33, 0.73, 0.73
15	308.89	308.80	1.85E+06	0.43	244.37	244.10	4.00E+04	0.65	376.33	--	--	--
17	245.00	244.90	4.80E+06	0.45	244.37	--	--	--	312.44	312.15	1.60E+06	1.68
19	259.01	258.90	7.40E+06	0.45	244.37	244.10	1.20E+05	0.83	326.45	326.30	5.20E+04	1.85

Table A.14 (continued)

20	260.99	260.90	5.50E+06	0.43	244.37	244.10	9.50E+04	0.75	328.43	328.95	6.00E+04	0.35
21	245.00	244.90	5.00E+06	0.4	244.37	244.10	3.25E+04	0.6	312.44	--	--	--
22	315.08	314.85	9.80E+06	1.35	244.37	244.15	2.15E+04	0.65	382.51	--	--	--
23	259.01	258.90	7.20E+06	0.5	244.37	244.10	5.00E+04	0.77	326.45	326.15	2.45E+05	1.85
24	230.98	230.90	5.30E+06	0.37	244.37	244.10	5.30E+04	0.7	298.42	--	--	--
25	272.94	272.85	4.80E+06	0.45	244.37	244.10	4.80E+04	0.67	340.38	340.05	5.30E+04	1.58 (3 peaks)
26	286.95	286.86	6.70E+06	0.45	244.37	244.10	3.00E+04	0.7	354.39	354.00	4.20E+04	0.35
27	272.94	272.80	5.00E+06	0.43	244.37	244.10	3.60E+04	0.65	340.38	340.10	7.00E+05	1.6
28	259.01	258.90	6.80E+06	0.55	244.37	244.10	3.00E+04	0.65	326.45	326.15	2.75E+04	1.85
29	259.01	258.85	7.40E+06	0.5	244.37	244.10	3.30E+04	0.67	326.45	326.25	3.10E+04	1.83
30	259.01	258.85	7.00E+06	0.45	244.37	244.05	3.70E+04	0.65	326.45	326.25	3.20E+04, 4.90E+04	1.85, 2.18
31	257.00	256.85	5.00E+06	0.45	244.37	244.10	2.60E+04	0.67	324.44	324.90	4.80E+04	0.35
32	257.00	256.80	7.00E+06	0.47	244.37	244.10	4.50E+04	0.67	324.44	--	--	--
33	242.98	242.85	5.00E+06	0.45	244.37	244.10	5.00E+04	0.67	310.42	310.95	4.40E+04	0.35
34	242.98	242.85	5.20E+06	0.45	244.37	244.10	4.30E+04	0.65	310.42	310.10	3.30E+04, 3.30E+04	0.33, 0.6
35	214.96	214.85	1.24E+06	0.43	244.37	244.10	3.80E+04	0.7	282.40	282.15	1.00E+05	1.33, 1.45 smear

Table A.15. LR-LC-MS analysis of CpaD reactions with cWG, looking for multiple prenylations. "--" = not detected.

	+2 alkyl, [M+H]				+3alkyl, [M+H]			
PP#	Calc	Exp	peak height	Rt (min)	Calc	Exp	peak height	Rt (min)
1	516.62	--	--	--	652.75	--	--	--
3	516.62	516.80	1.38E+05	1.4	652.75	--	--	--
4	476.50	476.20	5.30E+05, 4.00E+04	0.73,1.23	592.56	592.25	2.20E+05	0.73
5	432.53	432.20	4.60E+06	1.9	526.61	526.45	5.00E+04	2.5
6	348.44	--	--	--	400.47	--	--	--
7	352.47	--	--	--	406.51	--	--	--
8	426.46	--	--	--	517.50	517.15	5.50E+04	1.55
9	376.47	376.20	2.10E+04	1.95	442.51	--	--	--
10	404.42	--	--	--	484.45	484.20	3.20E+04	2.03
11	530.52	530.35	2.40E+04	2.45	673.59	673.40	1.05E+05	2.05
12	348.44	--	--	--	400.47	--	--	--
13	404.50	404.20	2.25E+04	1.6	484.56	484.25	3.50E+04, 2.25E+04	2.05, 2.3
15	508.29	--	--	--	640.24	--	--	--
17	380.50	--	--	--	448.56	448.25	7.70E+04	2.43
19	408.53	--	--	--	490.61	--	--	--
20	412.49	--	--	--	496.55	--	--	--
21	380.50	--	--	--	448.56	--	--	--
22	520.65	520.30	2.20E+04	1.3	658.80	658.45	2.80E+04	2.5
23	408.53	--	--	--	490.61	--	--	--
24	352.47	--	--	--	406.51	--	--	--
25	436.39	--	--	--	532.40	532.40	1.90E+04	2.3
26	464.41	--	--	--	574.43	574.30	2.00E+04	1.87
27	436.39	436.10	4.20E+04	1.6	532.40	532.15	5.30E+04	1.6
28	408.53	408.20	2.40E+04	2.5	490.61	--	--	--
29	408.53	408.15	1.90E+04	1.1	490.61	490.20	2.00E+04	1.45
30	408.53	--	--	--	490.61	--	--	--
31	404.50	404.85	2.60E+04	0.35	484.56	484.20	4.70E+04	2.05
32	404.50	--	--	--	484.56	--	--	--
33	376.47	--	--	--	442.51	--	--	--
34	376.47	--	--	--	442.51	--	--	--
35	320.43	--	--	--	358.45	--	--	--

Table A.16. LR-LC-MS analysis of CpaD-catalyzed prenylation of cWG, cWF, or cWY *in vivo*. "--" = not detected. CG = cWG, CF = cWF, CY = cWY; 11 and 12 = 10 mM, 21 and 22 = 5 mM, 31 and 32 = 2.5 mM, 41 and 42 = 1 mM.

	PP-H			CDP+H			Prod+H		
Sample	Calc mass	peak height	Rt (min)	Calc mass	peak height	Rt (min)	Calc mass	peak height	Rt (min)
CG11	245.00	--	--	244.37	115000	0.64	312.44	80000	1.67
CG12	245.00	--	--	244.37	100000	0.64	312.44	66000	1.67
CG21	245.00	--	--	244.37	44000	0.64	312.44	62000	1.67
CG22	245.00	--	--	244.37	42000	0.67	312.44	70000	1.67
CG31	245.00	--	--	244.37	35000	0.7	312.44	88000	1.67
CG32	245.00	--	--	244.37	23000	0.73	312.44	93000	1.67
CG41	245.00	--	--	244.37	68000	0.37	312.44	68000	1.67
CG42	245.00	--	--	244.37	65000	0.37	312.44	58000	1.67
CF11	245.00	--	--	334.40	116000	1.54	402.46	22000, 34000	1.95, 1.6
CF12	245.00	--	--	334.40	94000	1.54	402.46	26000, 33000	1.96, 1.6
CF21	245.00	--	--	334.40	55000	1.53	402.46	34000, 24000	1.94, 1.6
CF22	245.00	--	--	334.40	58000	1.53	402.46	32000, 22000	1.94, 1.6
CF31	245.00	--	--	334.40	68000	1.54	402.46	36000, 25000	1.96, 1.6
CF32	245.00	--	--	334.40	73000	1.53	402.46	30000, 18000	1.94, 1.6
CF41	245.00	--	--	334.40	92000	1.54	402.46	34000, 25000	1.94, 1.6
CF42	245.00	--	--	334.40	65000	1.54	402.46	45000, 40000	1.94, 1.6
CY11	245.00	--	--	350.15	38000	1.3	418.21	70000	1.77
CY12	245.00	--	--	350.15	35000	1.3	418.21	64000	1.76

Table A.16 (continued)

CY22	245.00	--	--	350.15	38000	1.28	418.21	84000	1.76
CY31	245.00	--	--	350.15	108000	1.3	418.21	95000	1.77
CY32	245.00	--	--	350.15	100000	1.3	418.21	118000	1.77
CY41	245.00	--	--	350.15	55000	1.3	418.21	95000	1.77
CY42	245.00	--	--	350.15	50000	1.3	418.21	150000	1.77
CY21	245.00	--	--	350.15	33000	1.3	418.21	100000	1.77

A.5. FtmPT1 *in vitro* and *in vivo*

Table A.17. LR-LC-MS analysis of FtmPT1 reactions with cWY *in vitro*. “--” = not detected.

	PP-H				cdp+H				Prod+H			
PP #	Calc	Exp	peak height	Rt (min)	Calc	Exp	peak height	Rt (min)	Calc	Exp	peak height	Rt (min)
1	313.06	312.95	2.60E+06	1.8	350.15	350.15	7.00E+05	1.3	486.28	486.25	1.85E+04	2.15
3	313.06	312.90	8.00E+06	1.6	350.15	350.10	6.00E+05	1.3	486.28	486.25	3.00E+04	2.15
4	293.00	292.85	6.50E+06	0.55	350.15	350.15	6.20E+05	1.3	466.21	466.20	3.50E+05, 1.50E+05	1.3, 1.7
5	271.01	270.85	7.80E+06	0.45	350.15	350.10	1.00E+06	1.3	444.23	--	--	--
6	228.97	228.90	1.70E+05	0.43	350.15	350.10	6.50E+05	1.3	402.18	--	--	--
7	230.98	230.90	4.10E+06	0.4	350.15	350.10	8.00E+05	1.27	404.20	--	--	--
8	267.98	267.85	1.04E+06	0.4	350.15	350.15	6.30E+05	1.3	441.19	--	--	--
9	242.98	242.80	1.80E+06	0.43	350.15	350.15	8.00E+05	1.3	416.20	416.15	6.40E+04	2.05
10	256.96	256.85	2.50E+05	0.45	350.15	--	--	--	430.18	430.15	4.80E+06	1.67
11	320.01	319.90	1.90E+06	0.6 smear	350.15	350.10	6.50E+05	1.3	493.22	--	--	--
12	228.97	228.85	4.30E+05	0.43	350.15	350.10	8.50E+05	1.3	402.18	--	--	--
13	257.00	256.90	6.30E+05	0.5	350.15	350.10	5.80E+05	1.3	430.21	430.20	4.00E+04, 1.20E+05, 2.00E+04	1.3, 1.85, 2.15
15	308.89	308.80	2.00E+06	0.45	350.15	350.20	6.50E+05	1.3	482.11	482.35	1.90E+04	2.5
17	245.00	244.90	1.80E+06	0.45	350.15	350.10	8.00E+04	1.7	418.21	418.15	4.80E+06	1.7

Table A.17 (continued)

19	259.01	258.90	4.75E+06	0.45	350.15	350.10	7.00E+05	1.3	432.23	432.30	1.20E+06, 6.00E+04	1.9, 1.23
20	260.99	260.85	4.20E+06	0.43	350.15	350.10	7.00E+05	1.27	434.21	434.30	2.25E+04	1.9
21	245.00	244.90	1.90E+06	0.45	350.15	350.15	8.00E+05	1.3	418.21	--	--	--
22	315.08	314.90	8.60E+06	1.7	350.15	350.10	6.00E+05	1.3	488.29	488.35	2.40E+04, 3.70E+04	2.05, 2.77
23	259.01	258.90	1.70E+06	0.6	350.15	350.15	7.00E+05	1.3	432.23	432.25	4.60E+06	1.9
24	230.98	230.90	4.10E+06	0.4	350.15	350.15	8.00E+05	1.3	404.20	--	--	--
25	272.94	272.85	2.40E+06	0.45	350.15	350.15	6.00E+05	1.3	446.16	446.10	2.40E+05	1.7
26	286.95	286.85	5.40E+06	0.4	350.15	350.10	7.00E+05	1.3	460.17	460.25	5.00E+05	2.05
27	272.94	272.85	3.60E+06	0.45	350.15	350.10	3.00E+05	1.3	446.16	446.10	3.60E+06	1.7
28	259.01	258.80	3.65E+06	0.5	350.15	350.10	1.00E+06	1.32	432.23	432.30	1.20E+06, 4.00E+04	1.9, 1.2
29	259.01	258.80	4.50E+06	0.55	350.15	350.10	8.00E+05	1.3	432.23	432.35	1.20E+06, 4.00E+04	1.9, 1.2
30	259.01	258.90	4.60E+06	0.5	350.15	350.10	8.00E+05	1.3	432.23	432.35	1.30E+05, 5.00E+04	1.9, 1.23
31	257.00	256.90	7.30E+06	0.5	350.15	350.10	6.30E+05	1.3	430.21	430.10	3.60E+04	1.3
32	257.00	256.85	5.50E+06	0.53	350.15	350.10	8.00E+05	1.27	430.21	430.10	4.00E+04	1.27
33	242.98	242.85	3.60E+06	0.4	350.15	350.15	7.00E+05	1.3	416.20	416.15	5.00E+04	2.05
34	242.98	242.85	4.80E+06	0.4	350.15	350.10	7.00E+05	1.3	416.20	416.15	6.00E+04	2.05

Table A.17 (continued)

35	214.96	214.85	1.54E+06	0.4	350.15	350.10	7.00E+05	1.32	388.18	388.20	2.50E+04, 3.10E+04	1.2, 1.57

Table A.18. LR-LC-MS analysis of FtmPT1 reactions with cWY, looking for multiple prenylations. "--" = not detected.

	+2 alkyl, [M+H]				+3alkyl, [M+H]			
PP#	Calc	Exp	peak height	Rt (min)	Calc	Exp	peak height	Rt (min)
1	622.40	622.35	2.25E+04	2.4	758.53	758.30	2.70E+04	2.65
3	622.40	622.35	5.00E+04	2.4	758.53	758.30	3.70E+05	2.65
4	582.28	582.30	1.10E+05	1.3	698.34	698.50	1.20E+05	3.07
5	538.31	538.20	2.90E+04	2	632.38	--	--	--
6	454.21	--	--	--	506.24	--	--	--
7	458.24	--	--	--	512.29	512.45	1.90E+04, 7.70E+04	1.3, 2.43
8	532.23	--	--	--	623.28	--	--	--
9	482.24	482.40	2.00E+04, 2.60E+04	0.5, 2.5	548.29	--	--	--
10	510.20	510.20	5.50E+04	1.83	590.23	--	--	--
11	636.30	--	--	--	779.37	--	--	--
12	454.21	454.20	1.20E+05	1.65	506.24	--	--	--
13	510.28	--	--	--	590.34	--	--	--
15	614.06	614.50	1.90E+04	2.5	746.02	--	--	--
17	486.28	486.20	5.20E+04	2.05	554.34	--	--	--
19	514.31	--	--	--	596.38	--	--	--
20	518.26	--	--	--	602.32	--	--	--
21	486.28	--	--	--	554.34	--	--	--
22	626.43	--	--	--	764.5725	764.10	2.00E+04	1.67
23	514.31	--	--	--	596.38	--	--	--
24	458.24	--	--	--	512.29	--	--	--
25	542.17	--	--	--	638.18	--	--	--
26	570.19	570.40	2.50E+04	2.5	680.21	--	--	--
27	542.17	542.20	3.50E+04	1.65	638.18	--	--	--
28	514.31	--	--	--	596.38	--	--	--
29	514.31		2.10E+04	2.05	596.38	--	--	--
30	514.31	--	--	--	596.38	--	--	--
31	510.28	--	--	--	590.34	--	--	--
32	510.28	--	--	--	590.34	--	--	--
33	482.24	481.95, 482.95	2.00E+04, 2.20E+04	0.5, 2.5	548.29	--	--	--
34	482.24		2.50E+04	2.5	548.29	--	--	--
35	426.20	--	--	--	464.23	463.9, 464.85	5.50E+04	0.27

Table A.19. LR-LC-MS analysis of FtmPT1 reactions with cWF *in vitro*. "--" = not detected.

	PP-H				cdp+H				Prod+H			
PP#	Calc	Exp	peak height	Rt (min)	Calc	Exp	peak height	Rt (min)	Calc	Exp	peak height	Rt (min)
1	313.06	312.95	5.30E+06	1.77	334.40	334.15	1.00E+06	1.55	470.52	470.25	7.40E+04, 4.30E+04	2.35, 0.53
3	313.06	312.95	4.30E+06	1.83	334.40	334.15	9.00E+05	1.54	470.52	470.25	2.80E+05, 2.70E+04	2.35, 0.55
4	293.00	292.80	6.70E+06	0.6	334.40	334.10	7.00E+05	1.55	450.46	450.20	2.40E+05, 1.00E+05	2.07, 1.55
5	271.01	270.85	7.50E+06	0.45	334.40	334.15	9.00E+05	1.55	428.48	--	--	--
6	228.97	228.85	1.75E+06	0.43	334.40	334.10	7.00E+05	1.55	386.43	--	--	--
7	230.98	230.90	5.10E+06	0.4	334.40	334.10	7.00E+05	1.55	388.45	388.20	2.40E+04	1.15
8	267.98	267.85	1.70E+06	0.4	334.40	334.15	8.00E+05	1.55	425.44	425.10	6.00E+04	0.27
9	242.98	242.85	3.40E+06	0.4	334.40	334.10	8.00E+05	1.55	400.45	--	--	--
10	256.96	256.85	1.80E+06	0.45	334.40	--	--	--	414.42	414.15	4.00E+06	1.9
11	320.01	319.85	3.60E+06	1.05 smear	334.40	334.10	7.50E+05	1.55	477.47	477.25	1.50E+04	1.27
12	228.97	228.85	1.32E+06	0.43	334.40	334.15	8.00E+05	1.55	386.43	--	--	--
13	257.00	256.85	3.90E+06	0.45	334.40	334.10	1.10E+06	1.55	414.46	414.20	2.90E+05	2.05
15	308.89	308.80	6.10E+05	0.5	334.40	334.10	7.20E+05	1.55	466.36	--	--	--

Table A.19 (continued)

17	245.00	244.90	3.90E+06	0.45	334.40	--	--	--	402.46	402.20	6.00E+05, 7.00E+05	1.9, 2.03 smear
19	259.01	258.90	5.10E+06	0.43	334.40	334.10	7.00E+05	1.55	416.48	416.20	1.20E+06	2.1
20	260.99	260.90	5.60E+06	0.43	334.40	334.10	8.00E+05	1.55	418.46	--	--	--
21	245.00	244.90	4.30E+06	0.45	334.40	334.10	8.00E+05	1.55	402.46	--	--	--
22	315.08	314.90	9.20E+06	1.7	334.40	334.15	1.04E+06	1.55 smear	472.54	472.15	1.40E+05	0.5
23	259.01	258.90	5.00E+05	0.65	334.40	334.15	7.00E+04	1.55	416.48	416.20	5.30E+06	2.1
24	230.98	230.90	5.10E+06	0.4	334.40	334.10	7.00E+05	1.55	388.45	388.25	3.00E+04	1.17
25	272.94	272.80	1.85E+06	0.45	334.40	334.15	6.00E+05	1.55	430.41	430.10	1.55E+06	1.9
26	286.95	286.80	5.90E+06	0.45	334.40	334.15	1.00E+06	1.55	444.42	--	--	--
27	272.94	272.80	3.20E+06	0.45	334.40	--	--	--	430.41	430.10	4.50E+06	1.95
28	259.01	258.90	1.17E+06	0.55	334.40	334.15	1.17E+06	1.55	416.48	416.15	6.50E+04	2.05
29	259.01	258.90	5.80E+06	0.55	334.40	334.10	9.00E+05	1.55	416.48	41.20	1.04E+05	2.1
30	259.01	258.90	1.90E+06	0.55	334.40	334.15	1.05E+06	1.55	416.48	416.15	6.00E+04	2.05
31	257.00	256.85	3.80E+06	0.45	334.40	334.10	8.50E+05	1.55	414.46	414.15	2.50E+04	1.55
32	257.00	256.85	4.80E+06	0.55	334.40	334.15	1.00E+06	1.55	414.46	414.25	2.60E+04	1.55
33	242.98	242.85	5.40E+06	0.4	334.40	334.15	1.00E+06	1.55	400.45	400.95	1.90E+04	0.4
34	242.98	242.85	6.20E+06	0.4	334.40	334.15	8.00E+05	1.55	400.45	400.20	1.80E+04	2.27
35	214.96	214.85	2.15E+06	0.4	334.40	334.10	8.00E+05	1.55	372.43	--	--	--

Table A.20. LR-LC-MS analysis of FtmPT1 reactions with cWF, looking for multiple prenylations. "--" = not detected.

	+2 alkyl, [M+H]				+3alkyl, [M+H]			
PP#	Calc	Exp	peak height	Rt (min)	Calc	Exp	peak height	Rt (min)
1	606.65	--	--	--	742.77	--	--	--
3	606.65	--	--	--	742.77	--	--	--
4	566.52	566.15	2.50E+04	1.95	682.59	--	--	--
5	522.56	--	--	--	616.63	--	--	--
6	438.46	--	--	--	490.49	--	--	--
7	442.49	--	--	--	496.54	--	--	--
8	516.48	--	--	--	607.53	--	--	--
9	466.49	466.00	2.85E+04	0.35	532.54	532.05	3.35E+04	0.37
10	494.45	494.20	2.85E+04	2.13	574.48	--	--	--
11	620.55	--	--	--	763.62	764.05	2.40E+04	1.05
12	438.46	--	--	--	490.49	--	--	--
13	494.52	--	--	--	574.59	--	--	--
15	598.31	--	--	--	730.27	--	--	--
17	470.52	--	--	--	538.59	538.30	2.30E+04	2.05
19	498.56	--	--	--	580.63	--	--	--
20	502.51	--	--	--	586.57	--	--	--
21	470.52	--	--	--	538.59	538.25	2.30E+04	2.05
22	610.68	--	--	--	748.82	--	--	--
23	498.56	--	--	--	580.63	--	--	--
24	442.49	--	--	--	496.54	496.00	2.20E+04	0.32
25	526.42	526.45	1.90E+04	2.5	622.43	--	--	--
26	554.44	--	--	--	664.46	--	--	--
27	526.42	526.40	2.50E+04	2.5	622.43	--	--	--
28	498.56	--	--	--	580.63	--	--	--
29	498.56	--	--	--	580.63	--	--	--
30	498.56	--	--	--	580.63	--	--	--
31	494.52	--	--	--	574.59	--	--	--
32	494.52	--	--	--	574.59	--	--	--
33	466.49	466.00	4.40E+04	0.37	532.54	532.95	5.10E+04	0.37
34	466.49	466.05	5.10E+04	0.35	532.54	532.95	4.00E+04	0.37
35	410.45	--	--	--	448.48	--	--	--

Table A.21. LR-LC-MS analysis of FtmPT1 reactions with cWG *in vitro*. "--" = not detected.

	PP-H				cdp+H				Prod+H			
PP#	Calc	Exp	peak height	Rt (min)	Calc	Exp	peak height	Rt (min)	Calc	Exp	peak height	Rt (min)
1	313.06	312.90	6.30E+06	1.77	244.37	244.15	4.10E+04	0.65	380.50	380.20	5.00E+04	2.1
3	313.06	312.95	5.60E+06	1.8	244.37	244.15	7.20E+04	0.65	380.50	380.25	6.40E+04	2.1
4	293.00	292.85	6.50E+06	0.57 smear	244.37	--	--	--	360.44	360.15	7.00E+05, 2.10E+05	1.8, 0.6
5	271.01	270.90	7.20E+06	0.5	244.37	244.10	2.10E+04	0.6	338.45	338.05	3.75E+04	0.3
6	228.97	228.85	1.48E+06	0.45	244.37	244.10	3.50E+04, 5.00E+04	0.6, 0.27	296.40	296.10	4.70E+04, 3.30E+04	0.35, 1.15
7	230.98	230.85	4.50E+06	0.45	244.37	244.10	3.00E+04, 4.20E+04	0.6, 0.27	298.42	298.95	2.10E+04	0.35
8	267.98	267.85	9.30E+05	0.4	244.37	244.10	1.24E+05	0.73	335.41	--	--	--
9	242.98	242.85	3.50E+06	0.43	244.37	244.10	5.40E+04, 5.80E+04	0.67, 0.27	310.42	--	--	--
10	256.96	256.85	1.50E+06	0.45	244.37	244.05	6.10E+04	0.27	324.40	324.10	9.00E+05, 3.70E+06	1.4, 1.55
11	320.01	319.85	5.30E+06	0.6	244.37	244.10	2.50E+04	0.65	387.45	--	--	--
12	228.97	228.85	1.60E+06	0.43	244.37	244.10	3.20E+04	0.65	296.40	296.10	6.00E+04, 6.30E+04	1.17, 0.3
13	257.00	256.85	4.00E+06	0.45	244.37	244.10	3.00E+04	0.65	324.44	324.15	9.50E+04	1.77

Table A.21 (continued)

15	308.89	308.80	2.30E+06	0.45	244.37	244.12	1.25E+05	0.72	376.33	375.95, 376.95	3.20E+04	0.3
17	245.00	244.90	4.40E+06	0.45	244.37	243.90	3.00E+04, 2.50E+04	1.57, 1.7	312.44	312.15	3.80E+06, 3.20E+06	1.57, 1.7
19	259.01	258.90	5.80E+06	0.45	244.37	244.10	3.40E+04, 3.20E+04	0.67, 0.27	326.45	326.20	1.10E+05	1.83
20	260.99	260.85	5.40E+06	0.4	244.37	244.15	2.50E+04	0.6	328.43	328.00	1.30E+04	0.3
21	245.00	244.90	4.60E+06	0.43	244.37	244.10	4.00E+04	0.67	312.44	312.10	1.90E+04	0.3
22	315.08	314.90	9.80E+06	1.6	244.37	244.15	4.30E+04	0.65	382.51	382.15	6.30E+04, 1.80E+04	1.3, 1.55
23	259.01	258.90	2.45E+06	0.6	244.37	244.10	1.90E+04, 5.70E+04	0.6, 0.27	326.45	326.15	1.50E+06	1.83
24	230.98	230.85	5.00E+06	0.4	244.37	244.10	5.00E+04	0.65	298.42	--	--	--
25	272.94	272.80	2.15E+06	0.45	244.37	244.10	2.30E+04	0.65	340.38	340.05	7.00E+04	1.6
26	286.95	286.85	5.70E+06	0.45	244.37	244.15	6.80E+04	0.72	354.39	--	--	--
27	272.94	286.80	1.30E+06	0.4	244.37	244.15	6.20E+04	0.67	340.38	340.10	8.40E+05	1.6
28	259.01	258.95	3.70E+06	0.5	244.37	244.10	6.50E+04	0.65	326.45	326.30	2.00E+04	1.85
29	259.01	258.80	5.80E+06	0.5	244.37	244.10	4.80E+04	0.65	326.45	326.25	2.60E+04	1.8
30	259.01	258.95	3.90E+06	0.6	244.37	244.10	4.30E+04	0.65	326.45	326.30	1.80E+04	1.8
31	257.00	256.90	4.60E+06	0.45	244.37	244.10	5.30E+04	0.65	324.44	--	--	--
32	257.00	256.90	4.10E+06	0.5	244.37	244.10	4.80E+04	0.65	324.44	324.05	1.50E+04	0.37

Table A.21 (continued)

33	242.98	242.90	4.30E+06	0.4	244.37	244.10	3.50E+04	0.6	310.42	--	--	--
34	242.98	242.85	5.20E+06	0.4	244.37	244.05	3.20E+04	0.65	310.42	--	--	--
35	214.96	214.90	1.60E+06	0.4	244.37	244.10	4.00E+04	0.6	282.40	282.15	1.13E+05	1.4

Table A.22. LR-LC-MS analysis of FtmPT1 reactions with cWG, looking for multiple prenylations. “--” = not detected.

	+2 alkyl, [M+H]				+3alkyl, [M+H]			
PP#	Calc	Exp	peak height	Rt (min)	Calc	Exp	peak height	Rt (min)
1	516.62	--	--	--	652.75	--	--	--
3	516.62	--	--	--	652.75	--	--	--
4	476.50	476.30	7.00E+04, 2.80E+05	1.27, 0.6	592.56	592.25	1.20E+05	0.6
5	432.53	432.30	2.40E+06	1.9	526.61	526.40	2.75E+04	2.5
6	348.44	--	--	--	400.47	--	--	--
7	352.47	352.10	2.10E+04	0.27	406.51	--	--	--
8	426.46	426.05	4.00E+04	0.27	517.50	--	--	--
9	376.47	--	--	--	442.51	--	--	--
10	404.42	404.15	2.20E+04	1.73	484.45	484.20	2.40E+04	2.05
11	530.52	--	--	--	673.59	--	--	--
12	348.44	--	--	--	400.47	--	--	--
13	404.50	--	--	--	484.56	484.25	1.80E+04	2.05
15	508.29	--	--	--	640.24	--	--	--
17	380.50	380.20	1.30E+05	2	448.56	448.15	2.70E+04	2.43
19	408.53	--	--	--	490.61	--	--	--
20	412.49	411.85	1.30E+04	1.27	496.55	496.40	1.30E+04	2.6
21	380.50	380.05	2.50E+04	0.27	448.56	448.25	4.70E+04	2.43
22	520.65	520.30	1.80E+04	1.3	658.80	--	--	--
23	408.53	--	--	--	490.61	--	--	--
24	352.47	--	--	--	406.51	--	--	--
25	436.39	436.25	2.00E+04	0.93	532.40	--	--	--
26	464.41	--	--	--	574.43	574.35	3.20E+04	1.83
27	436.39	436.10	1.30E+04	1.6	532.40	532.10	1.20E+05	0.65
28	408.53	--	--	--	490.61	--	--	--
29	408.53	--	--	--	490.61	--	--	--
30	408.53	--	--	--	490.61	--	--	--
31	404.50	404.00	4.30E+04	0.27	484.56	484.20	2.80E+04	2
32	404.50	403.95	2.30E+04	0.27	484.56	484.20	1.70E+04	2
33	376.47	--	--	--	442.51	--	--	--
34	376.47	--	--	--	442.51	--	--	--
35	320.43	--	--	--	358.45	--	--	--

Table A.23. LR-LC-MS analysis of FtmPT1-catalyzed prenylation of cWG, cWF, or cWY *in vivo*. "--" = not detected. FG = cWG, FF = cWF, FY = cWY; 11 and 12 = 10 mM, 21 and 22 = 5 mM, 31 and 32 = 2.5 mM, 41 and 42 = 1 mM.

	PP-H			CDP+H			Prod+H		
Sample	Calc mass	peak height	Rt (min)	Calc mass	peak height	Rt	Calc mass	peak height	Rt (min)
FG11	245.00	--	--	244.37	130000	0.73	312.44	42000	1.7
FG12	245.00	--	--	244.37	52000	0.37	312.44	--	--
FG21	245.00	--	--	244.37	33000	0.34	312.44	55000	1.7
FG22	245.00	--	--	244.37	40000	0.34	312.44	49000	1.7
FG31	245.00	--	--	244.37	25000	0.34	312.44	45000	1.7
FG32	245.00	--	--	244.37	24000	0.96	312.44	45000	1.7
FG41	245.00	--	--	244.37	43000	0.36	312.44	35000	1.7
FG42	245.00	--	--	244.37	52000	0.36	312.44	35000	1.7
FF11	245.00	--	--	334.40	100000	1.54	402.46	65000	2.04
FF12	245.00	--	--	334.40	105000	1.54	402.46	72000	2.04
FF21	245.00	--	--	334.40	--	--	402.46	--	--
FF22	245.00	--	--	334.40	45000	1.54	402.46	115000	2.04
FF31	245.00	--	--	334.40	135000	1.54	402.46	105000	2.04
FF32	245.00	--	--	334.40	120000	1.54	402.46	200000	2.04
FF41	245.00	--	--	334.40	175000	2.27	402.46	150000	3.1
FF42	245.00	--	--	334.40	130000	2.24	402.46	100000	2.77
FY11	245.00	--	--	350.15	35000	1.3	418.21	39000	1.8
FY12	245.00	--	--	350.15	30000	1.3	418.21	24000	1.8
FY21	245.00	--	--	350.15	38000	1.3	418.21	54000	1.8
FY22	245.00	--	--	350.15	36000	1.3	418.21	45000	1.7
FY31	245.00	--	--	350.15	67000	1.3	418.21	51000	1.7
FY32	245.00	--	--	350.15	100000	1.3	418.21	58000	1.7
FY41	245.00	--	--	350.15	64000	1.3	418.21	63000	1.8
FY42	245.00	--	--	350.15	64000	1.3	418.21	73000	1.7

A.6. CpaD I329G *in vitro*

Table A.24. LR-LC-MS analysis of CpaD I329G reactions with cWY.

	PP-H				cdp+H				Prod+H			
PP#	Calc	Exp	peak height	Rt (min)	Calc	Exp	peak height	Rt (min)	Calc	Exp	peak height	Rt (min)
1	313.06	312.90	9.70E+06	1.35	350.15	350.10	6.40E+05	1.3	486.28	486.25	3.70E+05, 5.30E+05	1.3, 2.1

Table A.24 (continued)

3	313.06	312.85	9.40E+06	1.4	350.15	350.10	6.00E+05	1.3	486.28	486.20	4.60E+05, 5.90E+05	1.3, 2.1
4	293.00	292.85	6.80E+06	0.5	350.15	350.10	6.70E+05	1.3	466.21	466.15	3.60E+05, 2.50E+04	1.3, 1.9
5	271.01	270.85	7.40E+06	0.5	350.15	350.10	8.00E+05	1.3	444.23	--	--	--
6	228.97	228.85	2.00E+06	0.45	350.15	350.10	6.50E+05	1.3	402.18	--	--	--
7	230.98	230.85	5.30E+06	0.4	350.15	350.10	8.00E+05	1.3	404.20	--	--	--
8	267.98	267.85	1.80E+06	0.4	350.15	350.10	8.50E+05	1.3	441.19	--	--	--
9	242.98	242.85	4.50E+06	0.45	350.15	350.10	8.00E+05	1.3	416.20	416.15	6.40E+04	2.05
10	256.96	256.85	2.40E+06	0.43	350.15	350.10	7.00E+05	1.3	430.18	430.10	5.00E+05, 7.00E+04, 5.00E+04	1.6, 1.3, 2.15
11	320.01	319.80	7.20E+06	0.5	350.15	350.10	8.00E+05	1.3	493.22	--	--	--
12	228.97	228.85	1.60E+06	0.45	350.15	350.10	9.50E+05	1.3	402.18	--	--	--
13	257.00	256.85	5.40E+06	0.43	350.15	350.10	7.00E+05	1.3	430.21	430.35	6.70E+04, 2.90E+04, 5.50E+04	1.3, 1.85, 2.15
15	308.89	308.80	2.10E+06	0.45	350.15	350.15	7.50E+05	1.3	482.11	482.20	1.50E+05, 2.40E+04	0.35, 0.25
17	245.00	244.85	4.60E+06	0.43	350.15	350.10	7.00E+05	1.3	418.21	418.15	4.00E+05	1.77
19	259.01	258.90	5.80E+06	0.5	350.15	350.10	7.00E+05	1.3	432.23	432.30	2.50E+06	1.9

Table A.24 (continued)

20	260.99	260.85	5.00E+06	0.4	350.15	350.10	7.00E+05	1.3	434.21	434.30	3.85E+04	1.9
21	245.00	244.85	6.00E+06	0.45	350.15	350.15	7.00E+05	1.3	418.21	--	--	--
22	315.08	314.85	1.03E+07	1.35	350.15	350.10	3.30E+06	1.3	488.29	488.25	9.00E+04, 2.50E+04	2.05, 2.75
23	259.01	258.80	5.80E+06	0.5	350.15	350.10	6.00E+05	1.3	432.23	432.20	2.50E+06	1.9
24	230.98	230.90	5.30E+06	0.4	350.15	350.05	8.00E+05	1.3	404.20	--	--	--
25	272.94	272.80	4.70E+06	0.43	350.15	350.10	9.80E+05	1.3	446.16	446.15	1.25E+04, 1.20E+04	1.7, 1.95
26	286.95	286.90	6.10E+06	0.45	350.15	350.10	7.00E+05	1.3	460.17	460.25	7.00E+05	1.25
27	272.94	272.80	5.30E+06	0.4	350.15	350.10	8.00E+05	1.3	446.16	446.10	1.32E+05	1.7
28	259.01	258.85	6.40E+06	0.5	350.15	350.05	7.00E+05	1.3	432.23	435.25	2.10E+06	1.9
29	259.01	258.85	6.70E+06	0.55	350.15	350.10	7.00E+05	1.3	432.23	432.30	2.40E+06	1.9
30	259.01	258.85	6.90E+06	0.45	350.15	350.10	8.00E+05	1.3	432.23	432.25	1.90E+06	1.9
31	257.00	256.85	5.00E+06	0.43	350.15	350.10	7.50E+05	1.3	430.21	430.10	6.00E+04, 3.40E+04	1.3, 2.15
32	257.00	256.80	6.50E+06	0.45	350.15	350.05	7.00E+05	1.3	430.21	430.05	6.00E+04, 5.00E+04	1.3, 2.15
33	242.98	242.85	4.80E+06	0.4	350.15	350.10	8.00E+05	1.3	416.20	416.15	5.70E+04	2.05
34	242.98	242.85	5.30E+06	0.4	350.15	350.10	8.00E+05	1.3	416.20	416.10	2.80E+04, 7.30E+04	1.3, 2.05

Table A.24 (continued)

35	214.96	214.85	1.85E+06	0.4	350.15	350.10	1.10E+06	1.3	388.18	388.20	2.60E+04, 1.00E+05, 2.40E+05	1.15, 1.57, 1.73

Table A.25. LR-LC-MS analysis of CpaD I329G reactions with cWY, looking for multiple prenylations. "--" = not detected.

	+2 alkyl, [M+H]				+3alkyl, [M+H]			
PP#	Calc	Exp	peak height	Rt (min)	Calc	Exp	peak height	Rt (min)
1	622.40	622.30	1.40E+05, 6.00E+04, 9.00E+04	1.3, 2.1, 2.4	758.53	758.30	2.70E+05	2.65
3	622.40	622.30	2.40E+05, 1.20E+05	1.3, 2.1	758.53	758.25	2.80E+05	2.65
4	582.28	582.25	7.00E+04	1.3	698.34	--	--	--
5	538.31	538.25	3.50E+04	2.05	632.38	632.20	4.00E+04, 1.80E04	0.35, 1.73
6	454.21	454.40	1.25E+04, 1.90E+04, 1.50E+04, 1.90E+04	1.65, 1.85, 2.3, 2.9	506.24	--	--	--
7	458.24	--	--	--	512.29	512.40	3.05E+05	2.45
8	532.23	--	--	--	623.28	623.30	2.50E+04	2.4
9	482.24	482.00	3.00E+04, 2.50E+04	0.63, 2.5	548.29	548.30	1.50E+04	2.6
10	510.20	--	--	--	590.23	590.70	2.30E+04	2.4
11	636.30	--	--	--	779.37	--	--	--
12	454.21	454.15	1.00E+05	1.65	506.24	506.20	2.00E+04, 3.00E+04	1.95, 2.1
13	510.28	--	--	--	590.34	--	--	--
15	614.06	614.45	2.40E+04	2.5	746.02	745.80	2.40E+04	2.5
17	486.28	486.20	9.60E+04	2.1	554.34	--	--	--
19	514.31	--	--	--	596.38	--	--	--
20	518.26	--	--	--	602.32	--	--	--
21	486.28	--	--	--	554.34	--	--	--
22	626.43	--	--	--	764.57	--	--	--
23	514.31	514.30	2.20E+04	2.05	596.38	--	--	--
24	458.24	--	--	--	512.29	x	x	x

Table A.25 (continued)

25	542.17	542.25	1.75E+05	3.2	638.18	638.40	2.00E+04, 2.10E+04	0.37, 2.9
26	570.19	570.35	3.50E+04	2.5	680.21	680.30	1.85E+04	2.9
27	542.17	542.00	2.60E+04, 2.30E+04	0.35, 2.9	638.18	--	--	--
28	514.31	514.30	2.30E+04	2.05	596.38	--	--	--
29	514.31	514.25	2.25E+04	2.05	596.38	--	--	--
30	514.31	514.70	2.00E+04	2	596.38	--	--	--
31	510.28	510.30	2.30E+04	3.1	590.34	--	--	--
32	510.28	510.30	2.00E+04	3.15	590.34	--	--	--
33	482.24	482.35	2.50E+04, 3.70E+04	0.57, 2.5	548.29	548.25	2.00E+04	2.63
34	482.24	482.30	3.50E+04	2.5	548.29	548.20	2.50E+04	2.6
35	426.20	--	--	--	464.23	--	--	--

Table A.26. LR-LC-MS analysis of CpaD I329G reactions with cWF. "--" = not detected.

	PP-H				cdp+H				Prod+H			
PP#	Calc	Exp	peak height	Rt (min)	Calc	Exp	peak height	Rt (min)	Calc	Exp	peak height	Rt (min)
1	313.06	312.85	9.80E+06	1.5 smear	334.40	334.10	5.50E+05	1.55	470.52	470.25	2.90E+06, 3.50E+04	2.27, 1.55
3	313.06	312.90	9.60E+06	1.4 smear	334.40	334.10	6.50E+05	1.55	470.52	470.25	6.50E+05, 1.35E+06	1.55, 2.27
4	293.00	292.80	7.50E+06	0.5	334.40	334.10	7.80E+05	1.55	450.46	450.15	9.00E+04, 5.00E+04, 3.30E+05	1.55, 1.87, 2.07
5	271.01	270.85	8.00E+06	0.45	334.40	334.10	8.00E+05	1.55	428.48	--	--	--
6	228.97	228.85	2.25E+06	0.4	334.40	334.10	9.00E+05	1.55	386.43	--	--	--
7	230.98	230.85	5.80E+06	0.4	334.40	334.10	7.00E+05	1.55	388.45	388.20	2.00E+04	1.17
8	267.98	267.85	1.90E+06	0.4	334.40	334.10	1.00E+06	1.55	425.44	--	--	--

Table A.26 (continued)

9	242.98	242.85	5.00E+06	0.4	334.40	334.10	8.00E+05	1.55	400.45	--	--	--
10	256.96	256.85	3.20E+06	0.43	334.40	334.10	5.00E+05	1.55	414.42	414.15	1.95E+06	1.8
11	320.01	319.85	7.40E+06	0.5 smear	334.40	334.15	9.00E+05	1.55	477.47	--	--	--
12	228.97	228.85	2.05E+06	0.43	334.40	334.10	1.05E+06	1.55	386.43	--	--	--
13	257.00	256.85	6.70E+06	0.43	334.40	334.15	1.20E+06	1.55	414.46	414.20	4.80E+04, 1.08E+05	1.55, 2
15	308.89	308.75	2.35E+06	0.45	334.40	334.10	8.50E+05	1.55	466.36	--	--	--
17	245.00	244.90	5.00E+06	0.4	334.40	334.10	6.50E+05	1.55	402.46	402.15	3.80E+05	1.95
19	259.01	258.80	7.70E+06	0.45	334.40	334.10	9.00E+05	1.55	416.48	416.15	5.40E+04, 1.05E+05	0.45, 2.07
20	260.99	260.85	5.50E+06	0.4	334.40	334.15	1.10E+06	1.55	418.46	--	--	--
21	245.00	244.85	5.80E+06	0.4	334.40	334.10	9.00E+05	1.55	402.46	--	--	--
22	315.08	314.90	1.00E+07	1.5 smear	334.40	334.10	1.70E+06	1.55	472.54	472.25	2.40E+04	2.3
23	259.01	258.85	5.90E+06	0.55	334.40	334.10	5.00E+05	1.55	416.48	416.20	5.00E+05	2.07
24	230.98	230.85	5.80E+06	0.4	334.40	334.10	1.00E+06	1.55	388.45	--	--	--
25	272.94	272.80	5.50E+06	0.43	334.40	334.15	9.50E+05	1.55	430.41	430.15	2.50E+05	1.9
26	286.95	286.80	6.80E+06	0.45	334.40	334.15	9.00E+05	1.55	444.42	--	--	--
27	272.94	272.80	6.40E+06	0.43	334.40	334.15	8.00E+05	1.55	430.41	430.15	1.40E+06	1.9
28	259.01	258.85	7.00E+06	0.5	334.40	334.10	1.00E+06	1.55	416.48	416.20	4.70E+04	2.05
29	259.01	258.85	7.20E+06	0.5	334.40	334.15	8.00E+05	1.55	416.48	416.15	5.30E+04	2.05

Table A.26 (continued)

30	259.01	258.85	7.70E+06	0.5	334.40	334.15	1.60E+06	1.55	416.48	416.15	6.70E+04, 6.90E+04	0.95, 2.05
31	257.00	256.85	5.70E+06	0.45	334.40	334.10	1.40E+06	1.55	414.46	414.15	4.30E+04	1.55
32	257.00	256.85	6.70E+06	0.45	334.40	334.10	1.10E+06	1.55	414.46	414.10	4.70E+04	1.55
33	242.98	242.85	5.20E+06	0.4	334.40	334.15	1.10E+06	1.55	400.45	--	--	--
34	242.98	242.85	5.80E+06	0.4	334.40	334.15	1.20E+06	1.55	400.45	--	--	--
35	214.96	214.85	1.85E+06	0.4	334.40	334.15	1.20E+06	1.55	372.43	372.20	1.70E+04	1.8

Table A.27. LR-LC-MS analysis of CpaD I329G reactions with cWF, looking for multiple prenylations. “--” = not detected.

	+2 alkyl, [M+H]				+3alkyl, [M+H]			
PP#	Calc	Exp	peak height	Rt (min)	Calc	Exp	peak height	Rt (min)
1	606.65	606.35	2.05E+05, 2.50E+04	1.55, 2.25	742.77	742.50	4.00E+04	1.55
3	606.65	606.40	4.00E+05, 6.00E+04	1.55, 2.27	742.77	742.50	1.50E+05	1.55
4	566.52	566.10	2.50E+04	1.93	682.59	--	--	--
5	522.56	--	--	--	616.63	--	--	--
6	438.46	438.35	2.25E+04	2.5	490.49	--	--	--
7	442.49	--	--	--	496.54	496.35	3.60E+04, 1.75E+04	2.45, 2.6
8	516.48	--	--	--	607.53	--	--	--
9	466.49	466.90	3.30E+04	0.35	532.54	532.90	1.00E+05	0.37
10	494.45	494.15	1.20E+05	2	574.48	--	--	--
11	620.55	--	--	--	763.62	764.10	3.70E+05	0.5
12	438.46	438.35	2.50E+04	2.5	490.49	--	--	--
13	494.52	--	--	--	574.59	--	--	--
15	598.31	--	--	--	730.27	--	--	--
17	470.52	470.25	1.70E+05, 5.00E+04	2.23, 1.4	538.59	538.25	3.50E+04	2.05
19	498.56	498.15	5.00E+04, 8.00E+04	1.85, 1.55	580.63	--	--	--
20	502.51	--	--	--	586.57	--	--	--

Table A.27 (continued)

21	470.52	470.10	2.10E+04, 1.50E+04	1.35, 1.5	538.59	538.25	4.90E+04	2.05
22	610.68	--	--	--	748.82	--	--	--
23	498.56	--	--	--	580.63	--	--	--
24	442.49	--	--	--	496.54	496.05	3.65E+04	0.3
25	526.42	526.20	2.50E+04, 3.50+04	2.15, 2.5	622.43	622.40	1.30E+04	2.4
26	554.44	--	--	--	664.46	664.85	6.80E+04	0.35
27	526.42	526.20	4.00E+04, 2.60E+05	1.55, 2.15	622.43	--	--	--
28	498.56	498.20	6.20E+04, 3.90E+04	1.7, 1.9	580.63	--	--	--
29	498.56	--	--	--	580.63	--	--	--
30	498.56	--	--	--	580.63	--	--	--
31	494.52	--	--	--	574.59	--	--	--
32	494.52	--	--	--	574.59	--	--	--
33	466.49	466.05	2.60E+04	0.35	532.54	532.90	1.00E+05	0.37
34	466.49	466.05	2.60E+04	0.35	532.54	532.95	1.00E+05	0.37
35	410.45	--	--	--	448.48	--	--	--

Table A.28. LR-LC-MS analysis of CpaD I329G reactions with cWG. "--" = not detected.

	PP-H				cdp+H				Prod+H			
PP #	Calc	Exp	peak height	Rt (min)	Calc	Exp	peak height	Rt (min)	Calc	Exp	peak height	Rt (min)
1	313.06	312.90	9.80E+06	1.45	244.37	244.10	9.00E+04	0.65	380.50	380.20	1.32E+05	2.05
3	313.06	312.90	9.80E+06	1.5	244.37	244.15	8.00E+04	0.67	380.50	380.20	5.20E+05	2.05
4	293.00	292.80	7.10E+06	0.55 smear	244.37	244.10	1.50E+04	0.65	360.44	360.10	2.60E+04, 2.00E+04, 1.75E+05	1.65, 1.8, 0.65
5	271.01	270.85	8.20E+06	0.45	244.37	244.15	2.15E+04	0.65	338.45	--	--	--
6	228.97	228.85	1.85E+06	0.4	244.37	244.10	2.95E+04	0.67	296.40	296.20	2.10E+04	0.33
7	230.98	230.85	5.40E+06	0.37	244.37	244.15	2.50E+04	0.65	298.42	298.90	3.10E+04	0.33

Table A.28 (continued)

8	267.98	267.90	1.65E+06	0.4	244.37	244.10	8.80E+04	0.67	335.41	335.90	3.80E+04	0.33
9	242.98	242.85	4.50E+06	0.4	244.37	244.10	3.00E+04	0.65	310.42	310.10	3.10E+04, 1.30E+04	0.33, 1.43
10	256.96	256.85	4.30E+06	0.43	244.37	244.10	1.80E+05	0.73	324.40	324.10	6.00E+04	1.5
11	320.01	319.90	8.20E+06	0.65	244.37	244.10	1.00E+05	0.73	387.45	--	--	--
12	228.97	228.90	2.25E+06	0.43	244.37	244.10	9.80E+04	0.65	296.40	296.20	1.80E+04	1.47 messy
13	257.00	256.85	5.80E+06	0.45	244.37	244.10	8.30E+04	0.67	324.44	324.90	2.80E+04	0.35
15	308.89	308.75	2.15E+06	0.43	244.37	244.10	2.90E+04	0.65	376.33	376.15	1.75E+04	1.95
17	245.00	244.80	5.70E+06	0.45	244.37	244.10	1.30E+05	0.7	312.44	312.15	8.80E+04	1.67
19	259.01	258.85	7.30E+06	0.45	244.37	244.10	8.40E+04	0.73	326.45	326.25	2.00E+04, 2.00E+04	0.3, 1.85
20	260.99	260.90	5.40E+06	0.4	244.37	244.10	3.00E+04	0.65	328.43	328.90	4.70E+04	0.33
21	245.00	244.90	5.30E+06	0.4	244.37	244.10	2.60E+04	0.65	312.44	312.95	2.40E+04	0.35
22	315.08	314.90	1.00E+07	1.5	244.37	244.10	2.00E+05	0.73	382.51	382.10	2.60E+04	1.17
23	259.01	258.90	5.80E+06	0.55	244.37	244.15	2.90E+04	0.67	326.45	326.20	1.85E+04, 2.50E+04	0.3, 1.83
24	230.98	230.85	5.50E+06	0.4	244.37	244.15	3.00E+04	0.65	298.42	298.90	2.85E+04	0.35
25	272.94	272.80	5.50E+06	0.43	244.37	244.10	5.40E+04	0.65	340.38	340.05	2.80E+04, 2.00E+04	0.65, 0.35
26	286.95	286.80	7.20E+06	0.43	244.37	244.10	4.60E+04	0.65	354.39	354.00	2.80E+04	0.35

Table A.28 (continued)

27	272.94	272.80	5.80E+06	0.65	244.37	244.10	4.20E+04	0.67	340.38	340.05	2.00E+04, 4.10E+04	0.35, 0.65
28	259.01	258.85	7.20E+06	0.45	244.37	244.10	3.30E+04	0.67	326.45	326.25	4.20E+04, 2.00E+04	1.85, 0.27
29	259.01	258.85	7.50E+06	0.55	244.37	244.15	1.60E+05	0.72	326.45	326.25	3.00E+04	1.85
30	259.01	258.85	7.40E+06	0.45	244.37	244.10	1.20E+05	0.7	326.45	326.30	3.40E+04	1.85
31	257.00	256.85	5.40E+06	0.45	244.37	244.10	5.50E+04	0.65	324.44	324.85	3.40E+04	1.85
32	257.00	256.85	7.00E+06	0.4	244.37	244.10	9.20E+04	0.67	324.44	324.05	2.30E+04	0.35
33	242.98	242.90	5.20E+06	0.4	244.37	244.10	8.00E+04	0.67	310.42	309.95,310.9	3.30E+04	0.33
34	242.98	242.85	6.30E+06	0.43	244.37	244.10	2.50E+05	0.72	310.42	--	--	--
35	214.96	214.85	1.80E+06	0.4	244.37	244.15	1.45E+05	0.7	282.40	282.15	2.20E+05	0.75 smear

Table A.29. LR-LC-MS analysis of CpaD I329G reactions with cWG, looking for multiple prenylations. "--" = not detected.

	+2 alkyl, [M+H]				+3alkyl, [M+H]			
PP#	Calc	Exp	peak height	Rt (min)	Calc	Exp	peak height	Rt (min)
1	516.62	--	--	--	652.75	--	--	--
3	516.62	516.80	1.10E+05, 7.00E+04	1.43, 2.05	652.75	--	--	--
4	476.50	476.20	2.50E+05	0.63	592.56	592.25	1.10E+05	0.65
5	432.53	432.25	4.40E+06	1.9	526.61	526.40	3.40E+04	2.5
6	348.44	--	--	--	400.47	--	--	--
7	352.47	--	--	--	406.51	--	--	--
8	426.46	--	--	--	517.50	--	--	--
9	376.47	376.20	1.85E+04	1.95	442.51	--	--	--
10	404.42	--	--	--	484.45	484.25	2.50E+04	2
11	530.52	--	--	--	673.59	673.15	5.50E+04	2.05
12	348.44	--	--	--	400.47	--	--	--

Table A.29 (continued)

13	404.50	--	--	--	484.56	484.25	2.90E+04	2.05
15	508.29	--	--	--	640.24	--	--	--
17	380.50	--	--	--	448.56	--	--	--
19	408.53	--	--	--	490.61	--	--	--
20	412.49	--	--	--	496.55	--	--	--
21	380.50	--	--	--	448.56	448.25	2.80E+04	0.65
22	520.65	520.30	1.80E+05	1.276	658.80	658.45	2.00E+04	2.5
23	408.53	--	--	--	490.61	--	--	--
24	352.47	--	--	--	406.51	--	--	--
25	436.39	--	--	--	532.40	--	--	--
26	464.41	--	--	--	574.43	574.25	2.70E+04	1.85
27	436.39	436.10	8.20E+04	1.93	532.40	--	--	--
28	408.53	--	--	--	490.61	--	--	--
29	408.53	--	--	--	490.61	--	--	--
30	408.53	--	--	--	490.61	--	--	--
31	404.50	--	--	--	484.56	484.25	3.40E+04	2.05
32	404.50	--	--	--	484.56	484.20	2.50E+04	2.05
33	376.47	376.25	2.00E+04	1.97	442.51	--	--	--
34	376.47	--	--	--	442.51	--	--	--
35	320.43	--	--	--	358.45	--	--	--

A.7. FtmPT1 M364G *in vitro*

Table A.30. LR-LC-MS analysis of FtmPT1 M364G reactions with cWY. “--” = not detected.

	PP-H				cdp+H				Prod+H			
PP#	Calc	Exp	peak height	Rt (min)	Calc	Exp	peak height	Rt (min)	Calc	Exp	peak height	Rt (min)
1	313.06	312.90	5.30E+06	1.65	350.15	350.10	3.40E+04	1.3	486.28	486.25	3.50E+06, 1.50E+06	2.05, 2.18
3	313.06	312.85	8.00E+06	1.6	350.15	350.10	4.00E+05	1.3	486.28	486.20	4.70E+06	2.18
4	293.00	292.85	7.50E+06	0.45	350.15	350.15	6.00E+05	1.3	466.21	466.20	2.40E+06, 3.50E+05	1.85, 1.3
5	271.01	270.85	7.70E+06	0.45	350.15	350.15	7.00E+05	1.3	444.23	444.30	2.20E+04	2.3
6	228.97	228.90	8.80E+05	0.4	350.15	350.15	7.00E+05	1.3	402.18	--	--	--
7	230.98	230.90	3.50E+06	0.4	350.15	350.15	7.50E+05	1.3	404.20	--	--	--
8	267.98	267.90	3.10E+05	0.45	350.15	350.15	6.00E+05	1.3	441.19	--	--	--
9	242.98	242.90	1.90E+06	0.45	350.15	350.15	6.50E+05	1.3	416.20	416.20	5.70E+04	2.05
10	256.96	256.85	5.00E+04	0.45	350.15	350.15	7.00E+04	1.3	430.18	430.15	4.70E+06	1.67
11	320.01	319.85	6.20E+06	0.65	350.15	350.10	7.00E+05	1.3	493.22	--	--	--
12	228.97	228.90	2.70E+05	0.45	350.15	350.10	7.00E+05	1.3	402.18	--	--	--
13	257.00	256.85	1.48E+06	0.45	350.15	350.15	5.80E+05	1.3	430.21	430.20	3.00E+04, 2.00E+04, 1.00E+05	1.3, 2.25, 1.85
15	308.89	308.90	6.40E+05	0.45	350.15	350.10	8.60E+05	1.3	482.11	482.35	1.90E+04	2.5

Table A.30 (continued)

17	245.00	244.90	1.00E+06	0.45	350.15	350.10	1.15E+05	1.8	418.21	418.20	3.00E+06, 5.50E+06	1.7, 1.83
19	259.01	258.85	7.80E+06	0.5	350.15	350.15	8.00E+05	1.3	432.23	432.20	1.70E+06, 1.50E+06	1.9, 2.05
20	260.99	260.85	3.30E+06	0.45	350.15	350.15	7.50E+05	1.3	434.21	434.30	2.30E+04	2.05
21	245.00	244.90	4.50E+06	0.45	350.15	350.15	1.00E+06	1.3	418.21	--	--	--
22	315.08	314.90	1.00E+07	1.35	350.15	350.10	3.25E+05	1.27	488.29	488.25	2.60E+04, 2.70E+04, 7.50E+04	2.05, 2.3, 2.77
23	259.01	258.90	4.00E+05	0.6	350.15	350.10	6.00E+05	1.3	432.23	432.20	3.10E+06, 1.00E+06	1.9, 2.05
24	230.98	230.90	4.70E+06	0.4	350.15	350.15	8.00E+05	1.27	404.20	--	--	--
25	272.94	272.80	2.40E+06	0.43	350.15	350.10	6.50E+05	1.3	446.16	446.10	6.00E+04	1.73
26	286.95	286.85	1.10E+05	0.4	350.15	350.10	5.20E+05	1.3	460.17	460.25	3.50E+05, 3.00E+04	2.03, 2.57
27	272.94	272.80	4.20E+06	0.4	350.15	350.10	5.00E+05	1.3	446.16	446.10	2.60E+06	1.73
28	259.01	258.90	1.08E+06	0.55	350.15	350.15	6.60E+05	1.3	432.23	432.35	1.10E+06	2.05
29	259.01	258.90	8.00E+05	0.55	350.15	350.10	7.20E+05	1.3	432.23	432.30	1.50E+06	2.05
30	259.01	258.90	1.24E+06	0.5	350.15	350.10	7.00E+05	1.3	432.23	432.30	1.38E+06	2.05
31	257.00	256.85	7.90E+05	0.5	350.15	350.10	7.70E+05	1.3	430.21	430.05	4.30E+05, 1.70E+04	1.3, 2.35

Table A.30 (continued)

32	257.00	256.85	2.90E+06	0.45	350.15	350.10	7.00E+05	1.3	430.21	430.10	4.10E+04, 1.50E+04	1.3, 2.35
33	242.98	242.90	4.30E+06	0.4	350.15	350.10	7.00E+05	1.3	416.20	416.15	6.20E+04	2.05
34	242.98	242.85	5.00E+06	0.4	350.15	350.10	7.00E+05	1.3	416.20	416.15	4.80E+04	2.05
35	214.96	214.80	6.10E+05	0.45	350.15	350.10	6.90E+05	1.3	388.18	388.25	3.65E+04	1.6

Table A.31. LR-LC-MS analysis of FtmPT1 M364G reactions with cWY, looking for multiple prenylations. "--" = not detected.

	+2 alkyl, [M+H]				+3alkyl, [M+H]			
PP#	Calc	Exp	peak height	Rt (min)	Calc	Exp	peak height	Rt (min)
1	622.40	622.40	5.00E+05	2.57	758.53	758.35	4.50E+04	2.65
3	622.40	622.35	1.85E+05	2.07	758.53	758.30	1.25E+05	2.65
4	582.28	582.30	1.00E+05	1.3	698.34	698.50	4.50E+05	3.05
5	538.31	538.25	2.80E+04	2.05	632.38	--	--	--
6	454.21	454.20	1.50E+04	1.65	506.24	--	--	--
7	458.24	--	--	--	512.29	512.45	5.00E+04	2.45
8	532.23	--	--	--	623.28	--	--	--
9	482.24	482.40	2.40E+04	2.5	548.29	548.25	1.70E+04	2.6
10	510.20	510.20	6.50E+04	1.9	590.23	--	--	--
11	636.30	--	--	--	779.37	--	--	--
12	454.21	454.20	7.00E+04	1.65	506.24	--	--	--
13	510.28	--	--	--	590.34	--	--	--
15	614.06	614.45	2.50E+04	2.5	746.02	--	--	--
17	486.28	486.25	3.50E+04	2.15	554.34	--	--	--
19	514.31	--	--	--	596.38	--	--	--
20	518.26	518.25	2.30E+04	2.05	602.32	--	--	--
21	486.28	--	--	--	554.34	--	--	--
22	626.43	--	--	--	764.57	--	--	--
23	514.31	--	--	--	596.38	--	--	--
24	458.24	--	--	--	512.29	--	--	--
25	542.17	--	--	--	638.18	--	--	--
26	570.19	570.40	2.50E+04	2.5	680.21	--	--	--
27	542.17	542.15	1.40E+05	2	638.18	--	--	--
28	514.31	--	--	--	596.38	--	--	--
29	514.31	--	--	--	596.38	--	--	--
30	514.31	--	--	--	596.38	--	--	--
31	510.28	--	--	--	590.34	--	--	--
32	510.28	--	--	--	590.34	--	--	--
33	482.24	482.40	3.20E+04	2.5	548.29	548.30	2.20E+04	2.6
34	482.24	482.35	2.60E+04	2.5	548.29	548.25	1.80E+04	2.6
35	426.20	--	--	--	464.23	--	--	--

Table A.32. LR-LC-MS analysis of FtmPT1 M364G reactions with cWF. "--" = not detected.

	PP-H				cdp+H				Prod+H			
PP#	Calc	Exp	peak height	Rt (min)	Calc	Exp	peak height	Rt (min)	Calc	Exp	peak height	Rt (min)
1	313.06	312.90	7.90E+06	1.65	334.40	--	--	--	470.52	470.25	4.90E+06	2.35
3	313.06	312.90	7.40E+06	1.65	334.40	--	--	--	470.52	470.25	3.30E+06	2.35
4	293.00	292.85	5.10E+06	0.6	334.40	334.10	1.90E+05	1.55	450.46	450.15	4.50E+06	2.07
5	271.01	270.85	7.80E+06	0.5	334.40	334.10	8.00E+05	1.55	428.48	--	--	--
6	228.97	228.90	1.60E+06	0.4	334.40	334.10	8.20E+05	1.55	386.43	--	--	--
7	230.98	230.90	4.40E+06	0.4	334.40	334.10	7.00E+05	1.55	388.45	--	--	--
8	267.98	267.85	1.60E+06	0.4	334.40	334.15	7.50E+05	1.55	425.44	425.05	7.80E+04	0.27
9	242.98	242.85	3.70E+06	0.4	334.40	334.10	8.50E+05	1.55	400.45	--	--	--
10	256.96	256.85	1.80E+06	0.45	334.40	--	--	--	414.42	414.10	1.50E+06, 5.30E+06	1.77, 1.9
11	320.01	319.85	4.50E+06	0.6	334.40	334.10	8.00E+05	1.55	477.47	--	--	--
12	228.97	228.85	1.40E+06	0.45	334.40	334.10	8.00E+05	1.55	386.43	--	--	--
13	257.00	256.85	4.30E+06	0.45	334.40	334.10	8.00E+05	1.55	414.46	414.20	1.15E+05	2.03
15	308.89	308.75	1.45E+06	0.45	334.40	334.10	6.80E+05	1.55	466.36	--	--	--
17	245.00	244.90	5.80E+06	0.4	334.40	344.20	5.00E+05	2.05	402.46	402.15	5.00E+06	2.05
19	259.01	258.85	5.30E+06	0.43	334.40	334.10	2.15E+05	1.55	416.48	416.15	5.80E+06	2.1
20	260.99	260.85	5.30E+06	0.4	334.40	334.10	9.00E+05	1.55	418.46	--	--	--
21	245.00	244.85	3.80E+06	0.4	334.40	334.15	5.00E+05	1.55	402.46	--	--	--

Table A.32 (continued)

22	315.08	314.85	1.00E+07	1.6	334.40	334.10	1.10E+06	1.6 smear	472.54	472.25	7.70E+04	2.33
23	259.01	258.90	2.20E+06	0.6	334.40	334.10	6.70E+04	1.55	416.48	416.20	5.80E+06	2.1
24	230.98	230.85	5.40E+06	0.4	334.40	334.10	8.00E+05	1.55	388.45	--	--	--
25	272.94	272.80	5.10E+06	0.4	334.40	334.10	6.00E+05	1.55	430.41	430.10	3.70E+05	1.93
26	286.95	286.80	6.20E+06	0.45	334.40	334.10	8.00E+05	1.55	444.42	444.30	2.70E+04	2.27
27	272.94	272.80	1.80E+06	0.45	334.40	334.15	4.50E+04	1.55	430.41	430.05	5.40E+06	1.95
28	259.01	258.90	2.10E+06	0.55	334.40	334.10	8.50E+05	1.55	416.48	416.15	7.20E+04	2.1
29	259.01	258.90	5.60E+06	0.65	334.40	334.15	1.00E+06	1.55	416.48	416.25	1.90E+05	2.1
30	259.01	258.90	5.30E+06	0.55	334.40	334.15	8.00E+05	1.55	416.48	416.20	4.90E+04	2.05
31	257.00	256.90	3.40E+06	0.45	334.40	334.15	1.10E+06	1.55	414.46	414.20	2.85E+04	1.55
32	257.00	256.85	5.80E+06	0.4	334.40	334.15	8.00E+05	1.55	414.46	416.15	2.30E+04, 1.70E+04	1.55, 1.65
33	242.98	242.85	4.80E+06	0.43	334.40	334.15	8.00E+05	1.55	400.45	--	--	--
34	242.98	242.85	5.20E+06	0.4	334.40	334.15	1.10E+06	1.55	400.45	--	--	--
35	214.96	214.85	1.60E+06	0.4	334.40	334.15	1.30E+06	1.55	372.43	372.25	3.40E+04	1.83

Table A.33. LR-LC-MS analysis of FtmPT1 M364G reactions with cWF, looking for multiple prenylations. "--" = not detected.

	+2 alkyl, [M+H]				+3alkyl, [M+H]			
PP#	Calc	Exp	peak height	Rt (min)	Calc	Exp	peak height	Rt (min)
1	606.65	--	--	--	742.77	--	--	--
3	606.65	--	--	--	742.77	--	--	--
4	566.52	--	--	--	682.59	--	--	--
5	522.56	--	--	--	616.63	--	--	--
6	438.46	--	--	--	490.49	--	--	--
7	442.49	--	--	--	496.54	--	--	--
8	516.48	--	--	--	607.53	--	--	--
9	466.49	466.00	5.50E+04	0.35	532.54	532.05	3.00E+04	0.37
10	494.45	494.20	2.00E+05	2.07	574.48	--	--	--
11	620.55	620.40	2.40E+04	2.3	763.62	763.25	7.50E+04	0.65
12	438.46	--	--	--	490.49	--	--	--
13	494.52	--	--	--	574.59	--	--	--
15	598.31	--	--	--	730.27	--	--	--
17	470.52	470.25	6.40E+04	2.33	538.59	538.25	1.60E+04	2.05
19	498.56	--	--	--	580.63	--	--	--
20	502.51	--	--	--	586.57	--	--	--
21	470.52	--	--	--	538.59	--	--	--
22	610.68	--	--	--	748.82	--	--	--
23	498.56	--	--	--	580.63	--	--	--
24	442.49	--	--	--	496.54	--	--	--
25	526.42	--	--	--	622.43	--	--	--
26	554.44	--	--	--	664.46	664.45	2.10E+04	2.3
27	526.42	526.10	2.70E+04, 2.80E+05	2.5, 2.2	622.43	--	--	--
28	498.56	--	--	--	580.63	--	--	--
29	498.56	--	--	--	580.63	--	--	--
30	498.56	--	--	--	580.63	--	--	--
31	494.52	--	--	--	574.59	--	--	--
32	494.52	--	--	--	574.59	--	--	--
33	466.49	466.05	5.70E+04	0.35	532.54	532.40	3.90E+04, 2.80E+04	2.3, 0.37
34	466.49	466.00	4.50E+04	0.35	532.54	532.35	4.00E+04, 4.30E+04	2.3, 0.37
35	410.45	--	--	--	448.48	--	--	--

Table A.34. LR-LC-MS analysis of FtmPT1 M364G reactions with cWG. “--” = not detected.

	PP-H				cdp+H				Prod+H			
PP#	Calc	Exp	peak height	Rt (min)	Calc	Exp	peak height	Rt (min)	Calc	Exp	peak height	Rt (min)
1	313.06	312.95	2.80E+04	2.1	244.37	244.15	2.00E+04	2.1	380.50	380.20	4.30E+06	2.1
3	313.06	312.95	7.50E+04	2.1	244.37	244.15	1.50E+04	2.1	380.50	380.20	3.90E+06	2.1
4	293.00	292.85	3.60E+05	1.1	244.37	--	--	--	360.44	360.15	1.45E+06	1.8
5	271.01	270.90	2.70E+06	0.6	244.37	--	--	--	338.45	--	--	--
6	228.97	228.85	5.30E+05	0.43	244.37	244.15	2.50E+04	0.65	296.40	--	--	--
7	230.98	230.90	2.00E+06	0.45	244.37	244.15	4.30E+04	0.65	298.42	298.25	1.20E+04	1.87
8	267.98	267.85	3.70E+05	0.4	244.37	244.15	2.10E+04	0.65	335.41	--	--	--
9	242.98	242.85	8.30E+06	0.4	244.37	244.15	4.30E+04	0.7	310.42	--	--	--
10	256.96	265.85	3.50E+05	0.45	244.37	--	--	--	324.40	324.15	1.70E+06, 2.00E+05	1.55, 1.4
11	320.01	319.85	2.00E+06	1, 1.3 smear	244.37	244.15	6.00E+04	0.73	387.45	--	--	--
12	228.97	228.85	5.40E+05	0.4	244.37	244.15	2.30E+04	0.65	296.40	296.00	1.85E+04	0.35
13	257.00	256.90	7.30E+05	0.45	244.37	244.15	2.75E+04	0.7	324.44	324.20	2.85E+05	1.75
15	308.89	308.75	1.24E+05	0.6	244.37	244.15	4.80E+04	0.65	376.33	--	--	--
17	245.00	244.85	1.20E+06	0.43	244.37	244.10	4.80E+04	1.65	312.44	312.15	1.65E+06, 2.80E+05	1.67, 1.55
19	259.01	258.90	9.00E+05	0.5	244.37	244.15	3.60E+04	0.65	326.45	326.20	3.40E+05	1.85
20	260.99	260.85	1.90E+06	0.4	244.37	244.15	1.90E+04	0.65	328.43	--	--	--

Table A.34 (continued)

21	245.00	244.90	7.00E+05	0.45	244.37	244.15	6.30E+04	0.73	312.44	--	--	--
22	315.08	314.95	1.25E+06	1.85	244.37	244.15	1.85E+04	0.67	382.51	382.50	2.90E+04	2.2
23	259.01	258.65	5.50E+04	0.65	244.37	244.15	2.00E+04	1.25	326.45	326.20	6.70E+05	1.83
24	230.98	230.90	2.85E+06	0.4	244.37	244.20	1.24E+05	0.73	298.42	--	--	--
25	272.94	272.80	2.85E+05	0.5	244.37	244.15	2.60E+04	0.65	340.38	340.10	3.60E+04	1.57
26	286.95	286.85	5.80E+05	0.55	244.37	244.15	2.40E+04	0.65	354.39	--	--	--
27	272.94	272.80	7.10E+05	0.45	244.37	--	--	--	340.38	340.10	6.70E+05	1.63
28	259.01	258.90	1.80E+05	0.6	244.37	244.15	1.50E+04	0.65	326.45	326.30	1.40E+04	1.87
29	259.01	258.90	1.90E+05	0.65	244.37	244.15	3.50E+04	0.67	326.45	326.30	1.35E+04	1.85
30	259.01	258.90	3.00E+05	0.6	244.37	244.15	2.10E+04	0.65	326.45	326.30	1.25E+04	1.85
31	257.00	256.85	5.70E+05	0.45	244.37	244.15	2.00E+04	0.65	324.44	--	--	--
32	257.00	256.85	9.00E+05	0.5	244.37	244.15	1.40E+04	0.65	324.44	--	--	--
33	242.98	242.85	2.00E+06	0.4	244.37	244.15	5.80E+04	0.73	310.42	--	--	--
34	242.98	242.85	2.40E+06	0.4	244.37	244.15	3.40E+04	0.7	310.42	--	--	--
35	214.96	214.85	6.20E+05	0.4	244.37	244.15	1.90E+04	0.65	282.40	282.10	3.20E+04	smear

Table A.35. LR-LC-MS analysis of FtmPT1 M364G reactions with cWG, looking for multiple prenylations. "--" = not detected.

	+2 alkyl, [M+H]				+3alkyl, [M+H]			
PP#	Calc	Exp	peak height	Rt (min)	Calc	Exp	peak height	Rt (min)
1	516.62	--	--	--	652.75	--	--	--
3	516.62	516.30	2.30E+04	2.1	652.75	--	--	--
4	476.50	--	--	--	592.56	--	--	--
5	432.53	432.35	7.50E+05	1.95	526.61	526.00	2.50E+04	1.15
6	348.44	--	--	--	400.47	--	--	--
7	352.47	--	--	--	406.51	--	--	--
8	426.46	426.10	2.90E+04	0.27	517.50	--	--	--
9	376.47	--	--	--	442.51	--	--	--
10	404.42	404.15	3.75E+04	1.85	484.45	484.20	1.00E+04	2.05
11	530.52	--	--	--	673.59	--	--	--
12	348.44	--	--	--	400.47	--	--	--
13	404.50	--	--	--	484.56	--	--	--
15	508.29	--	--	--	640.24	--	--	--
17	380.50	--	--	--	448.56	--	--	--
19	408.53	--	--	--	490.61	--	--	--
20	412.49	--	--	--	496.55	--	--	--
21	380.50	--	--	--	448.56	--	--	--
22	520.65	520.25	1.70E+04	1.3	658.80	--	--	--
23	408.53	--	--	--	490.61	--	--	--
24	352.47	--	--	--	406.51	--	--	--
25	436.39	--	--	--	532.40	--	--	--
26	464.41	--	--	--	574.43	--	--	--
27	436.39	436.15	5.00E+04	1.95	532.40	--	--	--
28	408.53	--	--	--	490.61	--	--	--
29	408.53	--	--	--	490.61	--	--	--
30	408.53	--	--	--	490.61	--	--	--
31	404.50	--	--	--	484.56	--	--	--
32	404.50	--	--	--	484.56	--	--	--
33	376.47	376.25	3.30E+04, 2.00E+04	2.05, 0.5	442.51	--	--	--
34	376.47	--	--	--	442.51	--	--	--
35	320.43	--	--	--	358.45	--	--	--